Role of the Reduced Sulfur Species in the Degradation of Selected Organophosphorus Pesticides in Simulated Natural Environment

by

Qiu Gan

A dissertation submitted to the Graduate Faculty in Chemistry in partial fulfillment of the requirements for the degree of Doctor of Philosophy, The City University of New York

2007

UMI Number: 3245038

UMI Microform 3245038

ProQuest Information and Learning Company
300 North Zeeb Road
P.O. Box 1346
Ann Arbor, MI 48106-1346

This manuscript has been read and accepted by the Graduate Faculty in Chemistry in satisfaction of the dissertation requirement for the degree of Doctor of Philosophy.

Prof. Urs Jans

Date July, 19, 2006

Chair of Examining Committee

Prof. Gerald W. Koeppl

Date July, 19, 2006

Executive Officer

Prof. Mahesh K. Lakshman

Prof. Alexander Greer

Supervisory Committee

The City University of New York

Abstract

Role of the Reduced Sulfur Species in the Degradation of Selected Organophosphorus Pesticides in Simulated Natural Environment

by

Qiu Gan

Research Advisor: Professor Urs Jans

Esters and thioesters of phosphoric acid and thiophosphoric acid are widely applied as pesticides in agricultural and urban environments, taking advantage of their inhibitory action on cholinesterase. Organophosphorus pesticides (OPs) are among EPA's highest priority for review under the Food Quality Protection Act due to their influence on the function of the nervous system and their reported neurodevelopmentally toxic effects at very low dose. They enter the environment primarily during their uses in crops, and in homes and gardens, which result in the release into sensitive costal environments such as estuaries, salt marshes and sediments. Anoxic conditions are common in such environments and relative high concentrations of reduced sulfur species are reported. This dissertation presents the kinetic, thermodynamic and mechanistical studies of the reactions of reduced sulfur species, including hydrogen sulfide (H_2S), bisulfide (HS^-), polysulfide (S_n^{2-}

), thiophenol (PhSH), thiophenolate (PhS^-) and thiosulfate ($S_2O_3^{2-}$) in the degradation of selected organophosphorus pesticides (OPs) under anoxic condition. Selected OPs investigated in this study include thiometon, disulfoton, phorate, terbufos, naled and dichlorvos. Reactions were monitored at varying concentrations of reduced sulfur species over a pH range to obtain the second-order reaction rate constants. The activation parameters were investigated via the temperature dependence of the reaction rate constants of selected OPs with reduced sulfur species. This study also represents an experimental investigation of structural effects on reactivity and reaction mechanism. The subtle difference in structure may result in drastic differences in reactivity and even mechanism. Studies of the structural analogs can provide invaluable, though indirect and unclear, information regarding the mechanisms through which OPs react with the reduced sulfur species. When the second-order rate constants at 25 °C are multiplied by the environmentally relevant concentration of the reduced sulfur species, half-lives of selected OPs can be predicted. The results indicated that reduced sulfur species could play a very important role in the chemical fate of selected OPs in coastal marine environments.

Dedicated to those who made this thesis possible:

My parents, my friends

Acknowledgments

I am sincerely grateful to my research mentor, Professor Urs Jans, for his professional guidance. He not only helped me in project design and development in my research work, but also took much time and energy to review all of my reports and papers and made valuable comments as well as corrections.

I thank Professor Mahesh K. Lakshman and Professor Alexander Greer who gave me many valuable suggestions.

I am very thankful to my colleagues and to all those people who offered me a great deal of help.

Special thanks are also given to my family and my friends for their consistent encouragement during my Ph.D. research work.

Finally, I acknowledge the financial support from National Science Foundation, the Herman Frasch Foundation and the Petroleum Research Fund.

Table of Contents

List of Schemes

Chapter III

Chapter IV

Chapter V

Part I

Part II

List of Tables

Chapter III

Chapter IV

Chapter V

Part I

Part II

List of Figures

Chapter I

Chapter II

Chapter III

Chapter IV

Chapter IV

Part I

Part II

Chapter I

Introduction

1. Background of Organophosphorus Pesticides (OPs)

Many organic chemicals in current commercial production are intentionally or inadvertently released into environmental systems every year. One class of chemicals that have great and lasting impact on the ecosystem are agrochemicals. Agricultural pollution poses a great threat to the environment. Runoff from croplands is the major nonpoint source for agrochemicals in the aquatic environment (Godfrey et al., 1995; Wauchope, 1978; Leonard, 1988; Thurman et al., 1994). At the same time, agrochemicals are also introduced into the environment through leaching (Thurman et al., 1991; Hallberg, 1989), improper application and incidents (Capel et al., 1988). The fates of these chemicals in the environment include transportation, in which the molecular structure of the chemical is not changed and a molecule will be carried between air, surface, water, groundwater, organism, aquatic sediments, and soils by various processes and transformations such as adsorption, hydrolysis, photolysis, oxidation, reduction and biodegradation and so on. Many agrochemicals in use show a relatively high persistence in surface water, which allows their transport over long distance and their migration into very sensitive aquatic environments or delicate ecosystem, which pose a real risk to the ecosystem. Fortunately, the environment has the capacity to “cleanse itself ” of many kinds of chemicals through a variety of

chemical and biological processes. An understanding of these processes, especially how rapidly the environment can degrade a specific chemical structure to a simpler and potentially less harmful chemical, is a key to the rational use of natural resources with minimal abuse. The ability to predict the probable fate of specific compounds in the environment is also essential for screening the chemicals that may be considered for applications leading to their ultimate introduction into water, soil, or air.

Nationally, approximately 1 billion pounds of conventional pesticides are used annually, ¾ of which are used in agriculture (U.S.EPA, 1996, OPP annual report for 1996 Part 1). Recent studies have demonstrated that environments throughout the world are commonly contaminated with pesticides, including organophosphates, carbamates, organochlorines, pyrethroids and herbicide compounds (Starr et al., 1974; Roinestad et al., 1993; Lewis et al., 1994; Whitmore et al., 1994; Simcox et al., 1995; Bradman et al., 1997; Buckley et al., 1997; Steen et al., 1997; Colt et al., 1998; Camann et. al, 1995; Camann et. al, 1997). Because of their significant biological activity, inhibitory activity towards cholinesterase, a key enzyme involved in the metabolism of acetylcholine (one of major neuron transmitter), esters and thioester of phosphoric acid and thio phosphoric acid are widely applied as insecticides. OPs are typically categorized into four subgroups: phosphates, phosphorothioates, phosphorodithioates and phosphorothiolates (Figure 1.1).

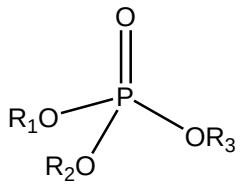

phosphate

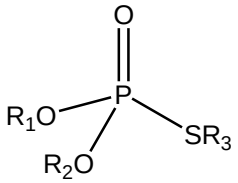

phosphorothiolate

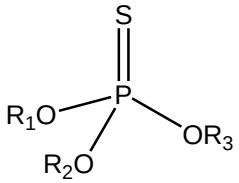

phosphorothioate

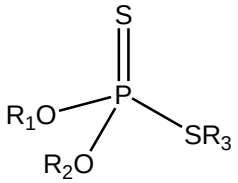

phosphorodithioate

Figure 1.1 Four structures of OPs

OPs were developed during the early 19th century, but their effects on insects, which are similar to their effects on humans, were discovered in 1932 (Ware and Whitacre, 2004). OPs are active against a broad spectrum of insects and are used on food crops as well as in residential and commercial buildings and on ornamental plants and lawns. The extremely toxic and specific molecules have been widely used throughout the world since the decline in the use of organochlorine pesticides in the 1960s and 1970s. OPs are tending to replace the organochline pesticides that are more or less prohibited for use because of their persistence in the environment and the bioaccumulation along the food chain. Now OPs account for about half of the insecticides used in the United States. Approximately 60 million pounds of organophosphate pesticides are applied to about 60 million acres of U.S. agricultural crops annually; nonagricultural uses

account for about 17 million pounds per year (U.S. EPA. 1999. 735-F-99-014). OPs are applied to the protected crops via a variety of methods. For example, the nighttime spraying of OPs from low-flying airplanes is a very common application. Soil pesticides can be applied as granules on the soil where the protected crop is cultivated. There is also a group of OPs that is applied directly to the fruit and/or leaves of the crop to be protected. And available formations of OPs include granular, fog, dust, emulsion concentrate, liquid, ULV formulation and so on. Note that the thionate (P=S) ester exhibit a lower mammalian toxicity than corresponding oxonate (P=O) ester and that, for this reason, they are more widely used. The thionate esters are converted to the oxonates by oxidation both inside and outside organisms. In addition to the use of the phosphoric acid esters as biocides, some trialkyl and triarkyl phosphates are used in very large quantities in fire-resistant hydraulic fluids and as fire-retardant plasticizers. Consequently, such compounds are of great environmental significance and concern.

Despite the undoubted advantages accruing from the use of OPs, concern has been expressed at the potentially harmful effects of using OPs which are rather stable and can accumulate in man and the environment. Many of the OPs are considered controlled substances and have very strict application instructions. Others may be controlled indirectly by the government bodies who set maximum allowable concentration standards of OPs in drinking water or residues of OPs in food, for instance. In recent years, EPA has started to reconsider the wide application of organophosphorus pesticides due to concern about their effects on

the central nervous system of humans, children in particular. They are in the first priority group of pesticides to be reviewed under the Food Quality Protection Act (U.S. EPA. 1996, Food Quality Protection Act (FQPA) of 1996). In order to evaluate the impact of OPs on the environment and to avoid the risk that OPs may put on the ecosystem, the knowledge concerning the transportation and transformation of OPs in the environment is desired.

2. Toxicity of OPs

To evaluate the effect of OPs on the environments, the toxicity of OPs has to be understood first. OPs act by interfering with the activity of cholinesterase, an enzyme that is essential for the proper working for the nervous systems of both humans and insects (Feldman, 1998). Electrical switching centers, called 'synapses' are found throughout the nervous systems of humans, other vertebrates, and insects. Muscles, glands, and nerve fibers called 'neurons' are stimulated or inhibited by the constant firing of signals across these synapses. Stimulating signals are usually carried by a chemical called 'acetylcholine'. Stimulating signals are discontinued by a specific type of cholinesterase enzyme, acetylcholinesterase, which breaks down the acetylcholine. These important chemical reactions are usually going on all the time at a very fast rate, with acetylcholine causing stimulation and acetylcholinesterase ending the signal. If cholinesterase-affecting insecticides are present in the synapses, however, this situation is thrown out of balance. The presence of cholinesterase inhibiting chemicals prevents the breakdown of acetylcholine. Since acetylcholinesterase is the enzyme that

degrades acetylcholine following stimulation of a nerve, its inhibition allows acetylcholine to accumulate and result in initial excessive stimulation followed by depression (EXTOXNET TIBs - Cholinesterase Inhibition, 1993).

The mechanism of action of OPs, on both target and nontarget species, is irreversible inhibition of acetylcholinesterase (Eskenazi and Maizlish, 1988). Acetylcholinesterase is found in red blood cells and in nicotinic and muscarinic receptors in nerve, muscle, and gray matter of the brain. Plasma acetylcholinesterase is found in CNS white matter, pancreas, and heart. It is a hepatic acute phase protein that often is decreased in liver dysfunction, malnutrition, neoplastic disease, pregnancy, and infectious processes as well as in narcotic or cocaine use. Decrease in plasma cholinesterase results in a decrease of cholinesterase activity in the central, parasympathetic, and sympathetic nervous systems.

Organophosphates phosphorylate the serine hydroxyl group at the site of action of acetylcholine. They bind irreversibly, deactivating the esterase and resulting in accumulation of acetylcholine at the endplate (Mileson et al., 1998). Accumulation of acetylcholine at the neuromuscular junction causes persistent depolarization of skeletal muscle, resulting in weakness and fasciculations. In the central nervous system, neural transmission is disrupted. In addition to the anti-acetylcholinesterase activity, some OPs may have carcinogenic activity such as dichlorvos (U.S.EPA. 1988a. Dichlorvos) and hexaethyl tetraphosphate.

3. Reduced Sulfur Species in the Natural Environments

Our research is focused on the investigation of the chemical fate of selected OPs in the reduced sulfuric environment under anoxic conditions. To understand the objective of our research, it is very important to know the occurrence of OPs in the natural environments containing reduced sulfur species. The pesticides already present in the surface water may associate with particles and can eventually become a part of the sediment phase. It is also likely that some pesticides are transported into salt marshes and into the bottom layer of estuaries. In sediment, salt marshes and the bottom layer of estuaries, anoxic conditions are typically prevalent. Transformation processes occurring under anoxic conditions may represent an important sink for pesticides. Anoxic conditions can give rise to high concentration of reduced sulfur species, which are versatile environmental "reagent" and are capable of reacting with a wide array of organic pollutants. Our laboratory approach is conducted in order to simulate environmental conditions.

It has been reported that inorganic and organic sulfur species are the most potent nucleophiles present in the environment (Barbash and Reinhard, 1989a; Barbash and Reinhard, 1989b; Haag et al., 1991). The potential therefore exists for such highly reactive reduced sulfur nucleophiles to serve as environmental "reagents" affecting the abiotic degradation of OPs. The most common sulfur nucleophiles encountered in natural waters are the following species: H_2S, HS^-, thiolate anions (RS^-), polysulfide (S_n^{2-}, where n>1), $S_2O_3^{2-}$, $S_4O_6^{2-}$, and SO_3^{2-}. Unlike sulfate, all of these nucleophiles are thermodynamically unstable in the presence of O_2. Hence, they are most commonly found in hypoxic environments

(i.e. natural waters containing very low or undetectable level of dissolved O_2), usually in the presence of high concentration of reduced organic matter. Environments of this type include marine, estuarine, and marsh porewaters, groundwaters containing high concentrations of leachate derived from domestic refuse (e.g., beneath landfills), and hydrogeologic zones located far down-gradient from their recharge areas. The speciation of sulfur among its various forms in a particular environment arises from a balance among several simultaneous chemical and biochemical processes (usually with microbiological mediation), including oxidation and reduction, hydrolysis, dissolution, and precipitation. The bacterial reduction of sulfate yields hydrogen sulfide (H_2S) (Stumm and Morgan, 1981), and hence HS^- and S^{2-}, as well, which are referred to collectively as $H_2S(T)$. Species which are partially reduced (i.e. forms in which sulfur exhibits an oxidation state between those of SO_4^{2-} (+VI) and $H_2S(T)$ (-II), such as S_n^{2-}, $S_2O_3^{2-}$, $S_4O_6^{2-}$, and SO_3^{2-} may be produced by the oxidation of $H_2S(T)$ and sulfide minerals, the reductive dissolution of goethite by HS^-, the hydrolysis of polysulfides, and microbial process (Stumm and Morgan, 1981; Boulegue et al., 1982; Luther et al., 1985; Pyzik and Sommer, 1981). Thiols may be produced biologically as results of sulfate reductions, biodegradation of organic matter or lithotrophic oxidation (i.e. the biological oxidation of inorganic compounds to obtain energy) (Brock et al. 1984); or abiotically through the reactions of dissolved organic matter with $H_2S(T)$ or elemental sulfur (Boulegue et al., 1982; Mopper and Taylor, 1986).

The concurrent operation of several of these processes in a particular environment may rise to a complex assemblage of sulfur nucleophiles. For example, Boulegue and his cowaorkers detected $H_2S(T)$, S_8, $S_2O_3^{2-}$, SO_3^{2-},S_n^{2-}, SO_4^{2-}, thiols, and organic polysulfides in the porewaters of a salt marsh along the Delaware estuary (Boulegue et al., 1982). They attributed the observed sulfur speciation to a steady-state interaction between the various reduced sulfur species diffusing upward from hypoxic sediments and O_2 diffusing downward from the sediment-water interface.

In this study, we focus on the reaction of OPs with reduced sulfur species in the aqueous solution under anoxic condition. The reduced sulfur species discussed here include $H_2S[T]$, S_n^{2-}, $S_2O_3^{2-}$ and PhSH(T) (PhSH and PhS^-). The selection of the investigated reduced sulfur species is based on their concentrations in the natural surrounding and their reactivity. The presence of reduced sulfur compounds in marine sediments has been the focus of a number of studies (Barbash and Reinhard, 1989a; MacCrehan and Shea, 1995; Boulegue et al., 1982; Berner, 1984; Schenau et al., 2002). When oxygen and nitrate are depleted, sulfate (abundant in seawater, but limited in fresh water) becomes the primary oxidant used for the bacterial diagenesis of organic detritus, which result in the formation of hydrogen sulfide. Subsequent reaction of HS^- with S_8, partial HS^- oxidation, or partial S(0) reduction gives rise to polysulfides, which are more highly reactive nucleophiles than HS^- (Reaction 1).

$$n\ S(0) + HS^- \rightleftharpoons S_{n+1}^{2-} + H^+ \quad (1)$$

The S_8 ring is cleaved by nucleophilic attack of HS^-. Much less polysulfide is formed at pH values below the pK_a of H_2S. Tetrasulfide (S_4^{2-}) and pentsulfide (S_5^{2-}) are the predominant species of polysulfide at pH > 6. Tetrasulfide and pentasulfide dismutate rapidly according to Reaction 2 (Giggenbach, 1972).

$$3\ S_5^{2-} + HS^- \rightleftharpoons 4\ S_4^{2-} + H^+ \quad (2)$$

Due to the velocity of Reaction 2, it is not known whether S_4^{2-} or S_5^{2-} is the preferred substrate of polysulfide reductase (Hedderich et al., 1999). For the same reason, the product of polysulfide reduction is not known. It is assumed that only one sulfur atom is cleaved from the polysulfide chain during reduction (Reaction 3).

$$H_2 + S_n^{2-} \rightleftharpoons HS^- + S_{n-1}^{2-} + H^+ \quad (3)$$

In very highly alkaline solution, S_5^{2-} has a lower concentration relative to the other polysulfide species. The relatively slow rate of polysulfide decomposition in highly alkaline solutions might be contributed to the decompositions via the pentasulfide species (Reaction 4) (Licht and Davis, 1997).

$$S_5^{2-} + 3\ OH^- \rightleftharpoons S_2O_3^{2-} + 3\ HS^- \quad (4)$$

Based the equilibrium distribution discussed by Giggenbach (1972) and Schwarzenbach and Fischer (1960), we can get a sample distribution of sulfur species over pH values under the condition of 5 mM $[H_2S]_T$ in presence of excess

of elemental sulfur. (Figure 1.2) The figure demonstrates that at pH < 6, H_2S is the predominant species in the aqueous solution. As pH increases, the portion of HS^- increases and reaches the maximum at pH ≈ 8. When pH > 9, polysulfide is the predominant species and only trace of bisulfide is present in the solution. The much lower proton dissociation constants of S_4^{2-} and S_5^{2-} (Schwarzenbach and Fischer, 1960) would result into the very low concentrations of HS_4^- and HS_5^- in solution. Therefore, in the system containing bisulfide and S(0), bisulfide and polysulfides are of much more importance than other species.

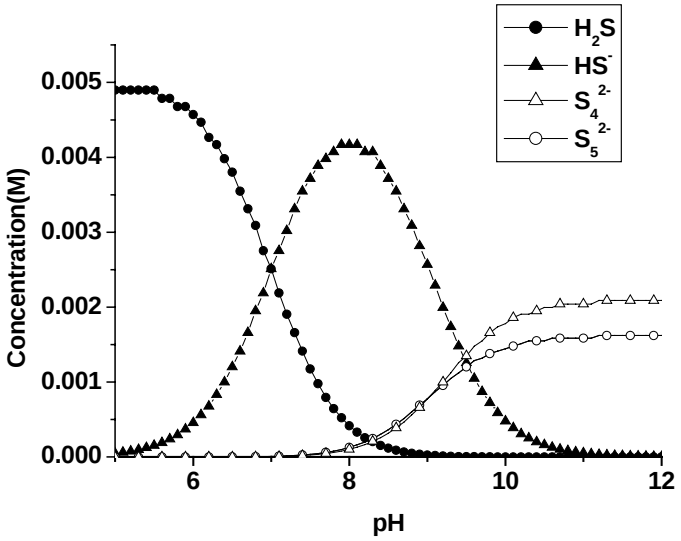

Figure 1.2 Calculated distribution of hydrogen sulfide/polysulfide species over pH 5 – 10. Assumptions: 5 mM $[H_2S]_T$ in equilibrium with excess elemental sulfur; based on equilibrium constants reported by Giggenbach (1972) and Schwarzenbach and Fischer (1960). S^{2-}, HS_4^- and HS_5^- have been included in the

calculations, but their concentrations are so small that they have been neglected in the figure.

Polysulfides are frequently employed as a 30% aqueous solution in commercial preparation used for agricultural soil conditioning and for fungal, mite, and insect control (Kohn et al., 1992). Elemental sulfur is also commonly added to soil in order to take advantage of its fungicidal quantities as well as its role as essential nutrients. Under hypoxic conditions, this elemental sulfur could undergo dissimilatory reduction by soil macroorganisms to generate polysulfides and bisulfide (Hedderich et al., 1998). Sediment thiosulfate may result from the abiotic reaction of elemental sulfur and sulfite. Thiosulfate is also produced by the oxidation of pyrite (FeS_2) under oxic condition. Many anaerobic sediment bacteria, which lack the ability to reduce sulfate directly, can instead use sulfur compounds of lower oxidation state, such as SO_3^{2-}, $S_2O_3^{2-}$ and S(0) as electron acceptors to produce HS^-.

The occurrence of organic sulfur compounds in the sediments was also reported (Damsté et al., 1989; Adam et al., 1998; Hofmann et al., 1993). Organic sulfur compounds are often abundant in sediment. As stated above, the anoxic environments are favorable for development of microorganisms implied in the formation of inorganic reduced sulfur species, which are liable to react with organic matter to produce low molecular weight organic sulfur compounds and macromolecules reticulated by sulfur. The mechanisms involved in the interaction between organic matter and inorganic sulfur species are still the

subject of many investigations (Brassell et al., 1986; Damsté et al., 1987, 1989; Kohnen et al., 1993). The paleoenvironments of the sediments were anoxic and H_2S has probably exceeded the amount of available iron. These conditions resulted in a sulfur of free H_2S, which reacted with organic matter, leading to the formation of organic sulfur species such as thiolanes, thianes, thiophenes, and so on (Damsté et al., 1989; Calvert and Karlin, 1991). Besides the addition of elemental sulfur and anionic sulfur species on organic matter (Schouten et al., 1993; Krein and Aizenshata, 1994; Rowland et al., 1993), a radical mechanism involving H_2S and elemental sulfur could also be considered as an effective process for the formation of organic sulfur entities. Radicals implied in the incorporation of sulfur into organic matter may be formed by various ways. For instance, the radicals present in humic substances could quench hydrogen from thiols or H_2S, leading to formation of sulfur radical (Senesi and Steelink, 1989*)*. Alternatively, photochemically–induced radical formation could be a potential process in natural environments (Adam, 1998).

4. Current Research Review

Despite the wide use of OPs, there are still few data available on the reactivity of such compounds in the aqueous solution. In addition, rate constants reported for a given compound often differ much between different authors. The degradations of OPs in water can occur via many pathways and are *in vivo* susceptible to all the normal degradation reaction such as salt formation, oxidation, hydrolysis, reduction, photodegradation, etc. The degradation of OPs and their kinetics in

aerobic aqueous solutions has been reported extensively (Meikle and Youngson, 1978; Holden et al., 2001; Liu et al., 2001; Kamiya and Kameyama, 2001). Oxidation of OPs can lead to the formation of the corresponding oxonates, sulfones, and sulfoxides. Photodegradation can occur either by a direct photolysis or by indirect photolysis, whereby dissolved humic and fulvic acids can act as a sensitizer (Noblet et al, 1996; Kamiya and Kameyama, 2001). Hydrolysis of OPs is perhaps the most thoroughly studied process. It can occur by a homogeneous mechanism, where H_2O and OH^- act as nucleophiles. Alternatively, some OPs are transformed through surface-catalyzed hydrolysis on particles. Research focusing on the chemical fate of OPs in the aquatic environment dates back to the 1950s and 1960s. Muhlmann (1957) and Faust and Gomaa (1972) studied the hydrolytic degradation of OPs and related the rate of hydrolysis with the OP molecular structure. Mortland (1967) and his coworkers investigated the influence of selected metal ions on the hydrolysis half-life of diazinon and other OPs in 1967. It has been shown that dissolved metal ions enhance the rate of hydrolysis by catalysis (e.g., Cu^{2+} and Pb^{2+} for chlorpyrifos-methyl, zinophos, diazinon, parathion-methyl, and fenchlorphos) (Smolen and Stone, 1997). Heterogeneous surfaces such as Fe and Al oxides and different clays can enhance the rate of hydrolysis by providing surface sites at which the nucleophiles and the OPs can react (Racke et al., 1996). Wolfe carried out a comprehensive study on the degradation of malathion in water (Wolfe et al. 1977). Wanner and co-works studied the fate of selected OPs in the Rhine River ecosystem after a chemical fire

in Basel, Switzerland, in 1986 (Wanner et al., 1989), and the subsequent release of a variety of chemicals into the Rhine River. Wang and Hoffman (1991) investigated the degradation of OPs in the coastal water. Fong and Pehkonen studied the degradation pathway and product of hydrolysis of phorate and terbufos in the simulated natural environment (Hong and Pehkonen, 1998; Hong et al., 2000 & 2001).

When trying to understand the reactivity of phosphate and thiophosphate esters, it is important to realize that such compounds may react like alkyl halides by nucleophilic displacement (S_N2) both at the phosphorus atom (with an alcohol moiety being the leaving group) and at the carbon bound to the oxygen of an alcohol moiety (with the diester being the leaving group) (Schwarzenbach et al., 2003). When dealing with phosphoric and thiophosphoric acid derivatives, we have to be aware that under different conditions, different mechanism may predominate.

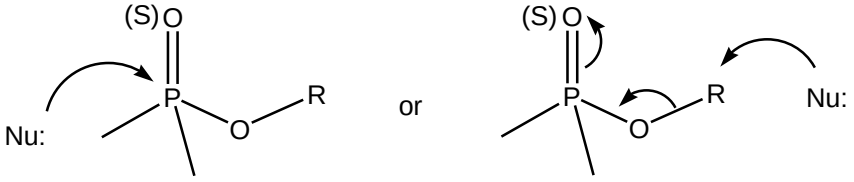

Figure 1.3 Possible nucleophilic attacks at OPs

The reaction at the phosphorus atom is postulated to occur by an S_N2 (no intermediate formed) rather than by an addition mechanism such as encountered with carboxylic acid derivatives (Kirby and Warren, 1967). For attack at a

saturated carbon atom, OH^- is a better nucleophile than H_2O by about a factor of 10^4. Toward phosphorus, which is a harder electrophilic center, however, the relative nucelophilicity increase dramatically. Consequently, the base-catalyzed reaction generally occurs at the phosphorus atom leading to the dissociation of the alcohol moiety that is the best leaving group (P-O cleavage).

Depending on the alcohol moieties present, the neutral reaction as well as reaction with soft nucleophiles (e.g., HS^-, PhS^-, CN^-) may also proceeded by nucleophilic substitution at a carbon atom (C-O cleavage). If such a reaction occurs, methyl esters will react faster than corresponding ethyl or other primary alkyl esters. Note that if a good leaving group is present, the neutral reaction may proceed by both reaction mechanisms, that is, C-O as well as P-O cleavage.

In most cases, hydrolysis is quite insensitive to acid catalysis unless there is a base function present in one of the alcohol moieties. If such a base is protonated, the reactivity is enhanced. Examples are diazoxon and diazinon (Figure 1.4), where protonation of one of the nitrogens of a pyrimidine ring renders the alcohol moiety a much better leaving group. Furthermore, comparison of the relative reactivity of phosphoric and thiophosphoric esters indicates that, the thionates hydrolyze somewhat slowly than the corresponding oxonate esters. This can be explained by the higher eletronegativity of oxygen as compared to sulfur. The presence of oxygen makes the phosphorus atom more electrophilic (enhancement of the reaction at the P atom) as well as the diester a better leaving group (C-O cleavage).

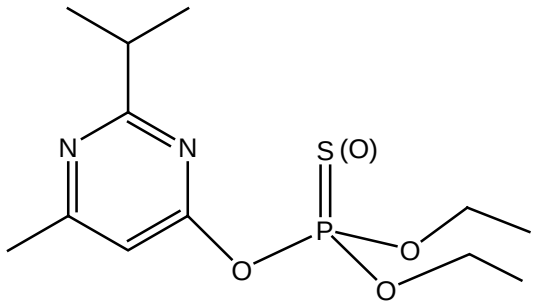

Figure 1.4 Structures of diazinon (diazoxon)

There are quite a few phosphoric and thiophosphoric acid derivatives exhibiting one thioester and two (often identical) ester groups (R_1=R_2=methyl or ethyl). In these cases, the situation is even more complicated. Depending on R_1, R_2, and R_3, the compound may react by P-O, P-S, C-O, and C-S cleavage, giving rise to a variety of possible products. If R_1 and R_2 are methyl or ethyl, the base-catalyzed reaction generally occurs by P-S cleavage with –S-R_3 being the leaving group. The neutral reaction as well as the reaction with soft nucleophiles, however, may proceed by cleavage of P-S, C-O, or C-S, each alone or in combination. The C-S cleavage may preferably occur if the R_3 moiety contains a nucleophilic group, which, by internal nucleophilic attack (S_Ni) may favor this reaction pathway. Such internal attacks accelerate the overall disappearance rate of the compound. In demeton-S, thiometon and disulfoton, a sulfur atom can serve as an internal nucelophile (Figure 1.5) (Schwarzenbach et al., 2003; Wanner, 1989). When R_3 group contains halogen atoms, there also exists the possibility of dehalogenation through nucleophilic substitution or nucleophile-induced elimination.

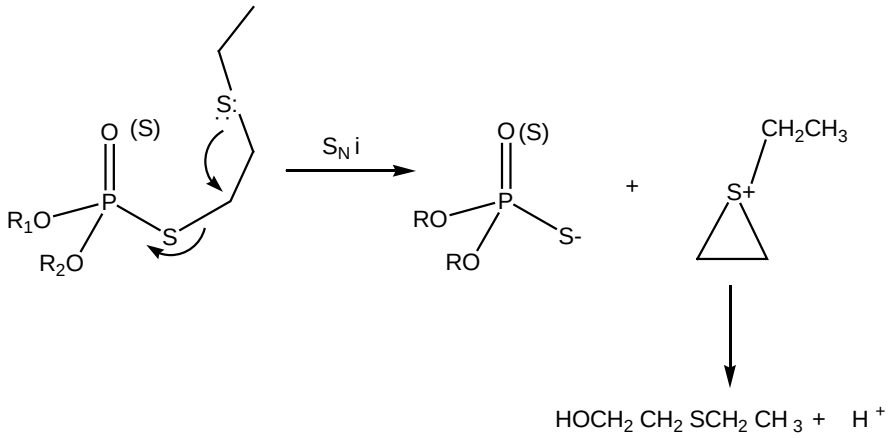

Figure 1.5 S_N i reaction for demeton-S, thiometon and disulfoton

Some investigators have shown that abiotic process can control the fate of organic contaminants under anaerobic conditions (Roberts and Gschwend, 1994; Weber, and Wolfe, 1987). It is possible that OPs undergo significant transformation under anoxic conditions by chemical rather than microbial process. The possible transformation processes are compound specific. Based on these findings of hydrolysis, it is hypothesized that OPs are likely to undergo a displacement reaction with sulfur nucleophile either with the attack occurring at α-carbon of alkoxy group or with the attack occurring at the central P atom. According to the principle of the hard-soft acid and base (Pearson and Songstadt, 1967), the later reaction would not readily happen. In addition, the specific structures of some OPs might result in the high reactivity on these specific sites, which would lead to the nucleophilic attack of sulfur nucleophiles occuring at these specific sites of the OPs and other reactions such as elimination induced by sulfur nucleophiles.

Chapter II

Experimental

1. Preparation

1.1. Reaction System

Our laboratory experiments are designed to simulate the natural conditions. To investigate the role of reduced sulfur species in the degradation of OPs, the experimental system is simplified to neglect the influence from other environmental factors. Therefore, the experiments were carried out in clean batch system under anoxic conditions.

All the reaction solutions were prepared in anaerobic glovebox (5% H_2, 95% N_2) and aqueous solutions were prepared from argon-purged deionized water (DW) (Mill-Q gradient system, Millipore, Bedford, MA). Glassware used with sulfidic solutions was washed with methanol/NaOH to remove traces of sulfur impurity before acid washing. All glassware was soaked in 1 M HNO_3 overnight, rinsed several times by deionized water, and dried at 200 ºC before use.

1.2. Preparation of Solution

1.2.1. Sodium sulfide stock solution

Sodium sulfide stock solutions were prepared under argon from $Na_2S{\cdot}9H_2O$ crystals (98%; EM Science) using deoxygenated distilled water accoding to the procedure described by Jans and Miah (2003). Crystals were rinsed with Ar-

purged water to remove surface oxidation products, blotted with cellulose wipe, and were then transferred to an Ar-purged three-necked flask. The flask was then connected to an Ar-purged closed glassware system consisting of a reservoir (containing distilled water), glass tubing, stopcocks and an argon tank. Before re-routing the argon flow and forcing the reservoir content into the flask containing the washed sodium sulfide crystals, the distilled water was purged with argon for one hour. Then the sodium sulfide stock solutions were transferred in the anaerobic chamber.

1.2.2. Polysulfide stock solution

Polysulfide stock solution was prepared in 100 mM borate buffer. Na_2S_4 crystal (Na_2S_4, 90% technical grade; Alfa Aesar) was grinded into powder in the mortar in the anaerobic glovebox and washed with deoxygenated toluene to remove sulfur. After decanting toluene, the powder was completely dried over argon. The treated powder was dissolved in prepared deoxygenated buffer (50 mM tetraborate buffer containing 100 mM NaCl) and stocked in the brown bottle to avoid the exposure to light. The polysulfide stock solutions were kept in the anaerobic chamber.

1.2.3. Thiophenol stock solution

The stock solution of ~100 mM thiophenol was prepared by dissolving thiophenol (99%, Lancaster Synthesis, Pelham, NH) in deoxygenated methanol and stored in glove box.

1.2.4. Pesticides stock and standard solutions

The stock solutions of pesticides were prepared by dissolving exactly weighed pesticides in deoxygenated methanol or ethyl acetate in volumetric flask and stored in brown bottle in glovebox. A series of standard solutions of pesticides were prepared by diluting the pesticides stock solution into methanol.

1.2.5. Reaction buffer

The reaction solutions containing bisulfide, polysulfide and thiophenol were prepared by dilution of the prepared stock solution into pH buffer (50 mM phosphate or tetraborate buffer, containing 100 mM NaCl, and 5% methanol). 5 % methanol was added into the reaction solution to improve the solubility of organophosphorus pesticides and thiophenol in the aqueous solution. The reaction solution containing thiosulfate was prepared by dissolving the $Na_2S_2O_3$ crystal directly into the pH buffer.

2. Experiment Setup and Sampling

The reaction solution was prepared and equilibrated overnight in the glovebox and transferred into a 20 mL syringe equipped with a polycarbonate stopcock and a PTFE needle tubing and preequilibrated at selected temperatures. Four glass rings were placed in the syringe to facilitate mixing of the reaction solution. Reactions were initiated by spiking the stock solution of the pesticides into the syringe and vigorously mixing for 30 seconds in the glovebox. The experimental setup is shown in Figure 2.1. The reaction mixtures were maintained anoxic and

the reactor syringes were incubated in a water bath at selected temperatures. During the reaction, ~ 10 samples were taken by spiking aliquots (~ 1 mL) of the reaction mixture into the test tubes containing ~1 mL ethyl acetate and 2-3 drops of 6 M HCl was added. The extraction served to quench the reaction. The resulting extracts were stored in the refrigerator and were subjected to later GC analysis.

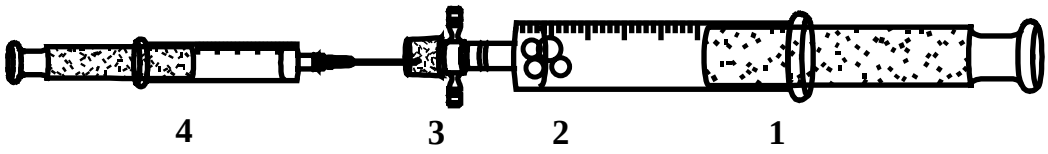

1. 20 mL syringe containing reduced sulfur species reaction solution.

2. four glass rings.

3. polycarbonate stopcock.

4.100 μL syringe containing stock solution of pesticide

Figure 2.1 Experimental setup: Spiking the stock solution of pesticides into the syringe containing reduced sulfur species reaction solution.

3. Analysis

3.1. Sulfur Measurement

The thermodynamics and kinetics of the H_2S/HS^- system in natural waters have been investigated in detail (Millero, 1986). pK_a of H_2S has been examined as function of temperature and salinity. In our experiments, the total hydrogen sulfide concentration ($[H_2S]_T$), the sum of all hydrogen sulfide species ($[H_2S]$ +

$[HS^-] + [S^{2-}]$), total thiophenol concentration ($[PhSH]_T$), the sum of [PhSH] and $[PhS^-]$, total S(II) concentration ($[S(II)]_T$), the sum of $[H_2S]_T$ and $[H_2S_n]_T$ ($[S_n^{2-}]$+ $[HS_n^-] + [H_2S_n]$, n = 2 – 5), in polysulfide solutions and thiosulfate concentration ($[S_2O_3^{2-}]$) were determined by iodometric titration using a starch endpoint. An Accument pH meter (Fisher Scientific, Pittsburgh, PA) with a Ross combination pH electrode (ThermoOrion, Beverly, MA) was used to measure the pH value in the reduced sulfur reaction solutions. Bisulfide and hydrogen sulfide concentrations were computed from $[H_2S]_T$ and measured pH values via ionization constants for H_2S reported by Millero (1986) that were corrected for ionic strength using activity coefficients γ_{HS^-} and $\gamma_{S^{2-}}$ determined from the Davies approximation using MacμQL 2.0. Thiophenolate and thiophenol ion concentrations were determined via the same way as $[HS^-]$ and $[H_2S]$ from $[PhSH]_T$ and the measured pH values. pK_a of thiophenol was reported to be 6.50 at 25 ^oC (Dean, 1985). The chemistry of aqueous polysulfide solution is complex. The equilibria between polysulfide ions in aqueous solution can generally be described by the equation:

$$(n\text{-}1)\ S_{n+1}^{2-} + HS^- + OH^- \rightleftharpoons n\ S_n^{2-} + H_2O \qquad n = 2 - 5 \qquad (1)$$

To the best of our knowledge, methods appropriate for determining concentrations of individual polysulfide species in complex matrixes have not been developed. In some studies, polysulfide concentrations were determined by the triphenylphosphine method previously developed by Borchardt and Easty

(1984), in which the total concentration of polysulfide was determined via the concentration of the dissolved sulfur(0). In our research, the total concentrations of polysulfide dianions, $\Sigma[S_n^{2-}]$, were determined via the speciation calculations from the measured $[S(II)]_T$ and pH values based on the reported equilibrium constants (Giggenbach, 1972; Schwarzenbach, 1960). Based on the assumption that polysulfides are very reactive species and no significant difference exists for the reactivity of individual polysulfide ions, the total polysulfide ions can be treated as one species in the investigation of kinetics of the reaction with polysulfide. $S_2O_3^{2-}$ is the only dominant species in the investigated pH range in this study, $[S_2O_3^{2-}]$ is equal to the concentration directly determined by titration.

3.2. Chromatographic Analysis

Ethyl acetate or hexane extracts were analyzed on a Fisons GC 8000 equipped with an AS 800 autosampler, a FID-80 flame ionization detector (Carlo Erba Instruments) or ECD-80 electron capture detector (Carlo Erba Instruments) containing ^{63}Ni beta emitting radioactive source of 370 MBq (10 mCi), a split/splitless injector and a 30 m DB-5, 0.25 mm i.d. × 0.25 μm fused-silica capillary column (J&W, Folsom, CA). The carrier gas was helium (99.999%). A Trio1000 quadrupole GC/MS system (Fisons Instruments) to identify and analyze the degradation products was equipped with a split/splitless injector and a 30 m AT-5ms, 0.25 mm i.d. × 0.25 μm fused-silica capillary column (Alltech, Deerfield, IL). EI mass spectra were generated using electron energy of 70 eV, monitoring for ions *m/z* 35-500 in full-scan and selected ion recording (SIR) modes. The

source temperature employed for the ionization technique was 200 ºC. Temperature programs are specific for each pesticide samples.

4. Kinetics model

Kinetics of most experiments in this study were determined assuming a pseudo-first-order reaction model, with the initial concentrations of pesticides much lower than that of reduced sulfur species. Noted that the second-order reaction model would be applied when the concentration of sulfur species is not high enough to meet the pseudo-first-order reaction assumption. Time courses were allowed to progress over approximately 2 half-lives. Pseudo-first-order rate constants (k_{obs}) were determined by regressing the natural logarithm of pesticide concentrations versus reaction time. The second-order rate constants can be obtained from the measured pseudo-first-order constants at varying concentration of the sulfur species. When the second-order reaction model is applied, the second-order rate constant can be obtained as the average of the second-order rate constants extracted from each experiment. For selected experiments, first-order rate constants of disappearance of parent compounds and formation of the products were determined by fitting observed data for parent compounds and reaction products to numerically integrated solutions of the system of governing differential rate expressions using *Scientist for Windows* v. 2.01 (MicroMath Scientific Software, Salt Lake City, UT).

Chapter III

Degradation of Thiometon and Disulfoton

1. Introduction

Thiometon and its ethyl analog, disulfoton, are systemic insecticides and acaricide belonging to the phosphorodithiolate subgroup. Thiometon is effective against sucking insects, mainly aphids, and mites on most crops. About 1.2 million pounds of disulfoton are used annually in United States, most of which is applied to cotton, wheat, potatoes, and tobacco (U.S.EPA, 2000, disulfoton summary). Asparagus and Christmas trees are also important use sites, with 40 and 65% of acres treated with disulfoton, respectively (U.S.EPA, 2000, disulfoton summary). Thiometon and disulfoton enter the environment primarily during their uses as insecide/acricide in crops and vegetables, and in homes and gardens. The processes that may introduce the pesticides to aquatic environmental media include leaching to groundwater and runoff to surface water (Holden, 1986; Mostaghimi et al., 1993; Nash, 1974; Plumb, 1991). Biotransformation, abiotic hydrolysis, to a lesser extent, sensitized oxidation are principally responbile for the loss of the pesticides from water (Capel et al., 1988; Mossman et al., 1988; Wanner et al., 1989). Wanner and coworkers reported a model prediction of the concentration-time courses of thiometon and disulfoton in the Rhine River (Wanner et al., 1989), concluding that biotransformation and abiotic reactions are important processes in the reduction of the total load from the river. The fate of

thiometon and disulfoton, once in the surface water and sediments, and the likely concentration therein, is very difficult to be modeled with the high degree of certainty since only few data are available for the aerobic and anaerobia aquatic degradation rates. There are only few studies available on the reactivity of organophosphorus compounds in aquatic systems despite their prevalence in the environment. Direct photolysis of thiometon and disulfoton is negligible, since the two compounds do not significantly absorb sunlight, while indirect photolysis can play a role in the degradation (Wanner et al., 1989; Gohre and Miller, 1986).

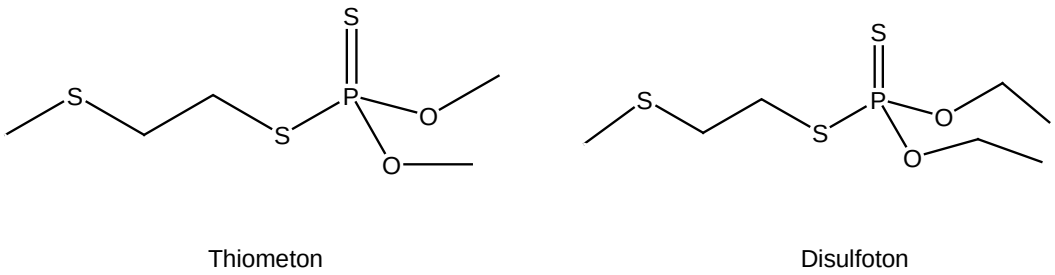

Figure 3.1 Structures of thiometon and disulfoton

Reduced sulfur species are versatile environmental reagent capable of reacting with a wide array of pollutants, including many organic contaminants that undergo nucleophilic substitution and dehalogenation. In recent years, the degradation of organic contaminants in the presence of reduced sulfur species has received increasing attention because of the reactivity of the reduced sulfur species and their occurrence in aquatic environments (Roberts et al., 1992; Miller et al., 1998; Loch et al.; 2002; Lippa and Roberts, 2002; Jans and Miah, 2003; Lippa et al., 2004; Gan et al., 2006; Wu and Jans, 2006). In addition to the

reaction with reduced sulfur species, hydrolysis (reaction with H_2O & OH^-) is a competing reaction. The most likely hydrolysis mechanisms for thiometon and disulfoton were summarized by Wanner and coworkers (Wanner et al., 1989). Based on the principle of hard and soft acid and bases (Pearson and Songstadt, 1967), the mechanism of the reactions of thiometon and disulfoton in the aqueous solutions containing reduced sulfur species are postulated (Scheme 3.1). The important pathways of the reaction of thiometon and disulfoton can be the nucleophilic attack by OH^-/H_2O on the phosphorus atom leading to the breakage of the P-S bond (Pathway I) and O-dealkylation of the side chain (Pathway II). At the same time, there is also the possibility of nucleophilic displacment at the 2-(ethylthio)ethyl group, which can be intramolecular and/or intermolecular (Pathway III).

I)

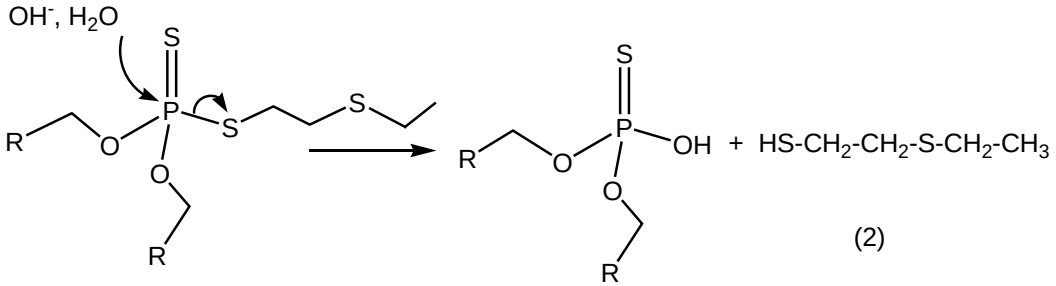

(1) (2)

1a. R=H, thiometon
1b. R=CH_3, disulfoton

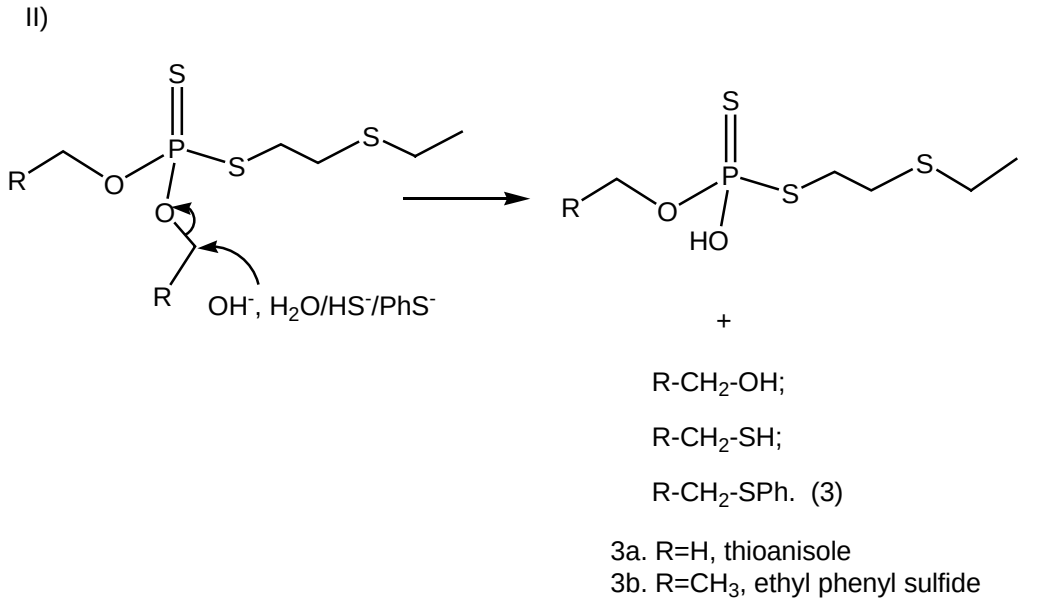

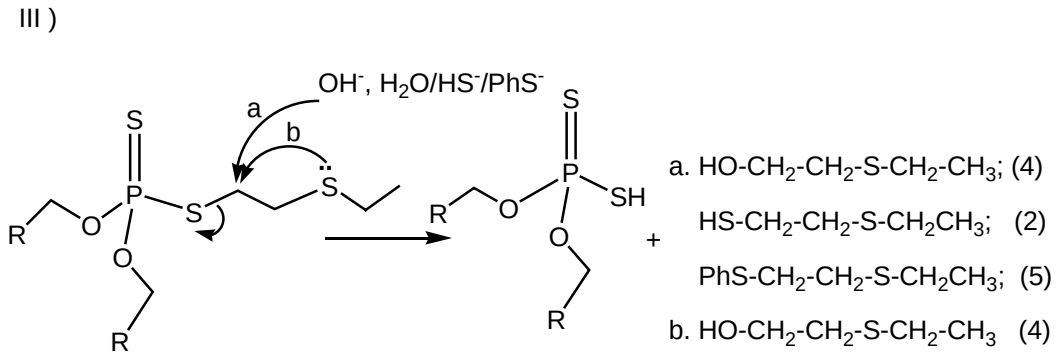

Scheme 3.1 Possible mechanisms of the reaction of thiometon and disulfoton in pH buffer containing reduced sulfur species. I: Nucleophilic attack on phosphorus atom leading to the breakage of P-S bond. II: O-dealkylation of the side chain III: Nucleophilic displacment at the 2-(ethylthio)ethyl group, including intermolecular (a) and intromolecular attack (b).

This chapter is focused on the chemical transformation of thiometon and disulfoton in simulated natural sulfidic environments. The primary purpose of the

research was to determine the role of reduced sulfur species in promoting the transformation of thiometon and disulfoton and to identify the degradation products. Kinetic and thermodynamic studies are the two most important tools for the elucidation of reaction mechanisms besides product identification. Reactions were monitored at varying concentrations of reduced sulfur species including bisulfide (HS^-), thiophenolate (PhS^-), polysulfide (S_n^{2-}) and thiosulfate ($S_2O_3^{2-}$) so as to obtain the second-order reaction rate constant and compare the reactivity of different sulfur species. The activation parameters were investigated via the temperature dependence of the reaction rate constants of thiometon and disulfoton with bisulfide. This study also represents an experimental investigation of substituent effects on reactivity and reaction mechanism. The subtle difference in structure may result in drastic differences in reactivity and even mechanism. Studies of the structural analogs can provide invaluable, though indirect and unclear, information regarding the mechanisms through which the pesticides react with the reduced sulfur species.

2. Materials and Methods

2.1. Chemicals

All chemicals were used as received. Thiometon (S-2-ethylthioethyl O,O-dimethyl phosphorodithioate; 95.0%) and disulfoton (S-2-ethylthioethyl O,O-diethyl phosphorodithioate; 99.1%) were obtained from Chem Service (West Chester, PA). 2-(ethylthio)ethanol, thioanisole and were obtained from TCI (Portland, OR). 2-chloroethyl ethyl sulfide was obtained from TCI (Tokyo, Japan).

And ethyl phenyl sulfide was obtained from Avocado Research Chemicals (Heysham, Lancashire, England). 2-(ethylthio)ethanethiol was prepared from 2-chloroethyl ethyl sulfide in our lab according to the method reported by Furukawa (1984). All solvents and reagents that were used were analytical grade or equivalent. Ethyl acetate and methanol were HPLC grade and were obtained from Fisher Scientific (Pittsburgh, PA). All the reaction solutions were prepared in an anaerobic glovebox (5% H_2, 95% N_2) and aqueous solutions were prepared from argon-purged deionized water (DW) (Milli-Q gradient system, Millipore, Bedford, MA).

2.2. Preparation of 2-(ethylthio)ethanethiol.

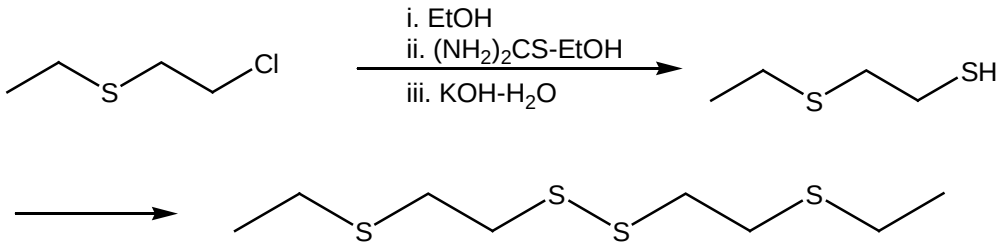

Scheme 3.2 Synthesis of 2-(ethylthio)ethanethiol

A solution of 2-chloroethyl ethyl sulfide (0.01 mol, 1.25g) in 30 mL ethanol was added to thiourea (0.012 mol, 0.92g) and heated for 24 hours under reflux. After concentration of the solution with a Turbovap 500 (Zymark Corp.), potassium hydroxide (0.071 mol, 4g) in 40 mL distilled water was added to the residue. The resulting mixture was refluxed for 5 hours under nitrogen and then cooled in ice-water bath. Cooled aqueous sulfuric acid was added dropwise until

the mixture was acidic. After the addition of acid, the reaction mixture was extracted with chloroform and dried over $MgSO_4$. After removal of the solvent, the residue was distilled under vacuum to obtain a colorless liquid. In the standard solutions prepared in methanol, 2-(ethylthio)ethanethiol was entirely present as dimer, 2-(ethylthio)ethyl disulfide.

2.3. Experimental System

The starting concentration of thiometon and disulfoton were ~ 30 μM. The concentrations of $[H_2S]_T$, $[PhSH]_T$ and $[S(II)]_T$ in the reaction with thiometon were 4.3 – 10.3 mM, 1.2 – 3.5 mM and 4.2 – 7.6 mM, respectively. And these concentrations in the reaction with disulfoton were 5.2 – 25 mM, 1.2 – 2.6 mM and 2.2 – 16.5 mM, respectively.

2.4. Chromatographic Analysis

Ethyl acetate extracts were analyzed on a Fisons GC 8000 equipped with an AS 800 autosampler, a FID-80 flame ionization detector (Carlo Erba Instruments), a split/splitless injector and a 30 m DB-5, 0.25 mm i.d. × 0.25 μm fused-silica capillary column (J&W, Folsom, CA). The carrier gas was helium (99.999%). GC/MS system to identify and analyze the degradation products was equipped with a split/splitless injector and 30 m AT-5ms, 0.25 mm i.d. × 0.25 μm fused-silica capillary column (Alltech, Deerfield, IL). EI mass spectra were generated using electron energy of 70 eV, monitoring for ions *m/z* 35-500 in full-scan modes. The source temperature employed for the ionization technique was 200 ºC.

Temperature program: Injector temperature and detector temperature were set at 250 ºC and 275 ºC, respectively. The column temperature was held at 80 ºC for one minute, then increased at a rate of 20 ºC/min to 275 ºC and finally held constant at 275 ºC for 4 minutes.

3. Discussion and Results

3.1. Hydrolysis of Thiometon and Disulfoton in pH Buffer

Hydrolysis is a major removal process for organophosphorus pesticides in the aqueous system. The hydrolysis of thiometon and disulfoton were investigated in aqueous solution at pH 9.20, 50 mM tetraborate buffer or phosphate buffer, 100 mM NaCl or $NaClO_4$ and 5% methanol at 25 ºC and 50 ºC. The influence of chloride ion was explored by comparing the experiments with NaCl and $NaClO_4$. The kinetics data of thiometon hydrolysis display good fit with the pseudo-first-order reaction model. The time courses of the degradation of thiometon in pH 9.20, 50 mM sodium tetraborate buffer, 100 mM NaCl, and 5% methanol at 25 ^{o}C and 50 ^{o}C are shown in the Figure 3.2a and Figure 3.3a. In the experiments, the degradation of thiometon yielded 2-(ethylthio)ethyl disulfide, the dimer of 2-(ethylthio)ethanethiol (2, Scheme 1), which forms readily in the presence of oxygen during the extraction. The formation of 2-(ethylthio)ethyl disulfide accounted for ~70% of the loss of thiometon and resulted from the attack of OH^- /H_2O on the central phosphorus atom (Pathway I) and was quantified with the standard prepared in our lab. At the same time, a small amount of 2-(ethylthio)ethanol (4, Scheme 1) was detected as another degradation product,

which was confirmed with a purchased standard. 2-(ethylthio)ethanol can result from the intramolemular and/or intermolemular nucleophilic attack of OH^-/H_2O at the carbon of 2-(ehtylthio)ethyl group (Pathway III) and accounted for only ~10% of the loss of thiometon. However, accurate quantification is very difficult for 2-(ethylthio)ethanol due to strong tailing of the peak in the chromatography. Comparison experiments were carried out in the pH buffer solution containing $NaClO_4$ rather than NaCl to investigate the influence of chloride ion on the degradation rate of thiometon. The observed rate constant for hydrolysis of thiometon, k_h, was determined to be 0.0032 h^{-1} in pH 9.20, 50 mM sodium tetraborate buffer, 100 mM NaCl, and 5% methanol at 25 °C, while k_h was 0.0022 h^{-1} in the comparing experiment carried out in the buffer solution containing 100 mM $NaClO_4$ instead of NaCl. Although thiometon reacted faster in the presence of Cl^-, no significant increased formation of 2-(ethylthio)ethyl disulfide and 2-(ethylthio)ethanol was observed when compared to the experiment with ClO_4^- (Figure 3.2b). The difference of the two rate constants is attributed to Cl^- acting as a nucleophile (accelerating effect), which accounted for ~30% of the loss of thiometon under the chosen conditions. The mass balance in Figure 3.2a illustrates that the sum of the three possible contributions accounted for almost 100% of the loss of thiometon, in which the accelerating effect of Cl^- is predicted based on the observed difference of disappearance rate of thiometon in the buffer containing NaCl versus $NaClO_4$. The influence from different buffer salts can be ignored since there is no difference observed between experiments in phosphate

buffer versus tetraborate buffer. A relative greater accelerating effect of Cl^- was observed in hydrolysis of thiometon at 50 °C. Based on the formation of 2-(ethylthio)ethyl disulfide, the nucleophilic attack at the central phosphorus atom (Pathway I) accounted for ~ 50% of the loss of thiometon at 50 °C. As for thiometon, the relative importance of Pathway I is larger at low temperature than high temperature. The time course of the degradation of disulfoton in pH 9.20, 50 mM sodium tetraborate buffer, 100 mM NaCl, and 5% methanol at 50 ^oC is shown in Figure 3.4. Hydrolysis of disulfoton is much slower than hydrolysis of thiometon. No accelerating effect of Cl^- on the disappearance rate of disulfoton was observed at 25 °C, while a significant accelerating effect was detected at 50 °C. The contributions from each pathway to the observed rate constants in hydrolysis of thiometon and disulfoton are dramatically different. The much smaller formation of 2-(ethylthio)ethyl disulfide in the hydrolysis experiment of disulfoton compared to the hydrolysis experiment of thiometon suggest that Pathway I in disulfoton is not as important as in thiometon. The accelerating effects of Cl^- was greater at higher temperature than at low temperature. The accelerating effect of Cl^- in hydrolysis of disulfoton is more temperature-dependent than in hydrolysis of thiometon. All of those findings may suggest that the accelerating effect of Cl^- is consistent with a nucleophilic attack of Cl^- at the α-carbon of the alkoxy groups. Such a hypothesis is in agreement with the fact that methyl esters will react faster than corresponding ethyl or other primary alkyl esters in such a reaction (Schwarzenbach et al., 2003). Our hydrolysis rates of

thiometon and disulfoton at 25 ^{o}C in phosphate or tetraborate buffer containing $NaClO_4$ are comparable to the calculated rate constants based on the second-order constants at 20 ^{o}C and activation parameters reported by Wanner et al. (1989).

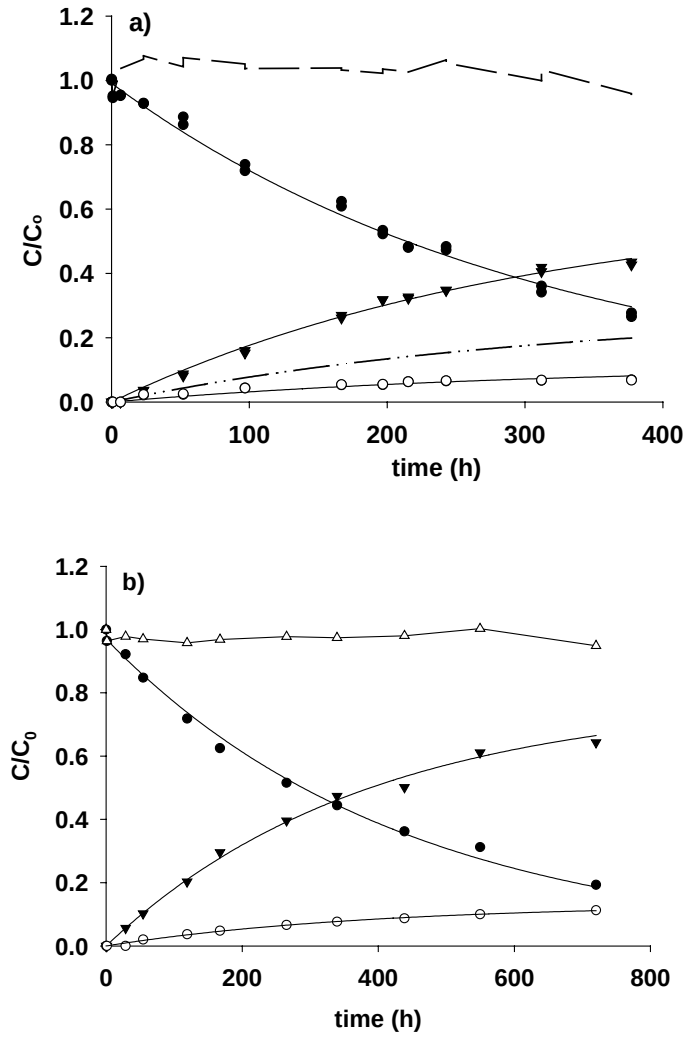

Figure 3.2 a) Hydrolysis of thiometon ([thiometon]$_{initial}$ = 29.8 μM) at pH 9.20 (50 mM tetraborate buffer, 100 mM NaCl, and 5% methanol) at 25 °C, indicating the degradation of thiometon (●, $k_h = 0.0032\ h^{-1}$), the formation of 2-

(ethylthio)ethanethiol (▼, 2 × 2-(ethylthio)ethyl disulfide, 0.0022 h^{-1}), the accelerating effect from Cl^- (—··—··—, 0.00092 h^{-1}), the formation of 2-(ethylthio)ethanol (o, 0.00037 h^{-1}) and the mass balance (- - - -); b) Hydrolysis of thiometon ([thiometon]$_{initial}$ = 30.3 μM) at pH 9.20 (50 mM tetraborate buffer, 100 mM $NaClO_4$, and 5% methanol) at 25 °C, indicating the degradation of thiometon (●, $k_h = 0.0023\ h^{-1}$), the formation of 2-(ethylthio)ethanethiol (▼, 2 × 2-(ethylthio)ethyl disulfide, 0.0020 h^{-1}), the formation of 2-(ethylthio)ethanol (o, 0.00033 h^{-1}) and the mass balance (Δ). Solid lines represent model fits to the data assuming exponential decay of thiometon to multiple degradation products simultaneously.

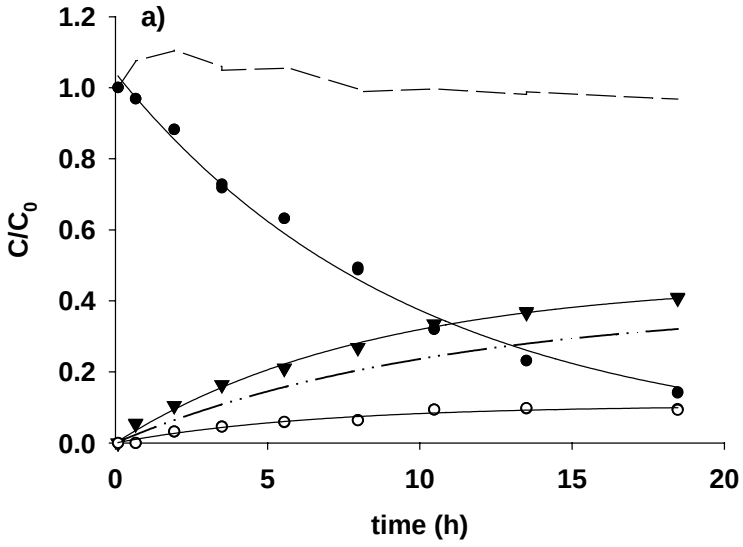

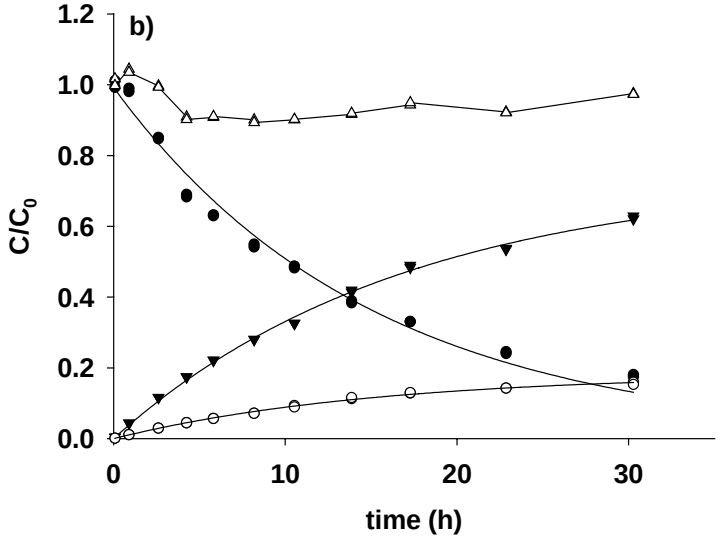

Figure 3.3 a) Hydrolysis of thiometon ([thiometon]$_{initial}$ = 29.2 μM) at pH 9.20 (50 mM tetraborate buffer, 100 mM NaCl, and 5% methanol) at 50 °C, indicating the degradation of thiometon (●, $k_h = 0.103\ h^{-1}$), the formation of 2-(ethylthio)ethanethiol (▼, 2 × 2-(ethylthio)ethyl disulfide, 0.049 h^{-1}), the accelerating effect from Cl^- (—··—··—, 0.037 h^{-1}), the formation of 2-(ethylthio)ethanol (o, 0.013 h^{-1}) and the mass balance (----);b)Hydrolysis of thiometon ([thiometon]$_{initial}$ = 29.5 μM) at pH 9.20 (50 mM tetraborate buffer, 100 mM $NaClO_4$, and 5% methanol) at 50 °C, indicating the degradation of thiometon (●, $k_h = 0.0066\ h^{-1}$), the formation of 2-(ethylthio)ethanethiol (▼, 2 × 2-(ethylthio)ethyl disulfide, 0.047 h^{-1}), the formation of 2-(ethylthio)ethanol (o, 0.012 h^{-1}) and the mass balance (Δ). Solid lines represent model fits to the data

assuming exponential decay of thiometon to multiple degradation products simultaneously.

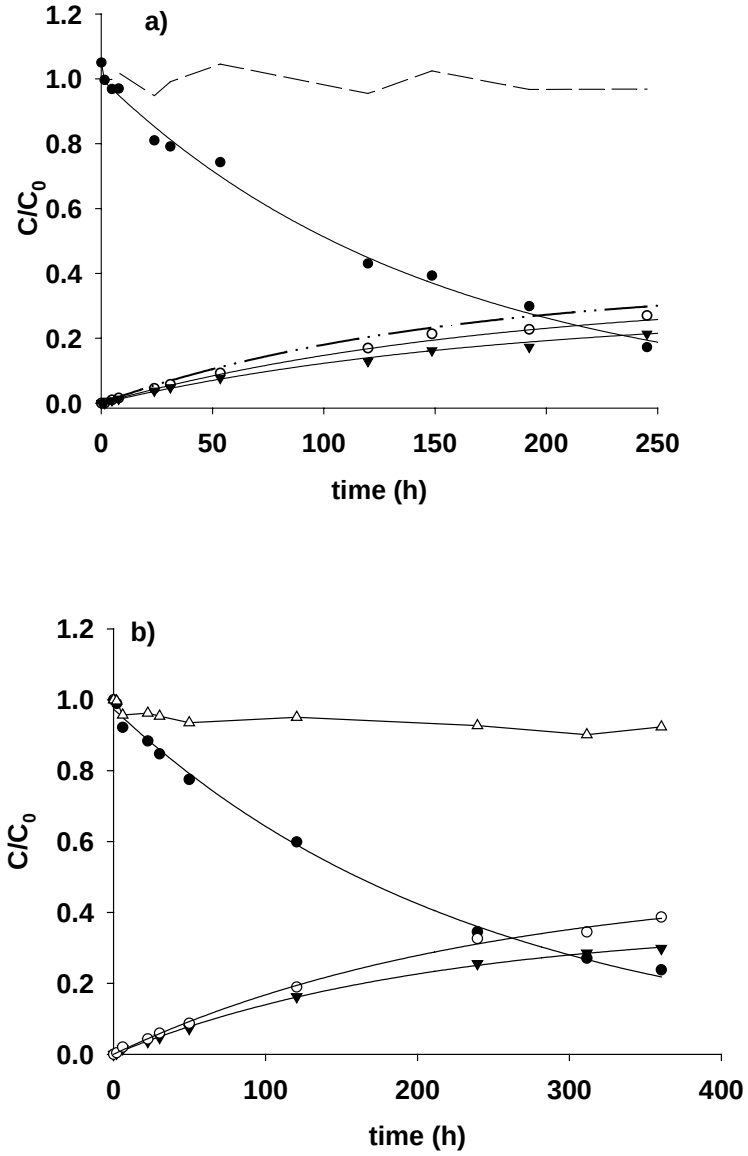

Figure 3.4 a) Hydrolysis of disulfoton ([disulfoton]$_{initial}$ = 28.6 μM) at pH 9.20 (50 mM tetraborate buffer, 100 mM NaCl, and 5% methanol) at 50 °C, indicating

the degradation of disulfoton (●, $k_h = 0.0067\ h^{-1}$), the formation of 2-(ethylthio)ethanethiol (▼, 2 × 2-(ethylthio)ethyl disulfide, 0.0017 h^{-1}), the accelerating effect from Cl^- (—··—··—, 0.0025 h^{-1}), the formation of 2-(ethylthio)ethanol (o, 0.0021 h^{-1}) and the mass balance (- - - -); b) Hydrolysis of disulfoton ($[disulfoton]_{initial}$ = 28.8 μM) at pH 9.20 (50 mM tetraborate buffer, 100 mM $NaClO_4$, and 5% methanol) at 50°C, indicating the degradation of disulfoton (●, $k_h = 0.0041\ h^{-1}$), the formation of 2-(ethylthio)ethanethiol (▼, 2 × 2-(ethylthio)ethyl disulfide, 0.0017 h^{-1}), the formation of 2-(ethylthio)ethanol (o, 0.0022 h^{-1}) and the mass balance (△). Solid lines represent model fits to the data assuming exponential decay of disulfoton to multiple degradation products simultaneously.

3.2. Kinetics of Reaction with HS^-, S_n^{2-}, PhS^- and $S_2O_3^{2-}$ at 25 °C

3.2.1. Reaction with HS^- at 25 °C

The degradation of thiometon in bisulfide was assessed with a pseudo-first-order reaction model. The experiments were conducted in the pH range of 8.90 – 9.35 and varying concentration of the sulfur nucleophile at 25 °C. Sample time course of the degradation of thiometon at pH 9.20, 5.43 mM $[H_2S]_T$ at 25 °C was shown in Figure 3.5a. The good linearity of the semilogarithmic plot for the decrease of thiometon over two half-lives is indicative of a first-order dependence on the thiometon concentration. No difference in reaction rates and product formation was observed for experiments in phosphate versus borate buffers.

Control experiments were conducted in the absence of HS^- to investigate the hydrolysis in the aquatic buffer system. The rate of reaction of thiometon in a bisulfide solution can hence be represented by the following expression:

$$k_{obs} = -d[thiometon]/dt = k_h + k_{corr}$$

$$= k_h + k''_{H_2S}[H_2S] + k''_{HS^-}[HS^-] \approx k_h + k''_{HS^-}[HS^-] \quad (1)$$

where k_h is the observed rate constant measured in the control experiment, k_{corr} is the rate constant which is obtained after k_{obs} is corrected for the contribution of k_h. The contribution from H_2S can be neglected due to its much lower reactivity and its small mole fraction in the pH range investigated. Linear regression analysis of $\log k_{corr}$ versus log [HS^-] yielded a slope equal to 1.08 ($\pm$0.06) (Figure 3.5b). The plot of k_{corr} versus [HS^-] (Figure 3.5c) fits a linear model quite well. Linear regression analysis yielded a slope (k''_{HS^-}) equal to 8.4 ($\pm$ 0.5)$\times 10^{-4}$ M^{-1} s^{-1} and an intercept not significantly different from zero at the 95% confidence level.

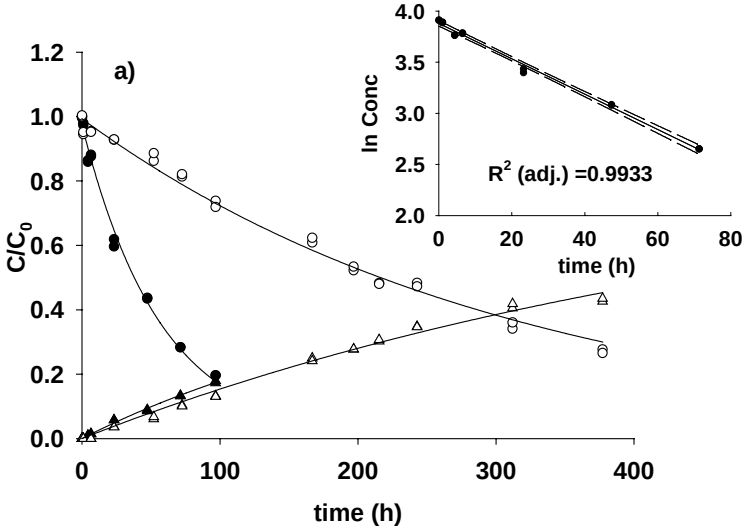

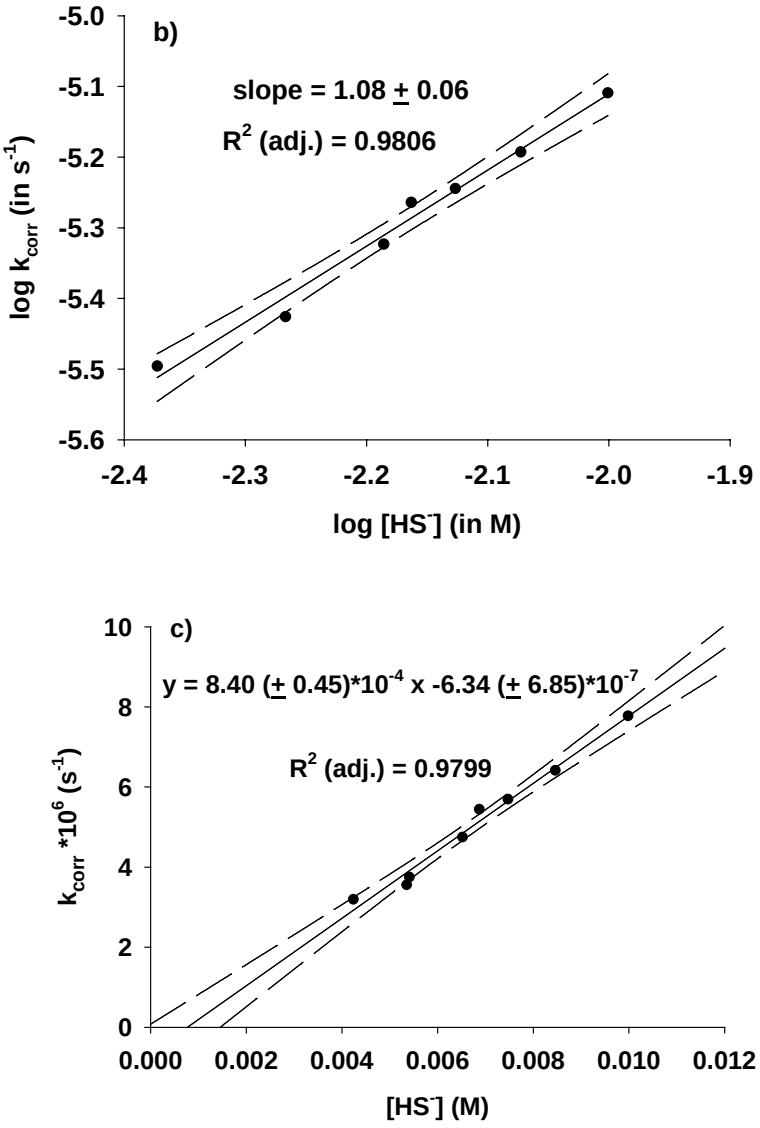

Figure 3.5 Degradation of thiometon ([thiometon]$_{initial}$ = 30.3 μM) at pH 9.20, 5.43 mM [H_2S]$_T$ (50 mM tetraborate buffer, 100 mM NaCl, and 5% methanol) at 25 °C, indicating the degradation of thiometon (●, $k_{obs} = 0.0175\ h^{-1}$), the formation of 2-(ethylthio)ethanethiol (▲, 2 × 2-(ethylthio)ethyl disulfide, 0.0037 h^{-1}) and hydrolysis of thiometon ([thiometon]$_{initial}$ = 30.3 μM) at pH 9.20, (50 mM

tetraborate buffer, 100 mM NaCl, and 5% methanol) at 25 °C, indicating the degradation of thiometon (o, $k_{obs} = 0.0032$ h^{-1}), the formation of 2-(ethylthio)ethanethiol (Δ, 2 × 2-(ethylthio)ethyl disulfide, 0.0022 h^{-1}). Inset depicts the data plotted in semilogarithmic form to obtain the observed pseudo-first-order reaction rate constants. (b) Plot of log k_{corr} versus log [HS^-]; (c) Plot of k_{corr} versus [HS^-] for the reaction of thiometon with biuslfide in 50 mM phosphate or tetraborate buffer, 100 mM NaCl, and 5% methanol at 25 °C. Solid line represents linear regression of the data; the dashed lines represent the 95% confidence interval.

3.2.2. Reaction with S_n^{2-} at 25 °C

To determine kinetics of the reaction of thiometon with polysulfide, the experiments were conducted at pH range of 8.85 – 9.30 and varying concentrations at 25 ^oC. Experimental solutions contained substantial concentration of HS^- besides S_n^{2-} species. The influence of HS_n^- can be neglected due to the extremely low concentration in the pH range investigated in the study. Hence, the rate of reaction of thiometon in a polysulfide solution can be given by the following expression:

$$k_{obs} = -d[thiometon]/dt \approx k_h + k''_{HS^-}\left[HS^-\right] + k_{corr}$$

$$\approx k_h + k''_{HS^-}[HS^-] + k''_{S_n^{2-}}\sum[S_n^{2-}] \qquad (2)$$

Corrections had to be made for the contribution from HS^- in addition to contribution from hydrolysis in computing the second-order rate constant, $k''_{S_n^{2-}}$. Linear regression analysis of $\log k_{corr}$ versus log $[S_n^{2-}]$ yielded a slope equal to 0.98 ($\pm$0.04). $k''_{S_n^{2-}}$ was determined by conducting linear regression of k_{corr} versus computed $\Sigma[S_n^{2-}]$, as shown in Figure 3.6.

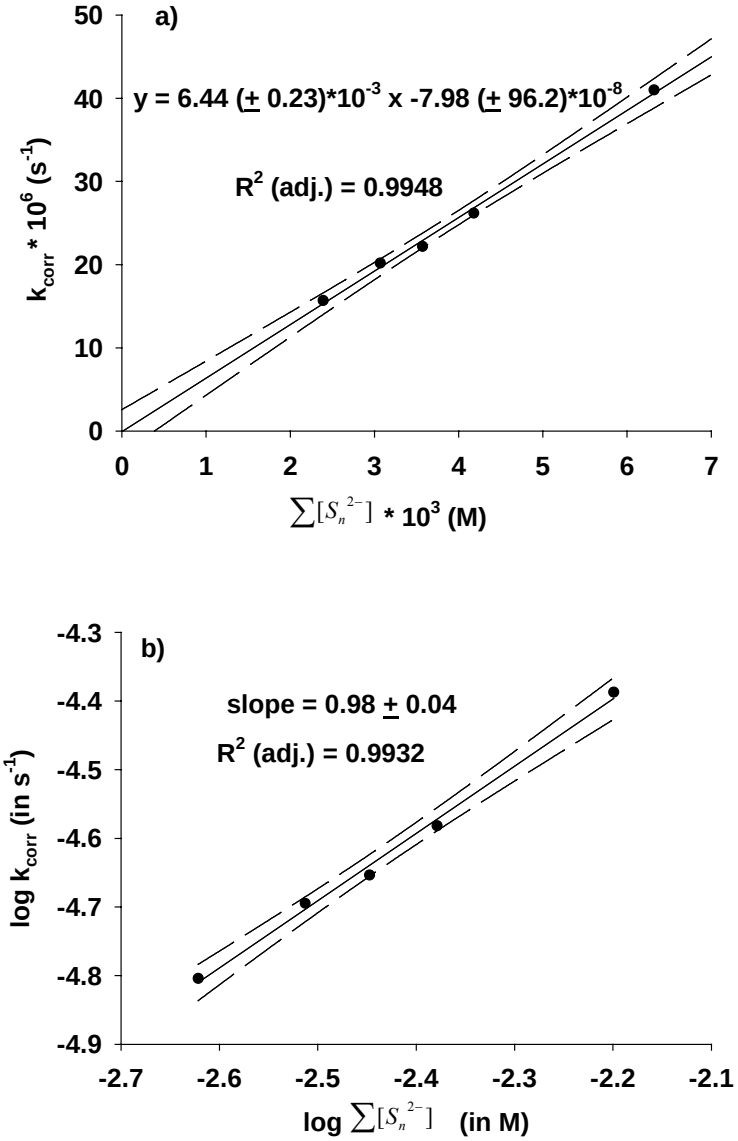

Figure 3.6 (a) Plot of k_{corr} versus $\sum[S_n^{2-}]$ for the reaction of thiometon with polysulfides in 50 mM phosphate or tetraborate buffer, 100 mM NaCl, and 5% methanol at 25 °C; (b) Plot of log k_{corr} versus log $\sum[S_n^{2-}]$. Solid line represents linear regression of the data; the dashed lines represent the 95% confidence interval.

3.2.3. Kinetics of reaction with PhS^- at 25 °C

The dependence of the pseudo-first-order rate constants on [PhS^-] and [$S_2O_3^{2-}$] were determined by conducting experiments at constant pH 9.2 and varying concentration at 25 °C. The contribution from PhSH to k_{obs} can be neglected following the same assumption as for H_2S in the reaction with bisulfide. After correction for hydrolysis, the second-order rate constants can be obtained via the linear regression of k_{corr} versus [PhS^-]

$$k_{obs} = -d[thiometon]/dt = k_h + k_{corr}$$

$$= k_h + k''_{PhSH}[PhSH] + k''_{PhS^-}[PhS^-] \approx k_h + k''_{PhS^-}[PhS^-] \quad (3)$$

Linear regression analysis of log k_{corr} versus log [PhS^-] yielded a slope equal to 0.82 ($\pm$ 0.08) (Figure 3.7).

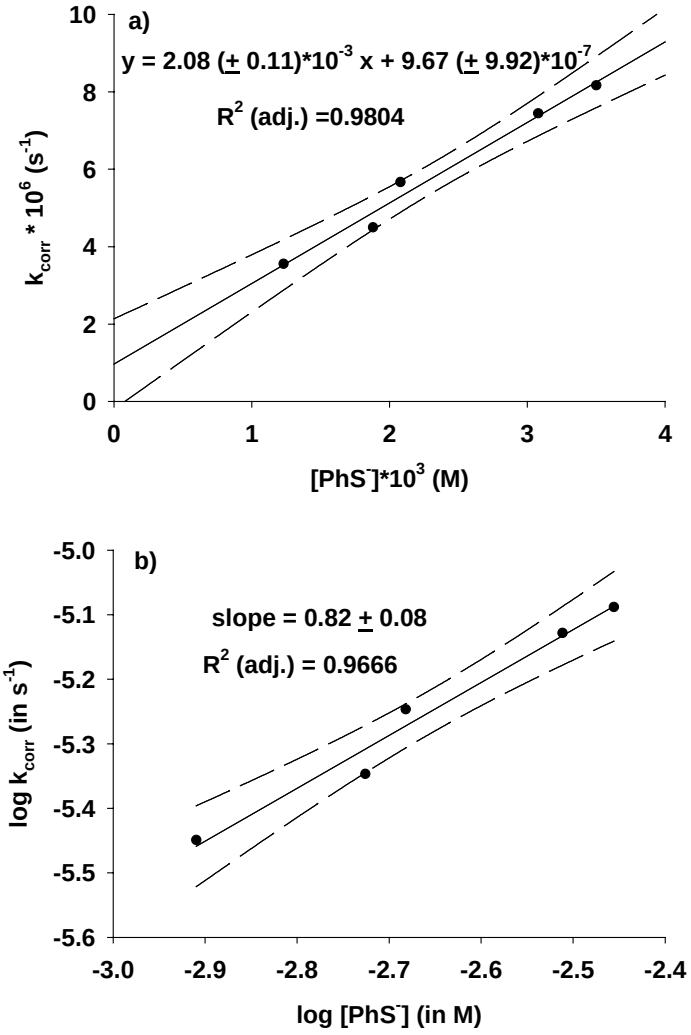

Figure 3.7 (a) Plot of k_{corr} versus [PhS⁻] for the reaction of thiometon with thiophenol in 50 mM phosphate or tetraborate buffer, 100 mM NaCl, and 5% methanol at pH 9.20, 25 °C; (b) Plot of log k_{corr} versus log [PhS⁻]. Solid line represents linear regression of the data; the dashed lines represent the 95% confidence interval.

3.2.4. Reaction with $S_2O_3^{2-}$ at 25 °C

$S_2O_3^{2-}$ is known to be the only dominant species in pH buffer solutions of sodium thiosulfate at the investigated pH 9.2. The linear regression of the observed rate constants after corrected for hydrolysis, k_{corr}, versus [$S_2O_3^{2-}$] would result in $k''_{S_2O_3^{2-}}$.

$$k_{obs} = -d[thiometon]/dt = k_h + k_{corr} = k_h + k''_{S_2O_3^{2-}}[S_2O_3^{2-}] \quad (4)$$

Linear regression analysis of $\log k_{corr}$ versus log [$S_2O_3^{2-}$] yielded a slope equal to 0.95 ($\pm$ 0.05) (Figure 3.8).

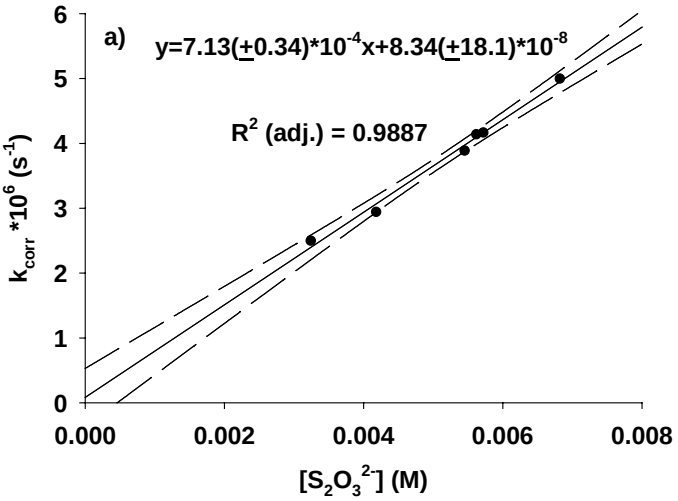

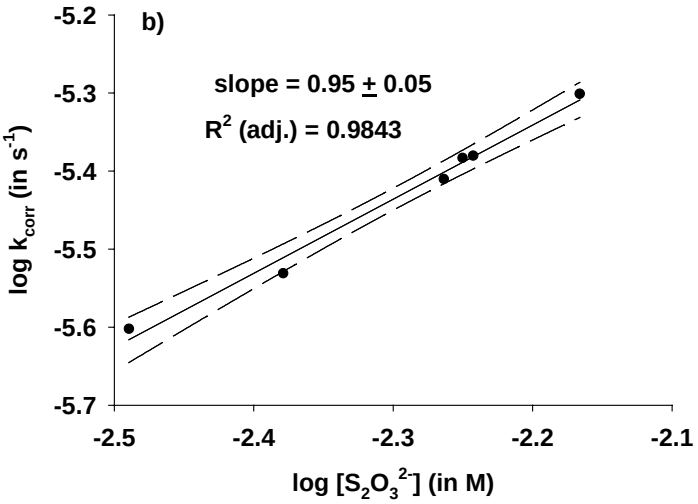

Figure 3.8 (a) Plot of k_{corr} versus $[S_2O_3^{2-}]$ for the reaction of thiometon with thiophenol in 50 mM phosphate or tetraborate buffer, 100 mM NaCl, and 5% methanol at 25 °C; (b) Plot of log k_{corr} versus log $[S_2O_3^{2-}]$. Solid line represents linear regression of the data; the dashed lines represent the 95% confidence interval.

The reactions of disulfoton with HS^-, S_n^{2-}, PhS^- and $S_2O_3^{2-}$ were assessed via the same method. There was no significant acceleration observed in bisulfide reaction solution containing up to 15 mM HS^- at pH 9.30, which demonstrated that k_{HS^-}(disulfoton) was too small to be determined exactly at 25 °C. Similarly, $S_2O_3^{2-}$ also did not show significant promotion to degradation of disulfoton in our experiments. Linear regression of log k_{corr} versus log $[S_n^{2-}]$ and log $[PhS^-]$ gave the slope of 1.10 ($\pm$ 0.05) and 1.10 ($\pm$ 0.05), respectively. The second-order rate constants for disulfoton were obtained via linear regression of k_{corr} versus $\Sigma[S_n^{2-}]$

and [PhS$^-$] as for thiometon (Figure 3.9 & 3.10). All the measured second-order rate constants are summarized in Table 3.1.

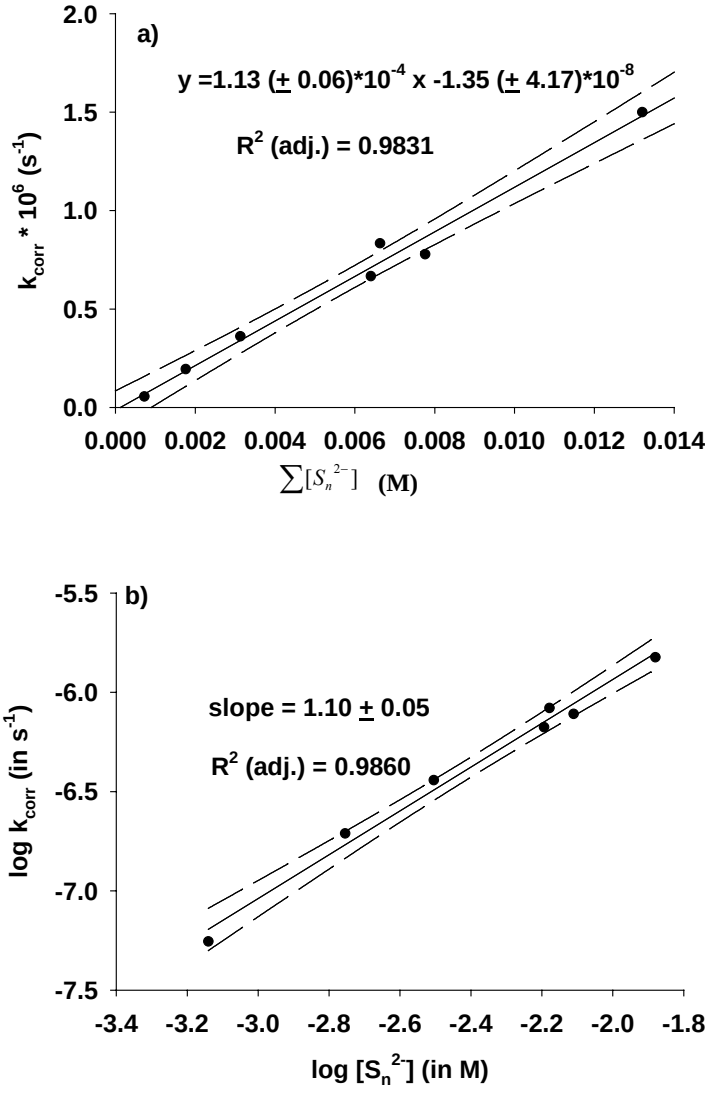

Figure 3.9 (a) Plot of k_{corr} versus $\sum[S_n^{2-}]$ for the reaction of disulfoton with polysulfides in 50 mM phosphate or tetraborate buffer, 100 mM NaCl, and 5% methanol at 25 °C; (b) Plot of log k_{corr} versus log [S_n^{2-}]. Solid line represents

linear regression of the data; the dashed lines represent the 95% confidence interval.

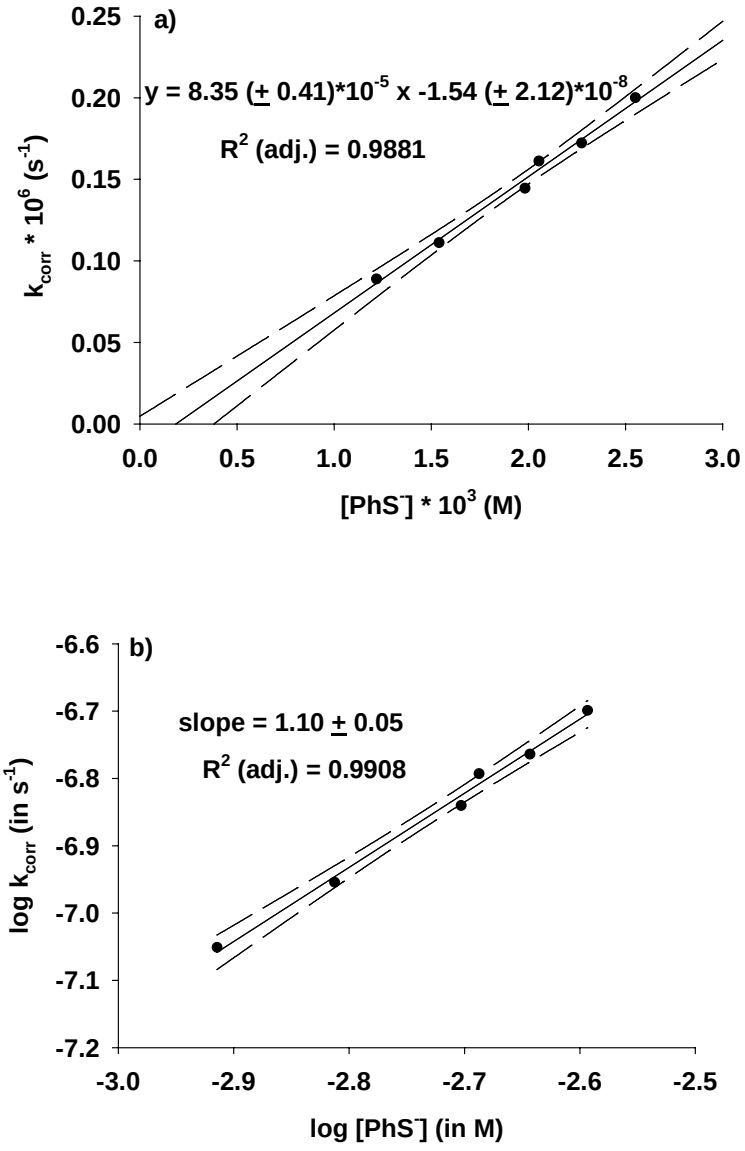

Figure 3.10 (a) Plot of k_{corr} versus [PhS⁻] for the reaction of disulfoton with thiophenol in 50 mM phosphate or tetraborate buffer, 100 mM NaCl, and 5%

methanol at 25 °C; (b) Plot of log k_{corr} versus log [PhS$^-$]. Solid line represents linear regression of the data; the dashed lines represent the 95% confidence interval.

Table 3.1 Second-order Rate Constants for Reaction of Thiometon and Disulfoton with Reduced Sulfide Species at 25 °C[a]

Pesticide	k''_{HS^-} (M^{-1} s^{-1})	k''_{PhS^-} (M^{-1} s^{-1})	$k''_{S_n^{2-}}$ (M^{-1} s^{-1})	$k''_{S_2O_3^{2-}}$ (M^{-1} s^{-1})
Thiometon	$8.4(\pm0.5)\times10^{-4}$	$2.1(\pm0.1)\times10^{-3}$	$6.4(\pm0.2)\times10^{-3}$	$7.1(\pm0.3)\times10^{-4}$
Disulfoton	Too small	$8.4(\pm0.4)\times10^{-5}$	$1.1(\pm0.1)\times10^{-4}$	Too small

[a] Stated uncertainties represent at 95% confidence interval.

While HS^- promoted the degradation of thiometon significantly, there is no significant accelerating effect from HS^- on the loss of disulfoton. At the same time, the degradations of disulfoton in pH buffer containing S_n^{2-} and PhS^- were much slower than of thiometon. The measured second-order rate constants for disulfoton were more than 20 times smaller than for thiometon, which is consistent with the greater accelerating effect of Cl^- for thiometon than disulfoton. The great difference in the reactivity of thiometon and disulfoton results from the substituent effect, which would support that methoxy group is more reactive than ethoxy group here. In the reaction with reduced sulfur species, the nucleophilic attack at the methyl or ethyl group (Pathway II) may be much more important than other pathways. For both thiometon and disulfoton, the reactivity of sulfur

species decreased in the following order: $S_n^{2-} > PhS^- > HS^- > S_2O_3^{2-}$. The relative order of the reactions of thiometon with three sulfur nucleophiles (S_n^{2-}, PhS^-, HS^-) tends to parallel that previously reported for S_N2 reactions of methyl bromide (Schwarzenbach et al., 2003). $S_2O_3^{2-}$ reacts 10 times faster than HS^- with CH_3Br, whereas thiometon reacts faster with HS^- than with $S_2O_3^{2-}$. It is quite likely that steric hindrance results into a lower reactivity of the larger $S_2O_3^{2-}$ nucleophile toward thiometon. The relative reactivity order is comparable to the results for chloroacetanilide herbicides reported by Lippa and Roberts (2004) and for chlorpyrifos-methyl reported by Wu and Jans (2006). Both thiometon and disulfoton displayed much greater reactivity towards polysulfide than bisulfide. The high reactivity of S_n^{2-} relative to HS^- might appear counterintuitive because HS^- is a slightly stronger base. Differences in charge and size between the two nucleophiles may also contribute to differences in reactivity. Polysulfides have an overall charges of -2, which can be distributed over several sulfur atoms (Meyer et al., 1977) via delocalization into d orbitals (Pickerling and Tobolsky, 1972). In contrast, HS^- has a localized charge of -1 and may, hence, be more strongly solvated despite its lower overall charge than a bulkier, more diffusely charged polysulfide dianion. If, in fact, repulsion between adjacent electron pairs contributes to increased nucleophilicity, one would predict S_2^{2-}, S_3^{2-}, S_4^{2-}, S_5^{2-}, and S_6^{2-}, to have markedly different ground-state energies and, hence, different reactivities. Previously summarized energies of the highest occupied molecular orbital (E_{HOMO}) of S_3^{2-} (-4.66 eV) and S_4^{2-}, (+1.36 eV) (Luther, 1990) confirm a

large difference in ground-state energies of these two nucleophiles; other factors being equal, more negative E_{HOMO} indicates an increase in stability and hence a decrease in nucleophilic reactivity. Differences in reactivity between polysulfide dianions would be difficult to demonstrate in our experimental systems, if polysulfides ions rapidly disproportionate to an equilibrium mixture in water.

3.3. Product Analysis

Product identification is a very important tool for the elucidation of reaction mechanisms. In the reaction of thiometon with 5.43 mM $[H_2S]_T$ in pH 9.20 50 mM tetraborate buffer containing 5% methanol and 100 mM NaCl at 25 ^oC, a faster formation of 2-(ethylthio)ethyl disulfide was observed than in the control experiment. The slight increase in the formation of 2-(ethylthio)ethyl disulfide accounts for ~10% of the increase in k_{obs} (Figure 3.2a). This would imply that HS^- attacked partly at the 2-(ethylthio)ethyl group (Pathway III(a)). The nucleophilic attack of HS^- at the central P atom would also lead to the formation of 2-(ethylthio)ethyl disulfide. However, it has been reported that such a nucleophilic attack does not occur for structurally related organophosphorus pesticides (Wu and Jans, 2006). The main reason for the increase in k_{obs} might be the nucleophilic attack of HS^- at the methoxy group (Pathway II). This hypothesis is supported by the reactions of thiometon with PhS^-, where thioanisole (3a, Scheme 1) was detected as a major product. The formation of thioanisole would result from a nucleophilic attack of PhS^- at a methoxy group (Pathway II). At the same time, another degradation product, 2-(ethylthio)ethylthio phenyl sulfide (5,

Scheme1) was detected in the reactions of thiometon with PhS^-, the EI mass spectrum is shown in Figure 3.11. The formation of 2-(ethylthio)ethyl phenyl sulfide may be attributed to the nucleophilic attack of PhS^- at the 2-(ethylthio)ethyl group (Pathway III(a)), which is consistent with the nucleophilic attack of HS^- at the 2-(ethylthio)ethyl group in the reaction with bisulfide. Unfortunately, 2-(ethylthio)ethyl phenyl sulfide was not quantified due to the lack of a standard. The time course of the reaction of thiometon with 1.82 mM $[PhSH]_T$ in pH 9.20, 50 mM borate buffer, 100 mM NaCl, and 5% methanol at 25 ºC is shown in Figure 3.12. The rate constants for the loss of thiometon (k_{obs}) and the formation of thioanisole (k_{PhSMe}) were determined by simultaneously fitting the data for thiometon and thioanisole to numerically integrated solutions of the system of governing differential rate expression using *Scientist*. k_{obs} and k_{PhSMe} were determined to be 0.188 h^{-1} and 0.104 h^{-1}, respectively. The formation of thioanisole therefore accounted for ~ 60% of the loss of thiometon. Similarly, ethyl phenyl sulfide (3b, Scheme 1) was detected as a major product in the reaction of disulfoton with PhS^-, which accounted for ~ 35% of the loss of disulfoton in the reaction of disulfoton with 2.55 mM $[PhSH]_T$ in pH 9.20, 50 mM borate buffer, 100 mM NaCl, and 5% methanol at 25 ºC (Figure 3.13). It can be concluded that the nucleophilic attack at the alkoxy group (Pathway II) is a very important pathway in the reaction of thiometon and disulfoton with reduced sulfur species. This pathway seems to be relatively more important for thiometon than

for disulfoton, which agrees well with the much slower reaction of disulfoton with reduced sulfur species than thiometon.

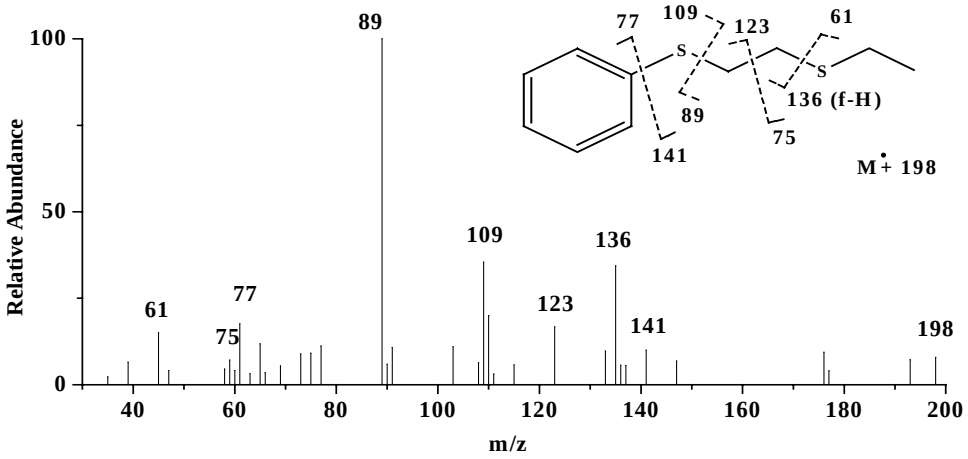

Figure 3.11 EI mass spectra for product (with retention time of 7.53 min) obtained in reaction of thiometon and disulfoton with thiophenolate. The retention time for thiometon and diusulfoton under these conditions were 7.89 min and 8.49 min, respectively.

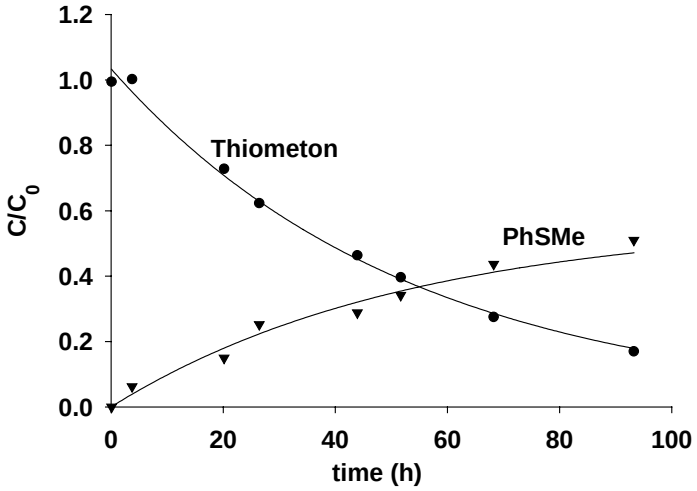

Figure 3.12 Degradation of thiometon ([thiometon]$_{initial}$ = 30.2 μM) at pH 9.20, 1.82 mM [PhSH]$_T$ (50 mM tetraborate buffer, 100 mM NaCl, and 5% methanol) at 25 °C, indicating the degradation of thiometon (●, $k_{obs} = 0.0188\ h^{-1}$), the formation of thioanisole (▼, 0.0104 h^{-1}). Solid lines represent model fits to the data assuming exponential decay of thiometon to degradation product thioanisole simultaneously.

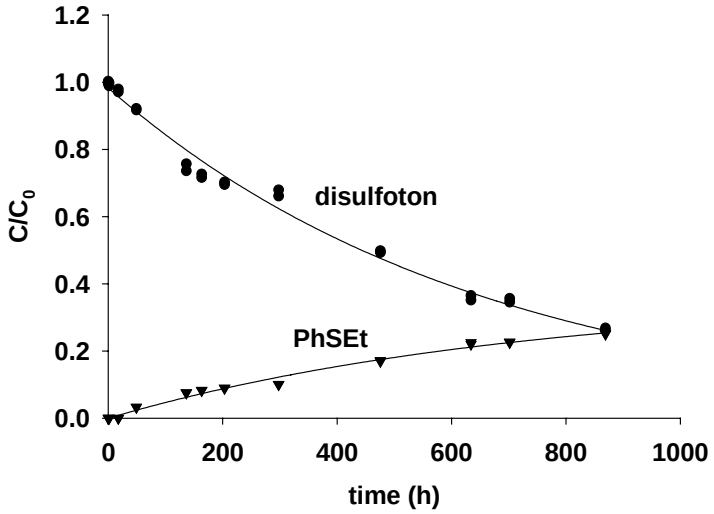

Figure 3.13 Degradation of disulfoton ([disulfoton]$_{initial}$ = 28.6 μM) at pH 9.20, 2.55 mM [PhSH]$_T$ (50 mM tetraborate buffer, 100 mM NaCl, and 5% methanol at 25 °C, indicating the degradation of disulfoton (●, $k_{obs} = 0.0015\ h^{-1}$), the formation of ethyl phenyl sulfide (▼, 0.00053 h^{-1}). Solid lines represent model fits to the data assuming exponential decay of disulfoton to degradation product ethyl phenyl sulfide simultaneously.

3.4. Activation Barrier for Reaction with Bisulfide

Thermodynamic studies are very useful in estimating the relative contribution of each pathway when multiple reaction pathways are present. To explore the multiple reaction pathways from enthalpic and entropic effects, the temperature dependence of k_{HS^-} of thiometon was determined in bisulfide solutions (pH 9.20, $[H_2S]_T$ = 9.63 mM) over the temperature range of 20.0 °C to 50.0 °C. The reaction of disulfoton was investigated in bisulfide solutions (pH 9.20, $[H_2S]_T$ =10.07 mM) from 25.0 °C to 60.0 °C, except that the reaction at 25.0 °C was carried out at pH 9.20 buffer containing 20.05 mM $[H_2S]_T$. The control experiments in the absence of bisulfide were conducted at these same temperatures. Data for thiometon and disulfoton were plotted as shown in Figure 3.14 according to a linearized version of the Eyring equation (Pross, 1995)

$$\ln(k''_{HS^-}/T) = \ln(k/h) - \Delta H^{\neq}/RT + \Delta S^{\neq}/R \qquad (3)$$

where k is the Boltzmann's constant, h is the Planck's constant, R is the gas constant, T is the temperature in Kelvin, and $\Delta H^{\neq}$ and $\Delta S^{\neq}$ are the enthalpic and entropic contributions to the overall activation barrier $\Delta G^{\neq}$, respectively. Linear regression analyses of the data yielded $\Delta H^{\neq}$ and $\Delta S^{\neq}$. Activation parameters are provided in Table 3.2.

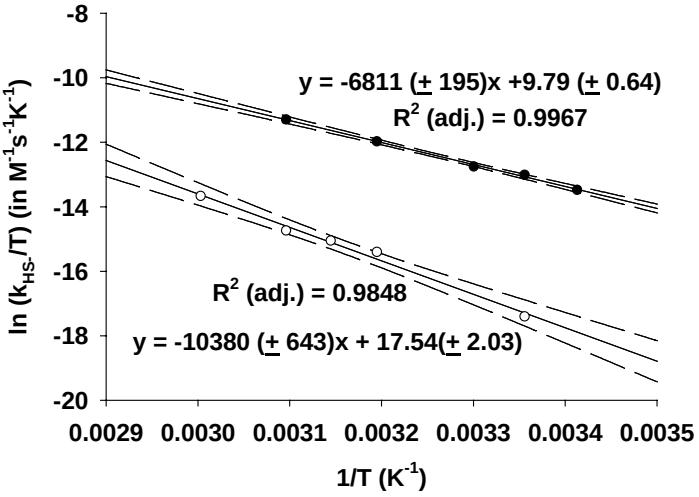

Figure 3.14 Temperature dependence of reaction of thiometon(•) and disulfoton(o) with bisulfide. The experiments of thiometon were conducted in pH 9.20, 9.63 mM $[H_2S]_T$, 50 mM tetraborate buffer, 100 mM NaCl, and 5% methanol over 20 – 50 °C. The experiments of disulfoton were conducted in pH 9.20, 10.07 mM $[H_2S]_T$, 50 mM tetraborate buffer, 100 mM NaCl, and 5% methanol over 25 – 60 °C. Solid line represents linear regression of the data; the dashed lines represent 95% confidence interval.

Table 3.2. Calculated Activation Barriers for Reaction of Thiometon and Disulfoton with Bisulfide[a]

Pesticide	$\Delta H^{\neq}$ (kJ/mol)	$\Delta S^{\neq}$ (J/mol·K)	$\Delta G^{\neq}$ (kJ/mol)[b]	E_a (kJ/mol)
Thiometon	56.6 (± 1.6)	- 116.2 (± 5.3)	91.3 (± 2.3)	59.1 (± 1.6)
Disulfoton	86.3 (± 5.3)	- 51.7 (± 16.8)	101.7 (± 9.4)	88.8 (± 5.3)

[a] Stated uncertainties represent at 95% confidence interval.

[b] Calculated at 298.15 K

The much lower $\Delta H^{\neq}$ of thiometon is consistent with the greater reactivity. Though precise experimental measurements of $\Delta S^{\neq}$ are difficult to determine (Petersen et al., 1961), the negative $\Delta S^{\neq}$ suggest that S_N2 reaction play a predominant role in the reaction with reduced sulfur species. The great difference of $\Delta S^{\neq}$ and $\Delta H^{\neq}$ in thiometon and disulfoton could be explained by the existence of multiple pathways and the different relative importance of each pathway for thiometon and disulfoton.

4. Environmental Significance

Our results demonstrate that bisulfide and polysulfides are reactive nucleophiles that could potentially control the environmental fate of thiometon within hypoxic coastal marine environments. Bisulfide is not reactive enough to influence the chemical fate of disulfoton in sulfidic environments while S_n^{2-} showed a little promotion for the transformation of disulfoton. The results demonstrate that polysulfide is the most reactive nucleophile with thiometon and disulfoton among the reduced sulfur species investigated in this study. PhS^- was chosen in this study as a model to investigate the role of aromatic sulfur nucleophiles in degradation of thiometon and disulfoton. Aromatic sulfur nucleophiles can form when natural organic matter (NOM) reacts with reduced sulfur species (e.g., H_2S and HS^-)

(Damste et al., 1989; Adam et al., 1998). Moreover, the investigation of the reaction with PhS^- is very helpful to elucidate the reaction mechanism.

The half-lives of thiometon and disulfoton at pH 7.0 in the absence of sulfur species at 25 ^oC can be calculated to be 39 d and 37 d according to the data reported by Wanner et al. (1989). Based on the measured second-order rate constants listed in Table 3.1, we can predict the persistence of thiometon and disulfoton under environmentally relevant sulfidic conditions. Half-lives for thiometon and disulfoton in marine porewaters containing reduced sulfur species were calculated by multiplying second-order rate constants in Table 3.1 by maximum concentration of $[HS^-]$ and $\Sigma[S_n^{2-}]$ reported by MacCrehan et al. (1995). The results indicate that the calculated half-life of thiometon at pH 7.0 containing 5.6 mM HS^- and 0.33 mM S_n^{2-} at 25 ^oC is 28.2 h, which is ~ 30 times shorter than only hydrolysis. Under the same conditions, the calculated half-life of disulfoton is 31 d, which was 6 days shorter. In particular, though polysulfide concentration is much lower than bisulfide, the contribution from polysulfide is still important due to its high reactivity. Hence, the reduced sulfur species at environmentally relevant concentration may represent an important sink for thiometon in anoxic coastal marine environments.

Polysulfides are actually applied as a 30% aqueous solution in commercial preparation used for agricultural soil conditioning and for fungal, mite and insect control (Kohn andd Baker, 1992). Elemental sulfur is also added to soil due to its fungicidal qualities as well as its role as an essential nutrient. Under anoxic

conditions, this elemental sulfur could undergo dissimilatory reduction by microorganisms to produce polysulfides and bisulfide (Hedderich et al., 1998). Therefore, abiotic reactions with reduced sulfur species may also represent important reactions in agricultural soils.

Chapter IV

Degradation of Phorate and Terbufos

1. Introduction

Phorate (O,O-dimethyl-S-[(ethylthio)-methyl] phosphorodithioate) and its structural analog, terbufos (S-[(1,1-dimethylethylthio)methyl]-O,O-diethyl phosphorodithioate) (Figure 4.1), are systemic insecticides used against soil pests, sucking pests and chewing pests. Phorate is used in pine forests and on root and field crops, including corn, cotton, coffee, some ornamental and herbaceous plants and bulbs (PIP-Phorate, 1993). Terbufos controls wireworms, seedcorn maggots, white grubs, corn rootworm larvae and other pests (PIP-terbufos, 1994). U.S. annual uses of phorate and terbufos were estimated at 3.2 million lb and 7.5 million lb, respectively (U.S. Environmental Protection Agency, 2001, 738-F-00-014, phorate; U.S. Environmental Protection Agency, 2001, 738-F-01-015, terbufos). They can be oxidized to corresponding oxon, sulfoxide, sulfone, etc. via either abiotic or biotic pathways (Chapman et al., 1982; Szeto et al., 1990; Chapman and Harris, 1980; Szeto et al., 1986). Hydrolysis and biodegradation are two primary dissipation processes for phorate and terbufos. Formaldehyde has been observed as a phorate and terbufos degradate in the studies where hydrolysis is a major route of dissipation (Hong and Pehkonen, 1998 & 2000; Hong et al., 2001). Photolysis does not become an important means of degradation. The

mechanisms of hydrolysis of the organophosphorus pesticides have been proposed over these years. The central phosphorus atom or the carbon atom on the ester side chain is susceptible to the attack from nucleophile. S_N2 mechanism usually dominates with a water molecule and/or hydroxide as the nucelophiles (Schwarzenbach et al., 2003). It is particularly noteworthy that the single carbon atom existing between two heteroatoms (e.g. sulfur in the case of phorate and terbufos) in the ester side chain resulted in its high reactivity. The instability of any carbon atom pocessing two functional groups is well known (Solomons, 1996). Hence, nucleophilic attack on the carbon atom between two sulfur atoms would be the main mode for hydrolysis of phorate and terbufos, which would result into much different kinetics and mechanism from the structural cousin, disulfoton. The hydrolysis of phorate and terbufos are much faster than disulfoton. And the identified degradation product confirmed the very different pathways for the hydrolysis of phorate and disulfoton. The hydrolysis of phorate and terbufos were reported by Pehkonen and his coworkers (Hong and Pehkonen, 1998; Hong et al., 2000 & 2001). And the rates, mechanisms and product analysis were discussed in detail. The dominant reaction is the nucleophilic attack at the carbon atom between two sulfur atoms from OH^- /H_2O. Formaldehyde and diethyl disulfide or di-*tert*-butyl disulfide were detected as degradation products (Scheme 4.1). In this study, emphasis is given on the reaction of phorate and terbufos with reduced sulfur species in the aqueous solution. Nucleophilicities of reduced sulfur species are higher than OH^-, which probably may result into two reactions in the

reaction with phorate and terbufos. Reduced sulfur species can attack both the carbon atom between the two sulfur atoms or ethoxy group (Scheme 4.2).

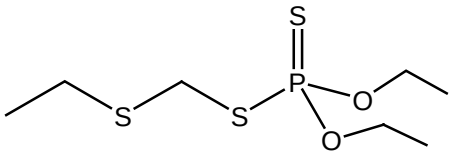

Phorate

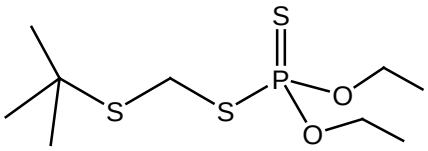

Terbufos

Figure 4.1 Structure of phorate and terbufos

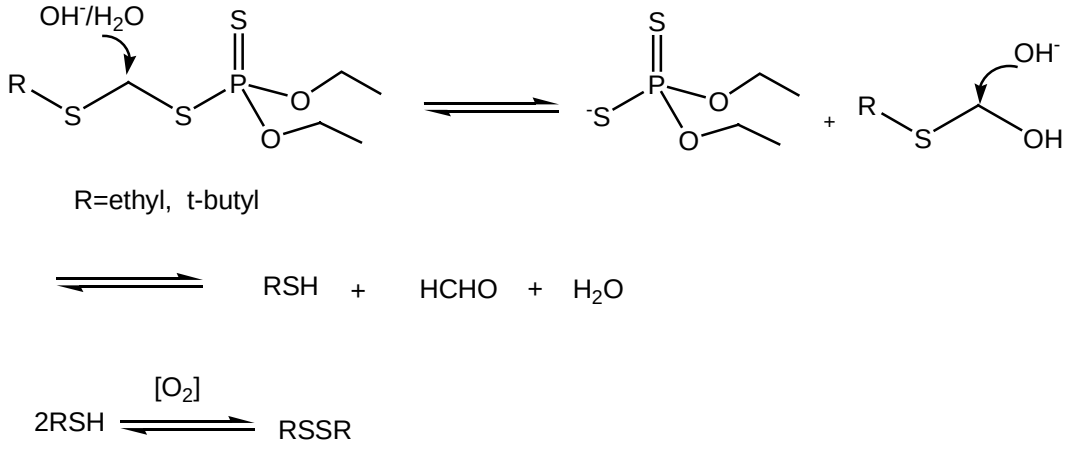

Scheme 4.1 Mechanism for the hydrolysis of phorate and terbufos

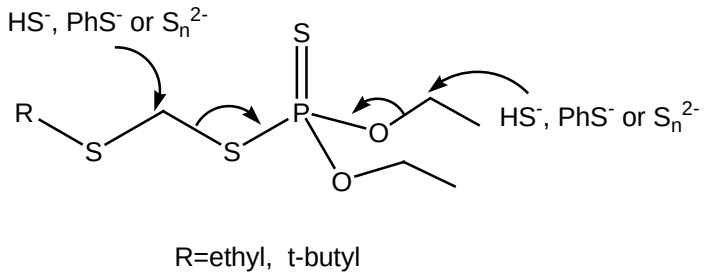

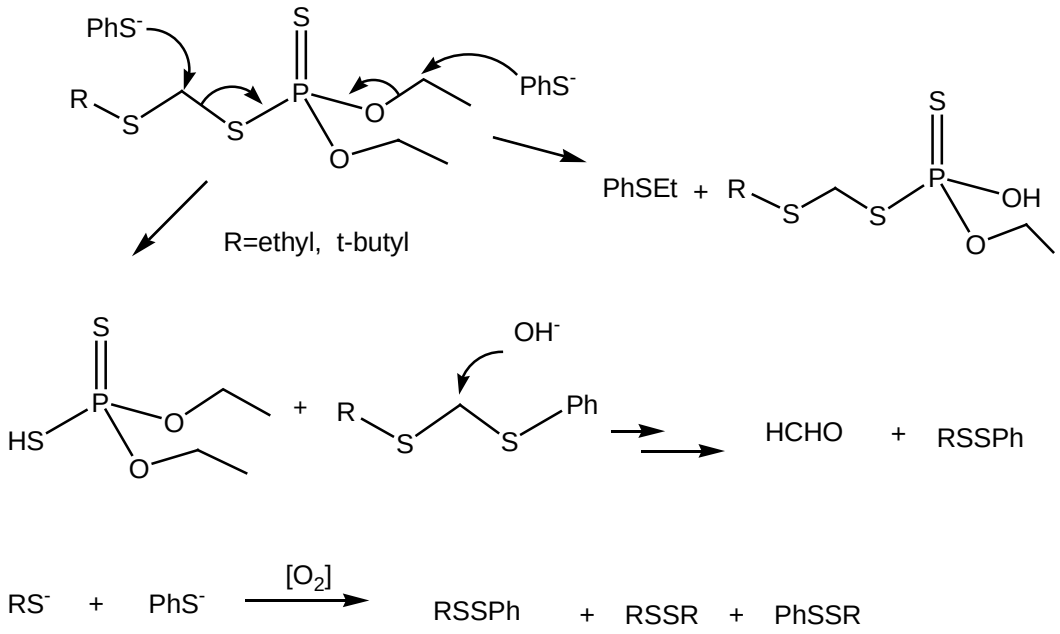

Scheme 4.2 Nucleophilic attack on phorate and terbufos by reduced sulfur species

This chapter is focused on the chemical transformation of phorate and terbufos in simulated natural sulfuric environments. The primary purpose of this study was to more closely examine rates and products of degradation of phorate and terbufos in the reduced sulfuric environments and determine the role of reduced sulfur species in the degradation of phorate and terbufos. Kinetic, thermodynamic studies and product identification are three important tools for the elucidation of reaction mechanisms. Reactions were monitored at varying concentrations of reduced sulfur species including bisulfide (HS^-), thiophenolate (PhS^-), polysulfide (S_n^{2-}) and thiosulfate ($S_2O_3^{2-}$) so as to obtain the second-order reaction rate constant and compare the reactivity of different sulfur species. PhS^- was chosen in this study as a model for investigation of role of aromatic sulfur nucleophiles in

degradation of phorate and terbufos. Aromatic sulfur nucleophiles would form when natural organic matter (NOM) reacts with reduced sulfur species. The activation parameters were investigated via the temperature dependence of the reaction of phorate and terbufos with bisulfide. This chapter also represents an experimental investigation of the influence of the substitute on reactivity and kinetics. Studies of the structural analogs can provide invaluable, though indirect and unclear, information regarding the mechanisms through which the pesticides react with the reduced sulfur species.

2. Materials and Methods

2.1. Chemicals

All chemicals were used as received. Phorate (O,O-dimethyl-S-[(ethylthio)-methyl] phosphorodithioate; 96%) and terbufos (S-[(1,1-dimethylethylthio)methyl]-O,O-diethyl phosphorodithioate; 99.5%) were obtained from Chem Service (West Chester, PA). Ethyl phenyl sulfide was obtained from Avocado Research Chemicals (Heysham, Lancashire, England). *o*-(2,3,4,5,6-pentafluorobenzyl)-hydroxylamine hydrochloride (PFBHA·HCl) were obtained from TCI-SU (Tokyo, Japan). All solvents and reagents that were used were analytical grade or equivalent. Ethyl acetate and methanol were HPLC grade and were obtained from Fisher Scientific (Pittsburgh, PA). Hexane (95% n-hexane) was for pesticides residue analysis and obtained from Mallinckrodt Baker, Inc. (Phillipsburg, NJ). All the reaction solutions were prepared in an anaerobic

glovebox (5% H_2, 95% N_2) and aqueous solutions were prepared from argon-purged deionized water (DW) (Milli-Q gradient system, Millipore, Bedford, MA).

2.2. Experimental System

The starting concentration of phorate and terbufos were ~ 50 μM and ~25 μM, respectively. The concentrations of $[H_2S]_T$, $[PhSH]_T$, $[S(II)]_T$ and $[S_2O_3^{2-}]$ in the reaction with phorate were 1.6 – 11.7 mM, 0.4 – 3.2 mM，3.5 – 17.3 mM and 4.2 – 6.8 mM, respectively. And these concentrations in the reaction with terbufos were 3.6 – 12.0 mM, 1.5 – 3.2 mM，2.9 – 13.1 mM and 3.8 – 7.2 mM, respectively. Reaction mixtures were maintained anoxic and incubated in a water bath at the selected temperature. The kinetics were monitored by extracting aliquots (~1 mL) of the reaction mixture with 1 mL ethyl acetate throughout the course of experiments. The resulting extracts were subjected to GC/FID and GC/MS analysis.

2.3. Chromatographic Analysis

Ethyl acetate extracts were analyzed on a Fisons GC 8000 equipped with an AS 800 autosampler, a FID-80 flame ionization detector (Carlo Erba Instruments), a split/splitless injector and a 30 m DB-5, 0.25 mm i.d. × 0.25 μm fused-silica capillary column (J&W, Folsom, CA). The carrier gas was helium (99.999%) and the make up gas was methane/argon. GC/MS system to identify and analyze the degradation products was equipped with a split/splitless injection and 30 m AT-5ms, 0.25 mm i.d. × 0.25 μm fused-silica capillary column (Alltech, Deerfield,

IL). EI mass spectra were generated using electron energy of 70 eV, monitoring for ions m/z 35-500 in full-scan modes. The source temperature employed for the ionization technique was 200 ºC. *Temperature program:* Injector temperature and detector temperature were set at 250 ºC and 275 ºC, respectively. The column temperature was held at 100 ºC for one minute, then increased at a rate of 20 ºC/min to 275 ºC and finally held constant at 275 ºC for 4 minutes.

2.4. Product Derivatization

The possible hydrolysis products in the buffer solutions were qualitatively analyzed by GC/MS. Formaldehyde can be determined via the analysis method for aldehyde and carbonyl compounds with PFBHA·HCl as a derivatizing agent. The method was first described by Yamada and Somiya (1989) and later improved by Glaze and coworkers (1989). The technique utilizes a direct aqueous derivatization with the reagent PFBHA, which reacts with the carbonyls to form the corresponding oximes. Two geometric isomers are formed (pentafluorobenzyloxime *(syn)* and pentafluorobenzyloxime *(anti)*) with most aldehydes except symmetrical carbonyls where only one isomer is formed (Scheme 4.3).

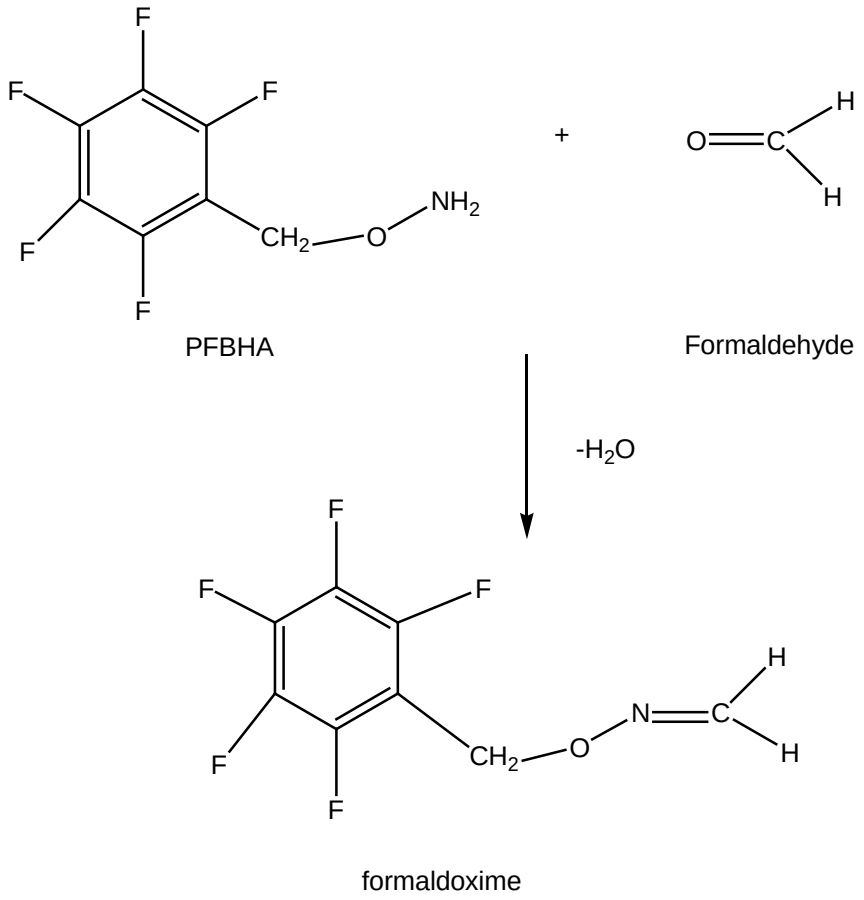

Scheme 4.3 Reaction of PFBHA and formaldehyde

About 2 mL aliquot of reaction solution or formaldehyde standard solution prepared in methanol was spiked into a test tube. To this was added 2 mL of PFBHA·HCl (prepared gravimetrically as 2 mg/ mL aqueous solution) and 5 mL of 50 mM pH 5 phosphate buffer. The test tube was kept in the 60 ± 0.5 ^{o}C water bath for 60 min. After the mixture had been allowed to cool to room temperature, 2~3 drops of concentrated sulfuric acid was added to quench the derivatization reaction. The derivatives were extracted into 1 mL of hexane. And the hexane extract was cleaned with 3 mL 0.1 M sulfuric acid and dried over magnesium

sulfate. The hexane extract was analyzed by GC/MS. The standards of the formaldoxime were prepared from the formaldehyde standard solutions treated with the same procedure. Good recovery of the derivatization method was reported for detection of concentration of formaldehyde in drinking water (Sclimenti, 1990).

3. Results and Discussion

3.1. Hydrolysis at 25 ^{o}C

Hydrolysis of phorate was investigated over a pH range of 7.40 – 9.30 in 50 mM phosphate or tetraborate buffer containing 100 mM NaCl and 5% methanol at 25 ^{o}C. Hydrolysis rate constants (k_h) are listed in Table 4.1. After the reaction, the sample was derivatized with PFBHA • HCl and formaldoxime was detected. The Electron Ionization spectrum of formaldoxime was available in the Figure 4.2. Based on the calibration curve of the prepared standards of formaldoxime from formaldehyde standard solutions, the formaldehyde concentration after the completion of experiments was measured to be ~45 μM in the hydrolysis of phorate at pH 9.0 at 25 ^{o}C with $[\text{phorate}]_{\text{initial}}$ = 50.3 μM.

Table 4.1 Hydrolysis Rate Constants of Phorate in 50 mM Phosphate or Tetraborate Buffer Containing 100 mM NaCl and 5% Methanol at 25 ^{o}C.

Reaction condition	k_h (s^{-1})*	$t_{1/2}$ (h)
pH 9.28, borate buffer	2.81 ($\pm$ 0.03) × 10^{-6}	68.8

pH 9.25, borate buffer	2.67 (± 0.03) × 10^{-6}	72.1
pH 8.90, phosphate buffer	2.72 (± 0.03) × 10^{-6}	70.7
pH 8.68, phosphate buffer	2.76 (± 0.02) × 10^{-6}	69.7
pH 8.33, phosphate buffer	2.81 (± 0.09) × 10^{-6}	68.8
pH 7.70, phosphate buffer	2.86 (± 0.06) × 10^{-6}	67.1
pH 7.65, phosphate buffer	2.66 (± 0.04) × 10^{-6}	72.4
pH 7.40, phosphate buffer	2.76 (± 0.05) × 10^{-6}	69.8

* The rate constant of hydrolysis of phorate was obtained at 95% confidence interval.

k_h = 2.76 (± 0.07) × 10^{-6} s^{-1}

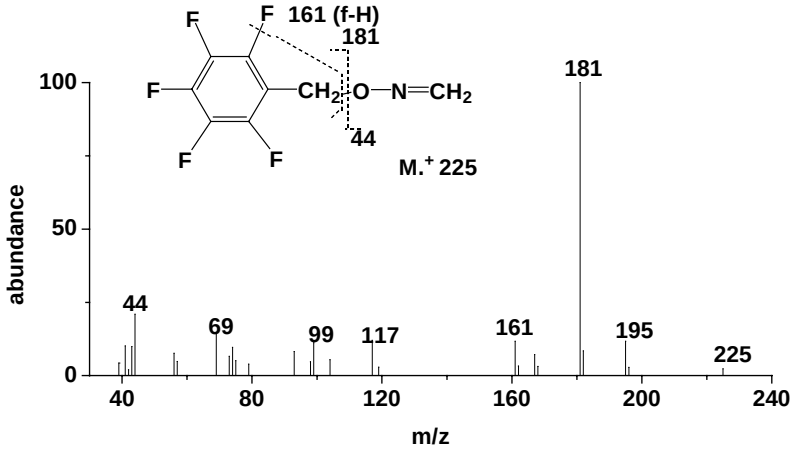

Figure 4.2 The EI chromatogram of derivatized sample in the hydrolysis of phorate at pH 9.0 (50 mM phosphate buffer, 100 mM NaCl, and 5% methanol, [phorate]$_{initial}$ = 50.3 μM) at 25 ^{o}C.

Diethyl disulfide was also identified during the reaction, which would result from oxidation of ethanethiol when the samples are exposed to the air during extraction. Diethyl disulfide was not constantly detected in the continuous samples due to uncertainty in the oxidation. The prolonged exposure time to oxygen would result into oxidation of ethanethiol beyond diethyl disulfide level. Ethanethiol would be oxidized to higher oxidation states (Capozzi and Modena, 1974), which are more hydrophilic and not extracted into organic solvent and detected by GC-MS. Therefore, it is problematic to quantify the formation of ethanethiol or diethyl disulfide exactly. In the investigated pH range of 7.40 – 9.30, hydrolysis rates lay in the narrow range of 2.76 ($\pm$ 0.07) $\times 10^{-6}$ s^{-1}, which demonstrated that no significant difference was observed in the 95% confidence interval. Our results were comparable to the hydrolysis rates reported by Hong and Pehkonen (1998). Their results also show that homogeneous hydrolysis rates of phorate at pH 8.5 and 9.4 were not much different, which are 3.15 ($\pm$ 0.50) $\times 10^{-6}$ s^{-1}, and 3.11 ($\pm$ 0.06) $\times 10^{-6}$ s^{-1}, respectively. The control experiments of hydrolysis of phorate in pH buffer containing 100 mM $NaClO_4$ rather than NaCl were carried out to investigate the influence of chloride ion on degradation. No significant difference of disappearance rate of phorate in the buffer containing NaCl or $NaClO_4$ was observed at 25 – 50 ^{o}C. Compared to the hydrolysis discussed in the previous chapter, the hydrolysis rate of phorate is more than 20 times faster than disulfoton. While chloride ion showed no acceleration at 25 ^{o}C and there was significant promotion effect at 50 ^{o}C to the degradation of

disulfoton, chloride ion showed no significant acceleration observed for degradation of phorate at 25 – 50 ^{o}C. There is structural difference for phorate compared to disulfoton: only one carbon between the two sulfur atoms on the thioester side chain in phorate, while there are two carbon atoms in disulfoton. The faster hydrolysis of phorate would strengthen the previous assumption of the much higher reactivity of the carbon atom in phorate than the two carbon atoms in disulfoton, which results from the presence of the two neighboring sulfur atoms. Hence, unlike the hydrolysis of disulfoton, which multiple pathways are present, the nucleophilic attack at the carbon between the two sulfur atoms on the thioester chain is the sole predominant pathway in the hydrolysis of phorate. These would explain why the hydrolysis of phorate is much faster than the hydrolysis of disulfoton, and no acceleration from chloride ion was observed over 20-50 ^{o}C. Hydrolysis of terbufos was also investigated in the same way. Hydrolysis of terbufos was ~ 50% faster than phorate. Formaldehyde was identified after the reaction to ~15 μM after reaction and di-tert-butyl disulfide was also detected as product. Hydrolysis rates of terbufos at pH 8.0 – 9.35 lay in the range of 4.27 ($\pm$ 0.10) $\times 10^{-6}$ s^{-1} (Table 4.2), which agree well with data reported by Hong et al. (2001). No acceleration from chlorine ions of the degradation of terbufos was observed over 20 – 50 ^{o}C. The hydrolysis rates of phorate and terbufos demonstrated that the influence of pH is not significant in the pH range investigated in this study. The faster hydrolysis rate of terbufos might be

attributed to tert-butylthio methylene group, a better leaving group than ethylthio methylene group.

Table 4.2. Hydrolysis Rate Constants of Terbufos in 50 mM Phosphate or Tetraborate Buffer Containing 100 mM NaCl and 5% Methanol at 25 ^{o}C.

Reaction condition	k_h (s^{-1})*	$t_{1/2}$ (h)
pH 9.42, borate buffer	4.39 ($\pm$ 0.04) × 10^{-6}	43.9
pH 9.27, borate buffer	4.28 ($\pm$ 0.05) × 10^{-6}	45.0
pH 8.90, phosphate buffer	4.08 ($\pm$ 0.03) × 10^{-6}	47.2
pH 8.49, phosphate buffer	4.22 ($\pm$ 0.03) × 10^{-6}	45.6
pH 8.32, phosphate buffer	4.33 ($\pm$ 0.03) × 10^{-6}	44.4
pH 7.95, phosphate buffer	4.36 ($\pm$ 0.04) × 10^{-6}	44.1
pH 7.65, phosphate buffer	4.25 ($\pm$ 0.04) × 10^{-6}	45.3

* The rate constant of hydrolysis of terbufos was obtained at 95% confidence interval.

k_h = 4.27 ($\pm$ 0.10) × 10^{-6} s^{-1}

3.2. Kinetics of Reaction with HS^-, PhS^-, $S_2O_3^{2-}$ and S_n^{2-} at 25 °C

All the reactions were treated as pseudo-first-order reactions in the presence of excess of reduced sulfur species. The great linearity of semilogarithmic plot for decay of phorate and terbufos over two to three half-lives is indicative of a first-order dependence on the pesticides concentration. No influence on the kinetics from phosphate and borate buffer was observed.

3.2.1. Reaction of phorate with HS^- at 25 °C

The reaction with bisulfide was investigated in the pH range of 8.50 – 9.40. The loss of the pesticides in the bisulfide solution was contributed to hydrolysis and to the reaction with sulfur species. The observed reaction rate in the bisulfide solution can hence be represented as follows:

$$k_{obs} = -d[phorate]/dt = k_h + k''_{H_2S}[H_2S] + k''_{HS^-}[HS^-] \approx k_h + k''_{HS^-}[HS^-]$$
$$k_{corr} = k_{obs} - k_h \approx k''_{HS^-}[HS^-] \quad (1)$$

in which k_h is the observed rate constant measured in hydrolysis experiment at the same pH. The contribution from H_2S can be neglected due to its much weaker reactivity and the extremely low concentration in the pH range investigated. Corrections were made for the contribution from k_h to obtain k_{corr}. Linear regression analysis of log k_{corr} versus log [HS^-] yielded the slope of 0.87 ($\pm$ 0.06). The plot of k_{corr} and [HS^-] fit a linear model very well (Figure 4.3). Linear regression analysis yielded a slope, the second-order rate cinstant (k''_{HS^-}), equal to 1.19 ($\pm$ 0.08) $\times 10^{-4}$ M^{-1} s^{-1} and an intercept not significantly different from zero at 95% confidence level.

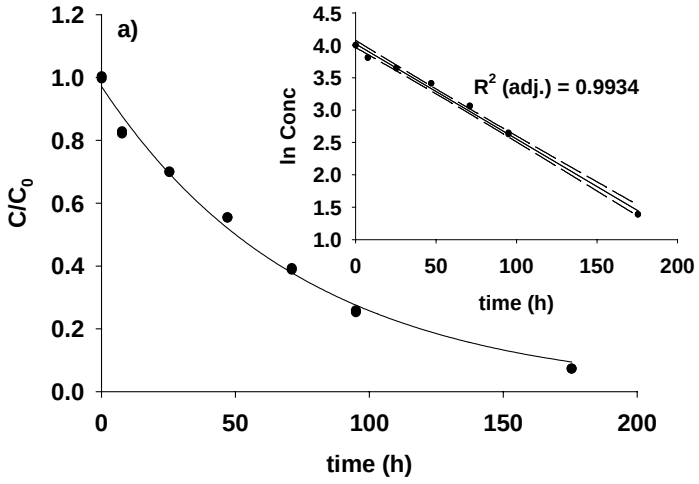
a)
C/C0
time (h)
ln Conc
R2 (adj.) = 0.9934
time (h)

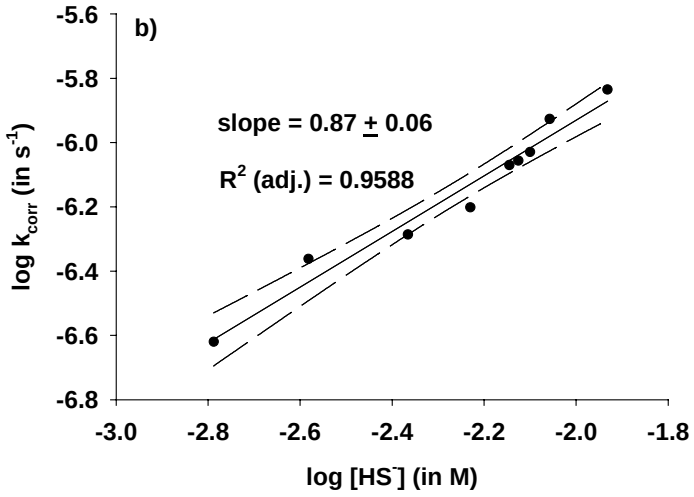
b)
slope = 0.87 ± 0.06
R2 (adj.) = 0.9588
log kcorr (in s-1)
log [HS-] (in M)

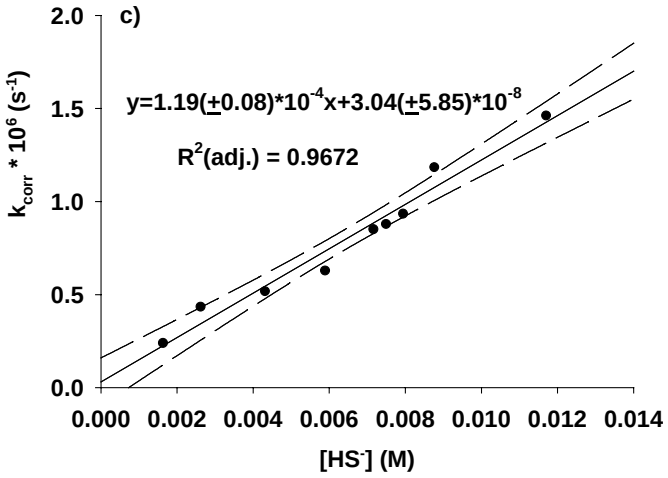
c)
y=1.19(±0.08)*10-4x+3.04(±5.85)*10-8
R2(adj.) = 0.9672
kcorr * 10^6 (s-1)
[HS-] (M)

Figure 4.3 (a) Reaction of phorate ([Phorate]$_{initial}$ = 52.2 μM) with 8.8 mM [H_2S]$_T$ at pH 9.42 (50 mM tetraborate buffer, 100 mM NaCl, and 5% methanol) at 25 °C, indicating the degradation of phorate (•). Solid lines represent model fits to the data assuming exponential decay of phorate. Inset depicts the data plotted in semilogarithmic form to obtain the observed pseudo-first-order reaction rate constants. (b) Plot of log k_{corr} versus log [HS^-] for the reaction of phorate with bisulfide in 50 mM phosphate/tetraborate buffer, 100 mM NaCl, and 5% methanol at 25 °C and (c) Plot of corrected reaction rate constants, k_{corr}, versus [HS^-] Solid line represents linear regression of the data; the dashed lines represent 95% confidence interval.

3.2.2. Reaction of phorate with PhS^- at 25 °C

The dependence of the pseudo-first-order rate constant on thiophenolate concentration was determined by conducting experiments at constant pH 9.2 and varying concentration at 25 ^oC. The kinetics fit the pseudo-first-order reaction model very well. Linear regression analysis of log k_{corr} versus log [PhS^-] yielded the slope of 1.00 ($\pm$ 0.03). The contribution from PhSH to k_{obs} can be ignored for the same reason as H_2S in the reaction with bisulfide. $k"_{PhS^-}$ can be obtained via the linear regression of observed rate constants corrected for hydrolysis, k_{corr}, versus [PhS^-] (Figure 4.4). And the intercept is also near zero.

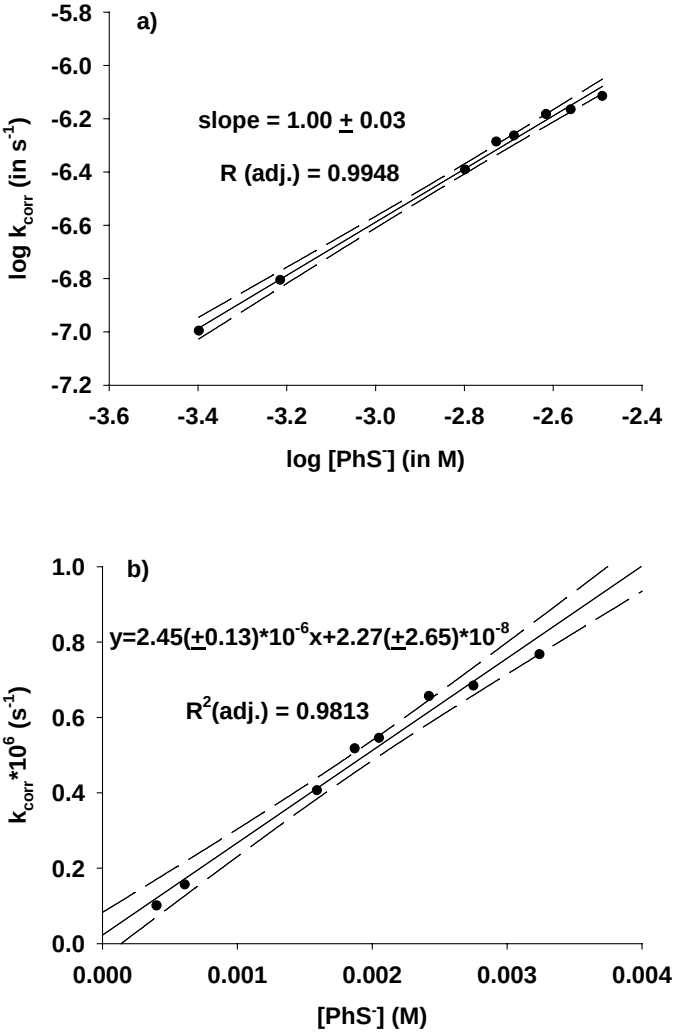

Figure 4.4 (a) Plot of log k_{corr} versus log [PhS^-] and (b) Plot of corrected reaction rate constants, k_{corr}, versus [PhS^-] for the reaction of phorate with thiophenol in 50 mM phosphate/tetraborate buffer, 100 mM NaCl, and 5% methanol at 25 °C. Solid line represents linear regression of the data; the dashed lines represent 95% confidence interval.

3.2.3. Reaction of phorate with $S_2O_3^{2-}$ at 25 °C

$S_2O_3^{2-}$ is known to be the only dominant species in pH buffer solutions of sodium thiosulfate over the investigated pH range of 8.5 – 9.2. The kinetics of the reaction of phorate also fit the pseudo-first-order reaction model quite well. Linear regression analysis of log k_{corr} versus log [$S_2O_3^{2-}$] yielded the slope of 0.93 (± 0.08). The linear regression of the observed rate constants corrected for hydrolysis, k_{corr}, versus [$S_2O_3^{2-}$] results in $k''_{S_2O_3^{2-}}$ (Figure 4.5).

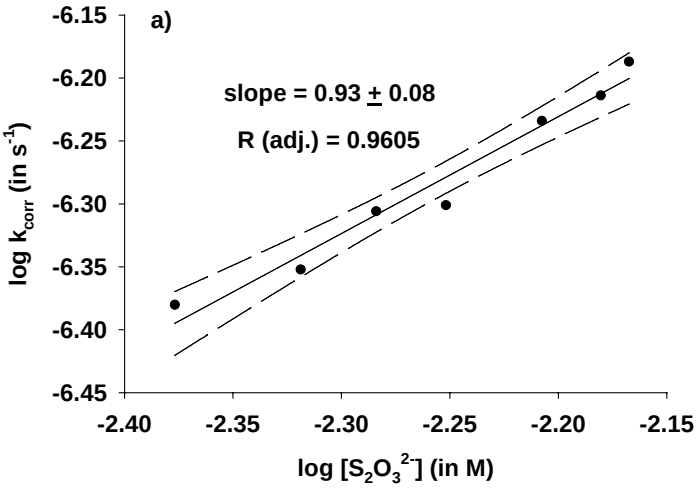

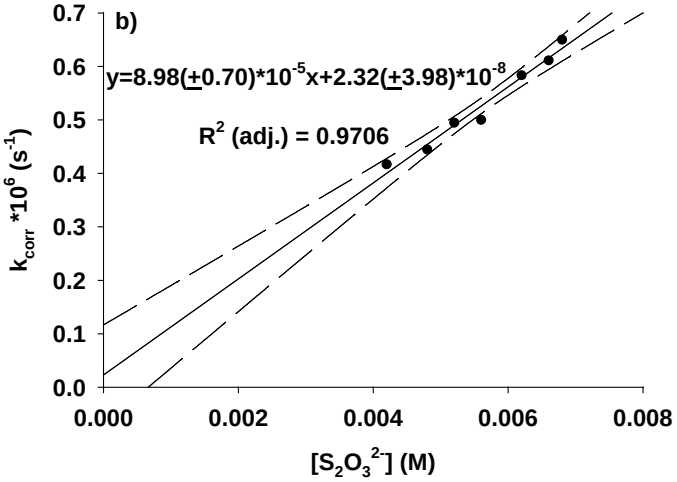

Figure 4.5 (a) Plot of log k_{corr} versus log [$S_2O_3^{2-}$] and (b) Plot of corrected reaction rate constants, k_{corr}, versus [$S_2O_3^{2-}$] for the reaction of phorate with thiosulfate in 50 mM phosphate/tetraborate buffer, 100 mM NaCl, and 5% methanol at 25 °C. Solid line represents linear regression of the data; the dashed lines represent 95% confidence interval.

3.2.4. Reaction of phorate with S_n^{2-} at 25 °C.

To determine kinetics of the reaction with polysulfide, the experiments were conducted at pH range of 8.85 – 9.30 and varying concentrations at 25 ^oC. Experimental solutions contained substantial concentration of HS^- besides S_n^{2-} species. Hence, the rate of reaction of thiometon in a polysulfide solution can be given by the following expression:

$$k_{obs} = -d[thiometon]/dt \approx k_h + k''_{HS^-}[HS^-] + k''_{S_n^{2-}} \sum [S_n^{2-}]$$
$$k_{corr} = k_{obs} - k_h - k''_{HS^-}[HS^-] \approx k''_{S_n^{2-}} \sum [S_n^{2-}] \quad (2)$$

The influence from hydropolysulfide HS_n^{2-} was neglected due to the extreme low concentration in the polysulfide solution in the pH range investigated. Corrections were made for the contribution from HS^- in addition to hydrolysis to compute second-order rate constant, $k''_{S_n^{2-}}$. Linear regression analysis of log k_{corr} versus log $\Sigma[S_n^{2-}]$ yielded the slope of 0.98 ($\pm$ 0.08). $k''_{S_n^{2-}}$ was determined by conducting linear regression of k_{corr} versus computed $\Sigma[S_n^{2-}]$ (Figure 4.6). The intercept is near zero in 95% confidence level.

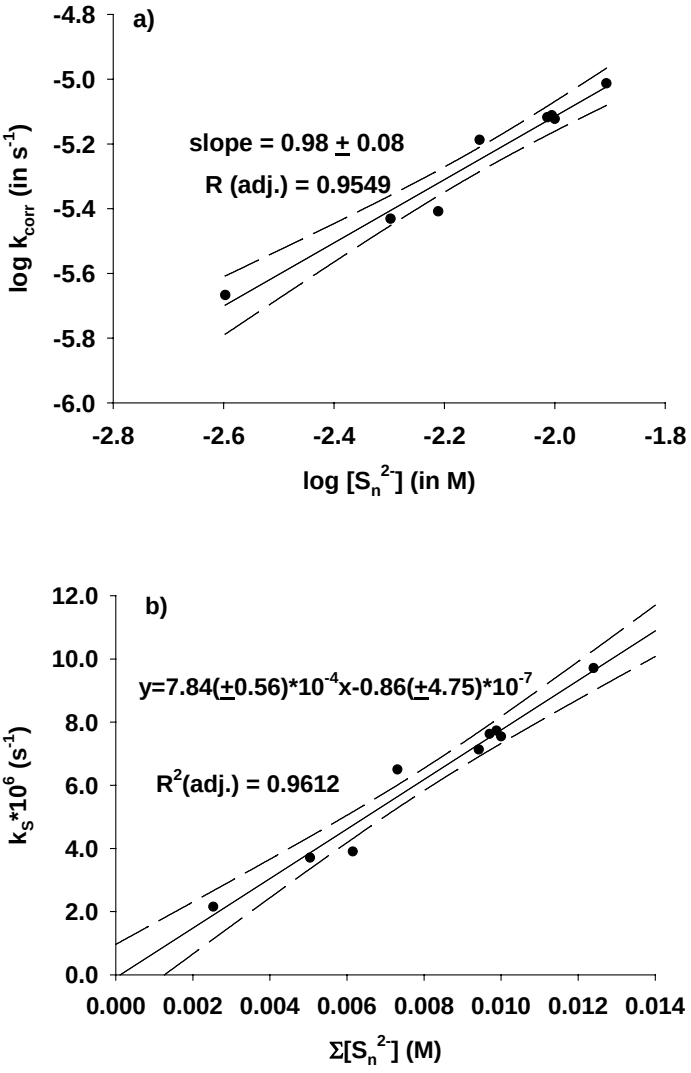

Figure 4.6 (a) Plot of log k_{corr} versus log $\Sigma[S_n^{2-}]$ and (b) Plot of corrected reaction rate constants, k_{corr}, versus $\Sigma[S_n^{2-}]$ for the reaction of phorate with polysulfide in 50 mM phosphate/tetraborate buffer, 100 mM NaCl, and 5% methanol at 25 °C. Solid line represents linear regression of the data; the dashed lines represent 95% confidence interval.

3.2.5. Reaction of terbufos with HS^-, PhS^-, $S_2O_3^{2-}$ and S_n^{2-} at 25 °C

The reactions of terbufos with HS^-, PhS^-, $S_2O_3^{2-}$ and S_n^{2-} were assessed via the same method. The kinetics of the reactions of terbufos with the sulfur species fit the pseudo-first-order reaction model well. The slopes of the plots of log k_{corr} and concentration of reduced sulfur species demonstrated that the reaction is roughly in first order in reduced sulfur species (Figure 4.7). All the measured second-order rate constants are listed in Table 4.3. Similar to hydrolysis, the degradations of terbufos in pH buffer containing HS^-, PhS^-, $S_2O_3^{2-}$ and S_n^{2-} were about 30 – 50 % faster than the degradation of phorate under the same condition. The slightly higher reactivity of terbufos would result from the more positive electrostatic charge at the carbon atom between the two sulfur atoms due to the presence of the tert-butyl group rather than the ethyl group.

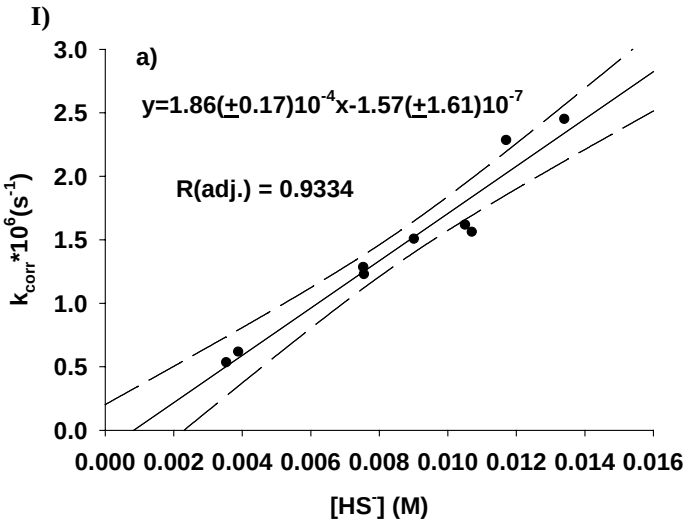

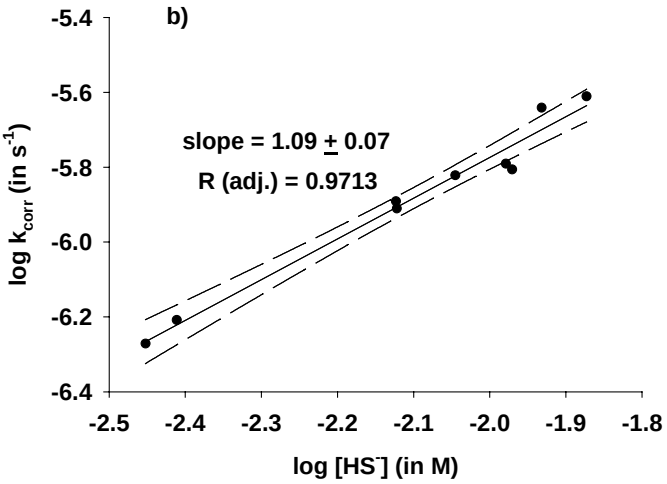
b)
slope = 1.09 ± 0.07
R (adj.) = 0.9713
log k_{corr} (in s^{-1})
log [HS^-] (in M)
-5.4
-5.6
-5.8
-6.0
-6.2
-6.4
-2.5
-2.4
-2.3
-2.2
-2.1
-2.0
-1.9
-1.8

II)

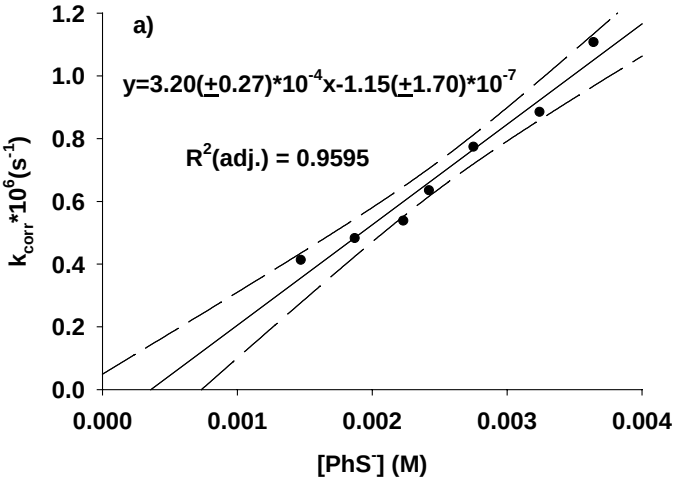
a)
y=3.20(±0.27)*10^{-4}x-1.15(±1.70)*10^{-7}
R^2(adj.) = 0.9595
k_{corr}*10^6(s^{-1})
[PhS^-] (M)
1.2
1.0
0.8
0.6
0.4
0.2
0.0
0.000
0.001
0.002
0.003
0.004

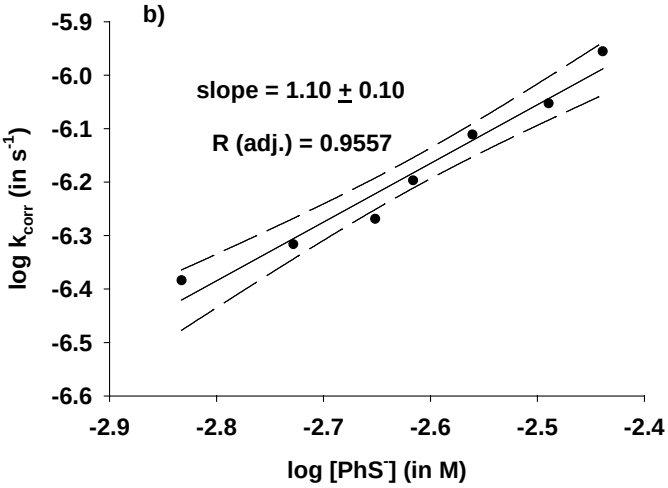
b)
slope = 1.10 ± 0.10
R (adj.) = 0.9557
log k_{corr} (in s^{-1})
log [PhS^-] (in M)
-5.9
-6.0
-6.1
-6.2
-6.3
-6.4
-6.5
-6.6
-2.9
-2.8
-2.7
-2.6
-2.5
-2.4

III)

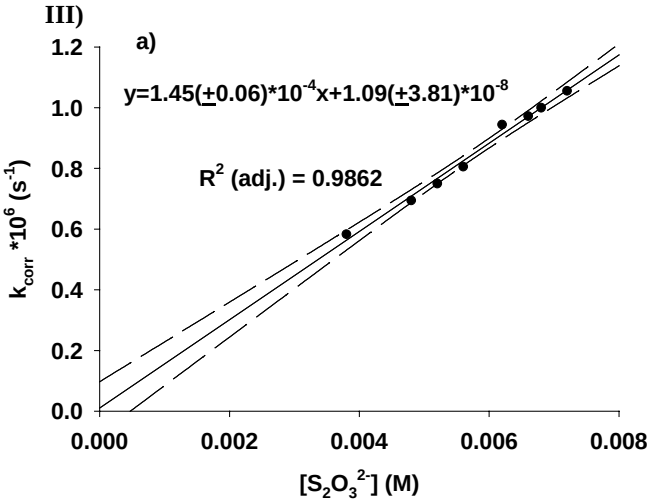
a)
y=1.45(±0.06)*10^-4x+1.09(±3.81)*10^-8
R^2 (adj.) = 0.9862
k_corr *10^6 (s^-1)
[S2O3^2-] (M)

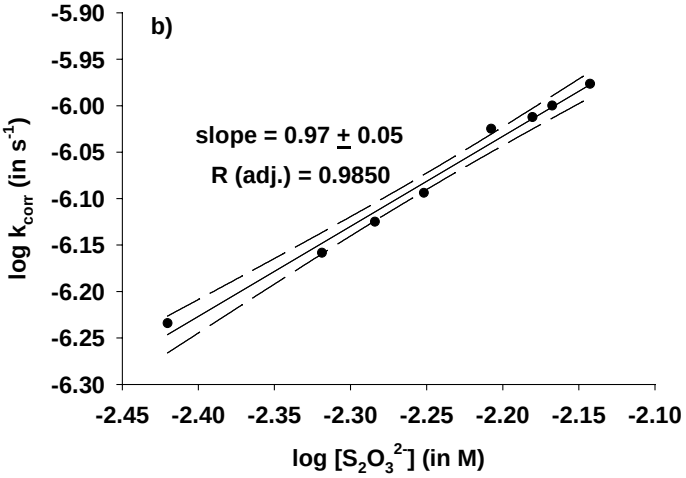
b)
slope = 0.97 ± 0.05
R (adj.) = 0.9850
log k_corr (in s^-1)
log [S2O3^2-] (in M)

IV)

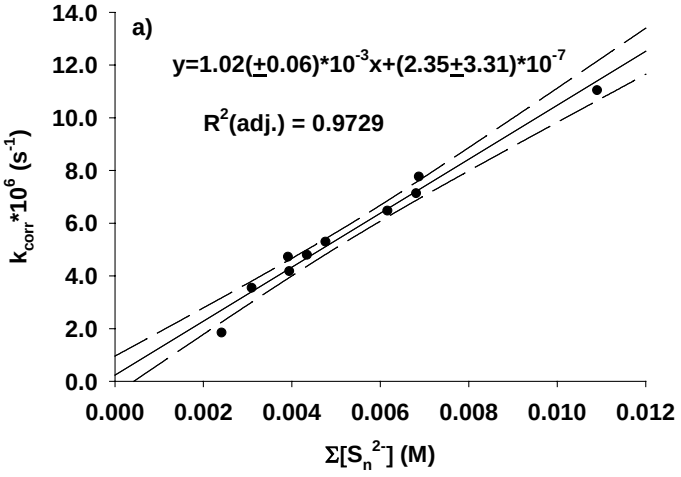
a)
y=1.02(±0.06)*10^-3x+(2.35±3.31)*10^-7
R^2(adj.) = 0.9729
k_corr *10^6 (s^-1)
Σ[Sn^2-] (M)

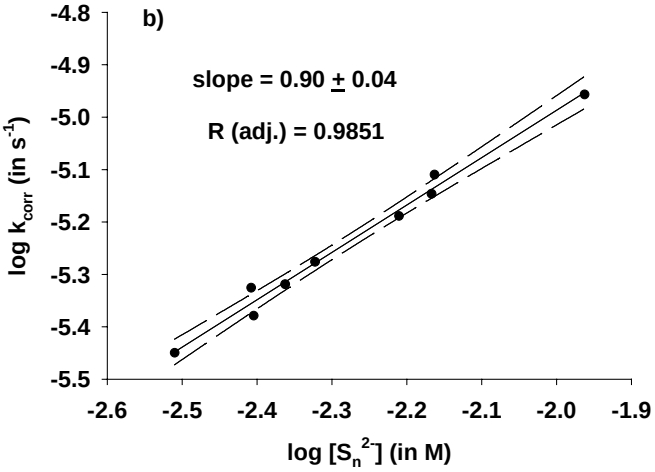

Figure 4.7 Plots of corrected reaction rate constants, k_{corr}, versus [HS⁻], [PhS⁻], [$S_2O_3^{2-}$] or Σ[S_n^{2-}] and plots of log k_{corr} versus log [HS⁻], log [PhS⁻], log [$S_2O_3^{2-}$] or log Σ[S_n^{2-}] for reaction of terbufos with I). bisulfide, II). thiophenolate, III). thiosulfate and IV). polysulfide in 50 mM phosphate/tetraborate buffer, 100 mM NaCl, and 5% methanol at 25 °C. Solid line represents linear regression of the data; the dashed lines represent 95% confidence interval.

Table 4.3 Second-order Rate Constants for Reaction of Phorate and Terbufos with Reduced Sulfide Species at 25 °C[a]

Pesticide	k''_{HS^-} ($M^{-1}\,s^{-1}$)	k''_{PhS^-} ($M^{-1}\,s^{-1}$)	$k''_{S_n^{2-}}$ ($M^{-1}\,s^{-1}$)	$k''_{S_2O_3^{2-}}$ ($M^{-1}\,s^{-1}$)
Phorate	1.2 (±0.1)×10^{-4}	2.5 (±0.1)×10^{-4}	7.8 (±0.6)×10^{-4}	9.0 (±0.7)×10^{-5}
Terbufos	1.9 (±0.2)×10^{-4}	3.2 (±0.3)×10^{-4}	1.0(±0.1)×10^{-3}	1.5 (±0.1)×10^{-4}

[a] Stated uncertainties represent at 95% confidence interval.

3.2.6. Relative reactivity of reduced s ulfur species

Our data indicated that the reduced sulfur species react with phorate and terbufos likely via a S_N2 mechanism. The Swain-Scott relationship will also allow us to evaluate the relative nucleophilicities of these important environmental sulfur nucleophiles. The Swain-Scott equation is given as (Swain and Scott, 1953)

$$\log k''_{Nuc} / k''_{H_2O} = sn \quad (3)$$

where k''_{Nuc} is the second-order rate constants for the nucleophilic displacement by a nucleophile, k''_{H_2O} is the second-order rate constant for nucleophilic attack by water, n is the nucleophilicity of the nucleophile reacting with MeBr, and s reflects the sensitivity of substrate to nucleophilic attack (s =1 for MeBr). Application of the Swain-Scott equation to the rate constants listed in Table 4.3 (Figure 4.8) demonstrated that the relative order of k''_{Nuc} values for reaction of phorate and terbufos tend to parallel that previously reported for S_N2 reactions of methyl bromide (Haag and Mill, 1988; Hine, 1962). The small derivation is quite likely explained by the steric hindrance, which is responsible for the lower reactivity of the larger thiosulfate and thiophenolate nucleophilies to phorate and terbufos. Similar observations for the relative reactivity order are observed for thiometon discussed in the previous chapter, and were also reported by Lippa and Roberts (2002) for the nucleophilic substitution reaction for chloroacetanilide herbicides and Wu and Jans (2006) for chlorpyrifos-methyl.

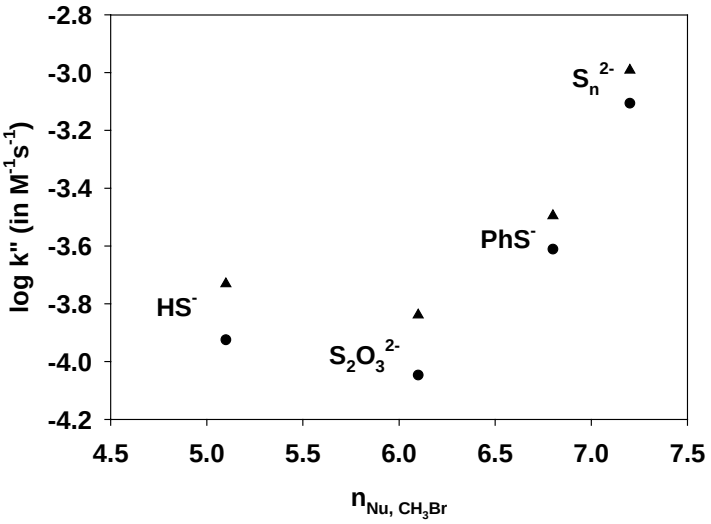

Figure 4.8 Logarithm of rate constants for reaction of phorate (●) and terbufos (▲) with various reduced sulfur nucleophiles versus n_{Nu,CH_3Br}.

3.3. Product Analysis

Product identification is a very important tool for elucidation of reaction mechanisms. Since the possible transformation products in the reactions of phorate and terbufos with thiophenolate were readily extracted into organic solvent and analyzed by GC-MS, the reaction with thiophenolate was chosen in this study as model to investigate the possible degradation products and the reaction pathways in the reactions with reduced sulfur species. The reaction with thiophenolate cannot be carried out at high concentration of thiophenolate due to the limited solubility. As our results show, the reaction of phorate with 3.2 mM $[PhSH]_T$ at pH 9.16 was only 30% faster than hydrolysis, which may make the investigation difficult. The kinetics of the reactions of phorate can be treated as

first-order reaction in the presence of excess of reduced sulfur species. The time course of the sample reaction of phorate with 3.2 mM $[PhSH]_T$ at pH 9.16 is shown in Figure 4.8. The concentrations of hydrolysis products were predicted based on the control experiment in pH 9.2 buffer in the absence of sulfur species. After the completion of the reaction, the sample was derivatized with PFBHA·HCl. The concentration of formaldehyde was determined to be 40.2 μM, which was slightly less than the formation of formaldehyde in the control experiment of hydrolysis of phorate at pH 9.20. Trace of ethyl phenyl sulfide was detected as a degradation product during the reaction of phorate and PhS^-, which amount for less than 10% after two half-lives. This indicates that the nucleophilic attack by PhS^- at the ethoxy group just makes a minor contribution to the loss of phorate. The rate constants for the loss of phorate (k_{obs}) and formation of ethyl phenyl sulfide (k_{PhSEt}) were determined to be 0.0127 h^{-1} and 0.001 h^{-1}, respectively, by simultaneously fitting the data for phorate and ethyl phenyl sulfide to numerically integrated solution of the system of governing differential rate expression using *Scientist.* The rate constant of the hydrolysis of phorate at pH 9.2 in the control experiment was measured to be 0.0099 h^{-1}. The hydrolysis and the nucleophilic attack from PhS^- at ethoxy group accounted for ~ 85% of k_{obs} in the experiment of degradation of phorate in the presence of 3.2 mM $[PhSH]_T$ at pH 9.16. These would suggest that there might be other pathway present. There exists the possibility of the nucleophilic attack of PhS^- at the carbon between the two sulfur atoms. Ethyl phenyl disulfide was detected in the

reaction, which results from the oxidation of PhS^- and EtS^- when exposed to air during the extraction. The EI mass spectroscopy is shown in Figure 4.11a. Unfortunately, like diethyl disulfide, the concentration of ethyl phenyl disulfide cannot be determined exactly in the reaction due to the uncertainty in the oxidation. Similar observation was obtained for terbufos (Figure 4.10). The formation of ethyl phenyl sulfide only accounted for less than 10% disappearance of terbufos. The mass balance therefore suggests the presence of another pathway in addition to hydrolysis and the nucleophilic attack of PhS^- at ethoxy group. Tert-butyl phenyl disulfide was detected during the reaction of terbufos and PhS^- (Figure 4.11b). The formation of ethyl phenyl disulfide in the reaction of phorate and terbufos with PhS^-, along with the formation of diethyl disulfide or di-tert-butyl disulfide in hydrolysis, implied that the carbon atom between the two sulfur atoms on the thioester side chain of phorate and terbufos might be very prone to the nucleophilic attack from H_2O/OH^- and the reduced sulfur nucleophile due to their higher reactivity. The high reactivity suggests the low selectivity towards attacking nucleophilies. Though the promotions from reduced sulfur species were observed, the contributions from the reduced sulfur species (excluding polysulfides) to the degradation of phorate were not as important as in the degradation of thiometon due to its fast hydrolysis rates. The high reactivity of polysulfide relative to bisulfide was discussed in the previous chapter. Since the polysulfides are much more reactive than HS^-, $S_2O_3^{2-}$ and PhS^-, the significant

acceleration effect was expected and also observed in the degradation of phorate in the presence of polysulfides.

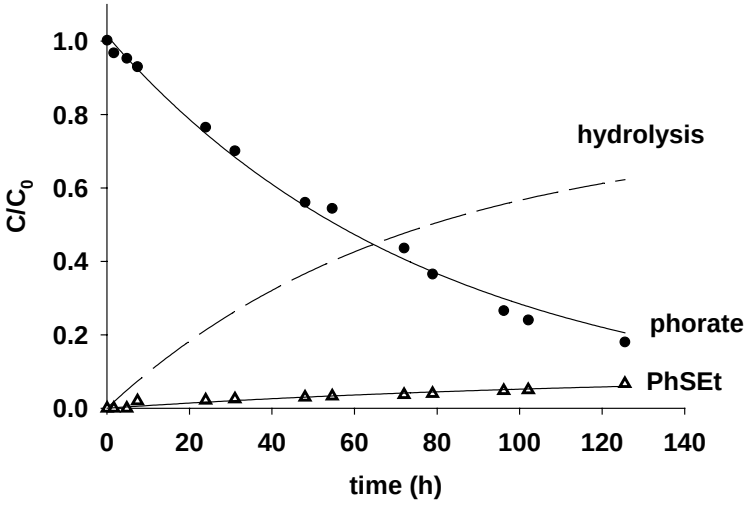

Figure 4.9 Degradation of phorate ([phoprate]$_{initial}$ = 52.2 μM) at pH 9.16, 3.2 mM [PhSH]$_T$ (50 mM tetraborate buffer, 100 mM NaCl, and 5% methanol) at 25 °C, indicating the degradation of phorate (●, $k_{obs} = 0.0127\ h^{-1}$), the formation of ethyl phenyl sulfide (▼, 0.001 h^{-1}) and hydrolysis (– – –, 0.0099 h^{-1}). Solid lines represent model fits to the data assuming exponential decay of phorate to degradation product ethyl phenyl sulfide simultaneously.

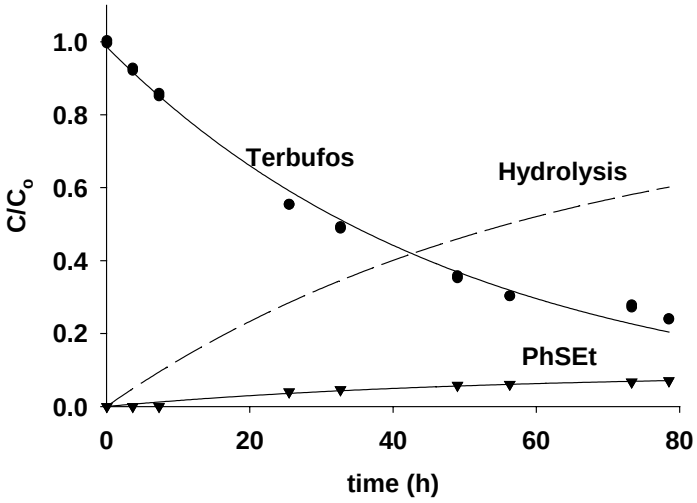

Figure 4.10 Degradation of terbufos ([terbufos]$_{initial}$ = 19.6 μM) at pH 9.26, 3.6 mM [PhSH]$_T$ (50 mM tetraborate buffer, 100 mM NaCl, and 5% methanol) at 25 °C, indicating the degradation of terbufos (•, k_{obs} = 0.0194 h^{-1}), the formation of ethyl phenyl sulfide (▼, 0.0018 h^{-1}) and hydrolysis (– – –, 0.0148 h^{-1}). Solid lines represent model fits to the data assuming exponential decay of terbufos to degradation product ethyl phenyl sulfide simultaneously.

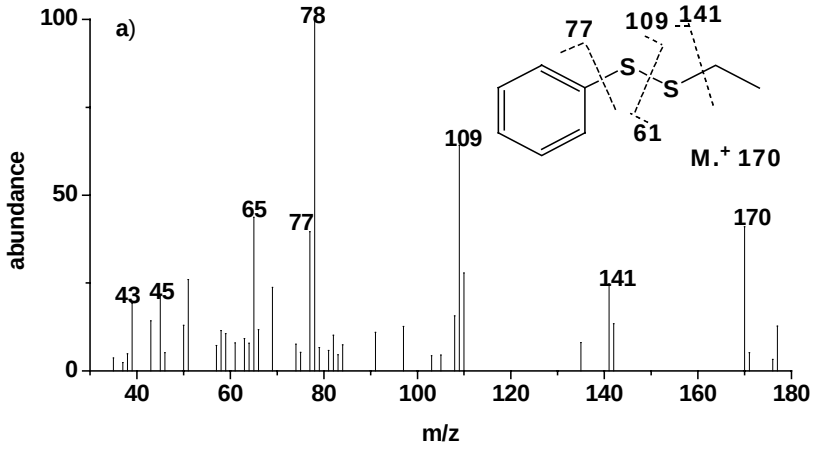

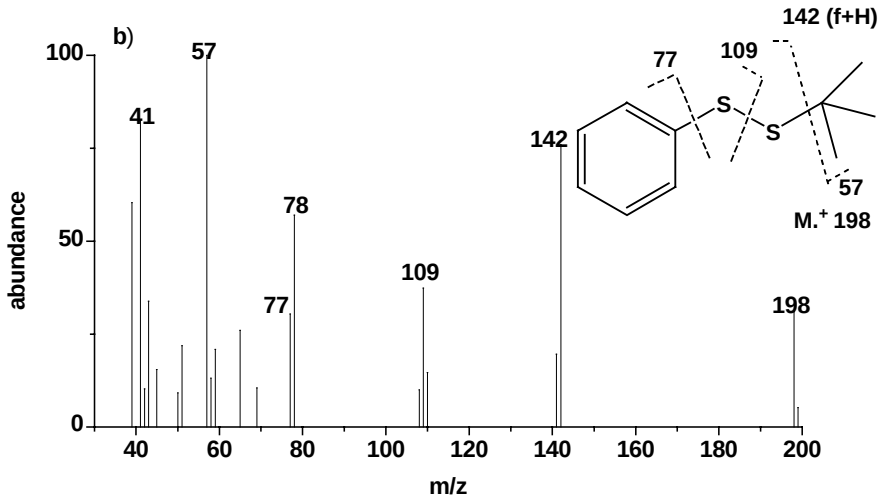

Figure 4.11 a) The EI mass spectra of the product (with the retention time of 5.71min) obtained in the reaction of phorate and thiophenolate. The retention time for phorate under these conditions was 7.81 min. b) The EI mass spectra of the product (with the retention time of 6.29 min) obtained in the reaction of terbufos and thiophenolate. The retention time for terbufos under these conditions was 8.31 min.

3.4. Temperature Dependce of the Reaction with HS^-

Thermodynamic studies are very useful in estimating the relative contribution of each pathway when multiple reaction pathways are present. The temperature-dependence of the hydrolysis of phorate and terbufos at pH 9.2 were investigated over a temperature range from 25 to 50 ^oC (Figure 4.12). The activation enthalpy, $\Delta H^{\neq}$ and activation entropy $\Delta S^{\neq}$ were determined based on the Eyring equation (Pross, 1995).

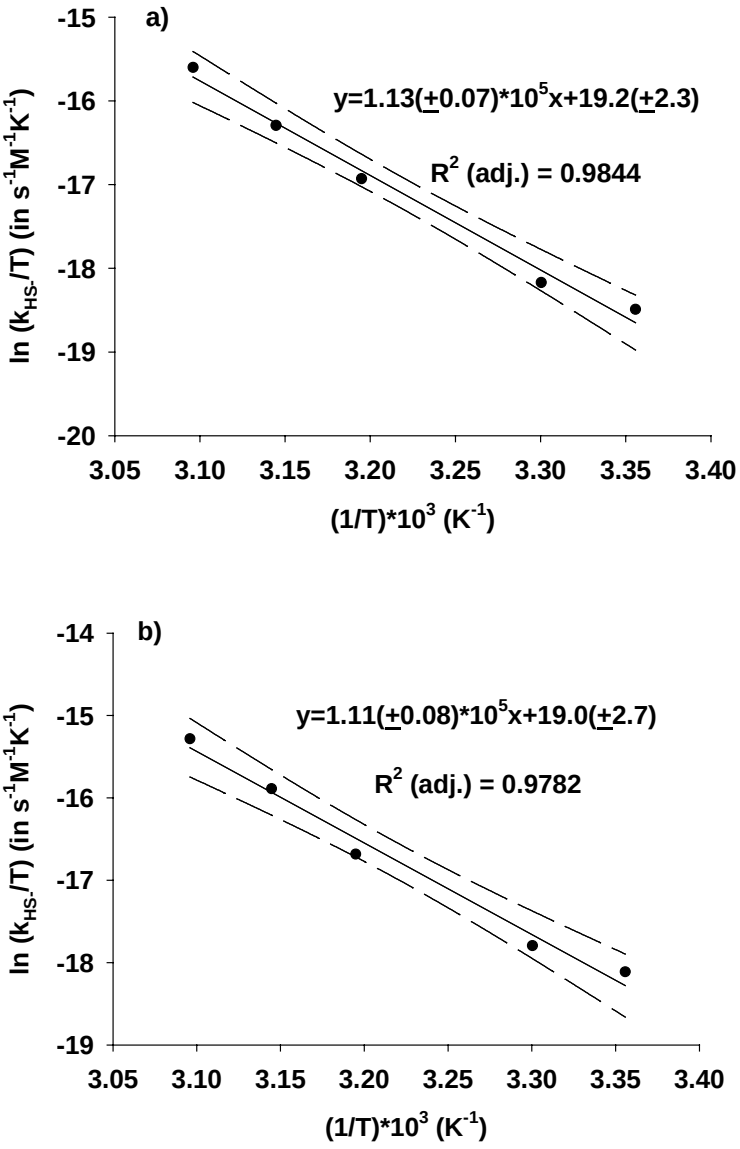

Figure 4.12 Temperature dependence of the hydrolysis of (a) phorate and (b) terbufos. The experiments were conducted in pH 9.2, 50 mM tetraborate buffer, 100mM NaCl and 5% methanol over 25 - 50 ^{o}C. Solid line represents linear regression of data; the dashed lines represent the 95% confidence level.

The reaction with HS^- was chosen to study the reactions of phorate and terbufos with reduced sulfur species from enthalpic and entropic effects. The temperature

dependence of k_{HS^-} was explored via the relationship between the rate constants corrected for hydrolysis and the experimental temperatures. Data for phorate and terbufos were plotted as shown in Figure 4.13 according to a linearized version of the Eyring equation (Pross, 1995). Linear regression analyses of the data yielded $\Delta H^{\neq}$ and $\Delta S^{\neq}$. Activation parameters in the reaction of phorate and terbufos are summarized in Table 4.4.

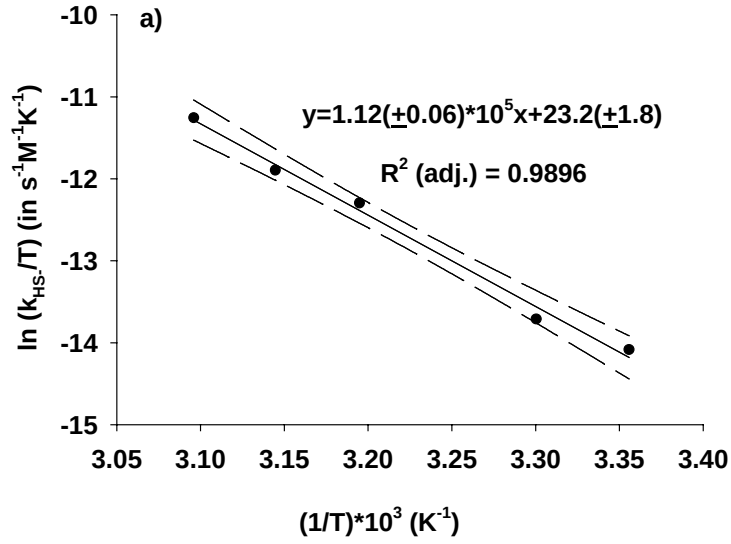

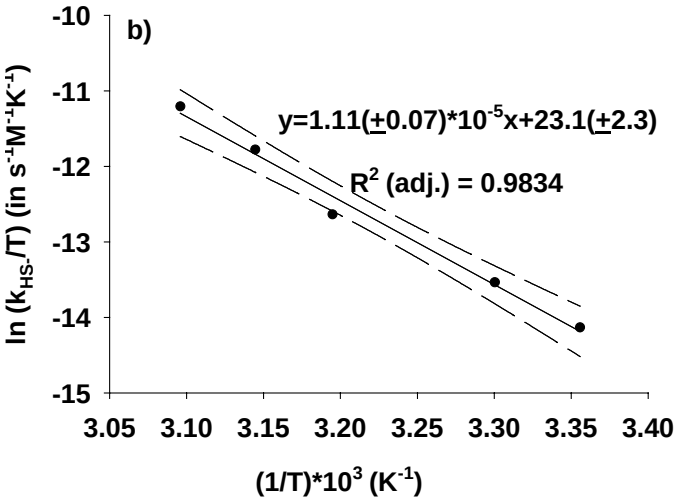

Figure 4.13 Temperature dependence of the reactions of (a) phorate and (b) terbufos with bisulfide. The experiments were conducted in pH 9.2, 5.12 mM $[H_2S]_T$, 50 mM tetraborate buffer, 100mM NaCl and 5% methanol over 25 – 50 ^oC. Solid line represents linear regression of data; the dashed lines represent the 95% confidence level.

Table 4.4 Calculated Activation Barriers for Hydrolysis and Reaction of Phorate and Terbufos with Bisulfide [a]

Pesticide	Reaction	$\Delta H^{\neq}$ (kJ/mol)	$\Delta S^{\neq}$ (J/mol·K)	$\Delta G^{\neq}$ (kJ/mol)[b]
Phorate	Hydrolysis at pH 5.7[c]	120	39	130
Phorate	Hydrolysis at pH 8.5 [c]	104	-2.8	103
Phorate	Hydrolysis at pH 9.20	93.9 (± 5.9)	-34.3 (± 19.0)	104.1 (± 5.8)
Terbufos	Hydrolysis at pH 9.20	92.4 (± 6.9)	-39.4(± 22.2)	104.2 (± 6.8)
Phorate	Reaction with HS^-	92.6 (± 4.7)	-4.5 (± 15.2)	94.0 (± 4.6)
Terbufos	Reaction with HS^-	92.5 (± 6.0)	-5.2 (± 19.3)	94.1 (± 5.9)

[a] Stated uncertainties represent at 95% confidence interval.

[b] Calculated at 298.15 K.

[c] The data reported by Hong et al. (2000)

There is no significant difference in the activation parameters for phorate and terbufos, either in hydrolysis at pH 9.2 or in the reaction with bisulfide, which might suggest a similar reactivity of phorate and terbufos. This is not surprising considering the similar structures of phorate and terbufos. This would tend to support that similar reaction pathways are present for phorate and terbufos. Comparing our data to the data repored by Hong et al. (2000), the activation parameters of the hydrolysis of phorate at pH 9.2 followed the order of activation parameters of hydrolysis at pH 5.7 and 8.5. Activation entropy reflects the loss or gain of degrees of freedom between the starting compounds and the transition states. Since multiple pathways may simultaneously contribute to the reactions of phorate and terbufos with bisulfide, the magnitude and the sign of $\Delta S^{\neq}$ can be used to evaluate the relative significance of the individual pathways. The negative $\Delta S^{\neq}$ suggest that the reaction with reduced sulfur species happen via S_N2 mechanism.

4. Conclusions

Our results demonstrated that the presence of the reduced sulfur species would accelerate the loss of phorate and terbufos from the aquatic environment. The understanding of the chemical fate in sulfidic environment is of much importance not only to the hypoxic coastal marine environments in which the reduced sulfur species are present at sufficiently high concentrations, but also to agricultural soil.

Phorate and terbufos are moderately persistent in the soil and bind to the soil organic matter and clay particles. Polysulfides and elemental sulfur are actually applied to agricultural soil. Elemental sulfur could undergo dissimilatory reduction by microorganisms to produce polysulfides and bisulfide under anoxic conditions. Hence, the abiotic reactions with reduced sulfur species may represent important reactions in agricultural soil.

Considering the hydrolysis rates of phorate and terbufos, the half-lives of phorate and terbufos at pH 7.0 in the absence of sulfur species at 25 ^{o}C can be calculated to be 70 h and 45 h, respectively, according to our hydrolysis data of phorate and terbufos. Based on the measured second-order rate constants listed in Table 4.3, we can predict the persistence of phorate and terbufos under environmentally relevant sulfidic conditions. Half-lives for phorate and terbufos in marine porewaters containing reduced sulfur species were calculated by multiplying second-order rate constants by maximum concentration of [HS^-] and $\Sigma[S_n^{2-}]$ reported by MacCrehan (1995). The results indicate that the calculated half-life of phorate and terbufos at pH 7.0, 5.6 mM HS- and 0.33 mM S_n^{2-} at 25 ^{o}C are 52 h and 34 h, respectively, which are 30 % shorter than only hydrolysis. In particular, though polysulfide concentration is much lower than bisulfide, the contribution from polysulfide is still important due to its high reactivity. Hence, the reduced sulfur species at environmentally relevant concentration may represent an important sink for phorate and terbufos in anoxic coastal marine environments.

Chapter V

Degradation of Naled and Dichlorvos

Part I Naled

1. Introduction

In the previous chapter, the degradation mechanisms of the four organophosphorus pesticides involved reduced sulfur species are nucleophilic substitutions, wherever the initial attack center is. In addition, reduced sulfur species are also the reactive agents for dehalogenation of halogenated organic compounds in natural waters. The dehalogenation mechanisms which are generally believed to be of great environmental significance include nucleophilic substitution, dehydrohalogenation and reductive dehalogenation. Recent work by a number of investigators has demonstrated that displacement of halide from bromoaliphatic compounds, as well as from chloroaliphatic compounds by sulfur nucleophiles (Schwarzenbach et al., 1985; Barbash and Reinhard, 1989; Roberts et al., 1992; Miller et al., 1998; Loch et al., 2002; Lippa et al., 2002). In this part, we will examine the potential importance of different sulfur nucleophiles as agents for the reductive dehaloganation in natural waters.

Mosquito-borne diseases affect millions of people worldwide each year. In the United States, some species of mosquitoes can transmit diseases such as West Nile Virus, encephalitis, dengue fever, and malaria to humans, and a variety of diseases

to wildlife and domestic animals. Naled (1,2-dibromo-2,2-dichloroethyl dimethyl phosphate) (Figure 5.1) is an adulticide used to kill adult mosquitoes. Naled is an organophosphate pesticide with contact and stomach poison activity and short residual effect (Thompson, 1985), which has been registered since 1959 for use in the United States. Naled is used primarily for controlling adult mosquitoes, but it is also used to control aphids, mites, and flies on crops and in greenhouses, mushroom houses, animal and poultry houses, kennels, food processing plants, and aquaria. Naled is recommended for mosquito control by the New York State's West Nile Virus Response Plan (New York State Department of Health, 2000). State and local authorities apply naled by truck-mounted or aircraft-mounted sprayers. Naled is manufactured by bromination of dichlorvos (2,2-dichlorovinyl dimethyl phosphate) (Figure 5.1) and has a much lower vapor pressure than dichlorvos (Howard and Meylan, 1997). It is postulated that dichlorvos may be the "insecticidal principle" of naled (Morifusa, 1974). A complex process of molecular transport and degradation, including volatilization, photolysis, hydrolysis and microbial breakdown, controls the fate of naled, as well as of other organophosphate pesticides (Racker, 1992). A study of pesticide drift and degradation in the Florida Keys found that naled drifted 750 m into a wildlife refuge (Hennessey, 1992). This study also reported that no significant loss of naled residue was detected during a 4 h period based on control degradation experiments. A later study by Valent USA Corporation (Walnut Creek, CA) reported that naled breaks down and dissipates rapidly in the environment, with half-life on soil of

approximately 0.5 h under light or dark conditions (Valent USA Corporation, 1993).

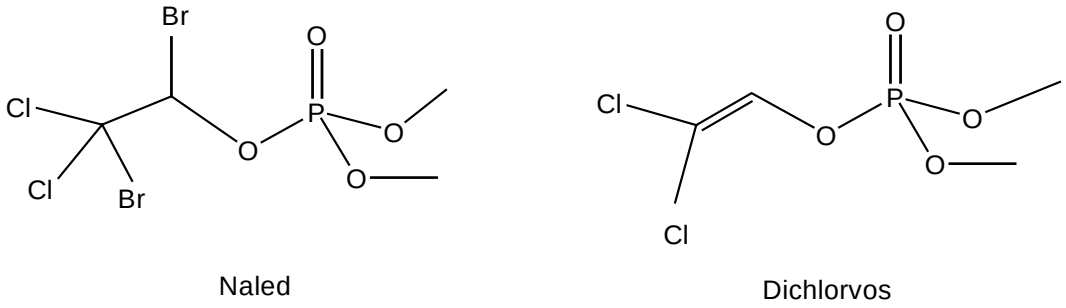

Figure 5.1 Structures of naled and dichlorvos

The reductive transformation of halogenated organic compounds has been widely reported to occur in reducing environments (Zoro et al., 1974; Klecka and Gonsior, 1984; Jafvert and Wolfe, 1987; Criddle et al., 1986; Peijnenburg et al., 1991; Roberts et al., 1996; Arnold et al., 2002; Totten et al., 2001). Dehalogenation of vicinal dihalides can be promoted by a great variety of nucleophiles or two-electron reductants, which include halide ions (Baciocchi and Schiroli, 1969; Tsai et al., 1970; Kwok et al., 1970) except fluorides, sulfur nucleophiles (Janout et al., 1976; Ramasamy et al., 1978; Ibne-Rasa et al., 1966), phosphorus nucleophiles (Borowitz et al., 1971; Devlin and Walker, 1972; Schroeder et al., 1970), organometallic compounds (Posner and Ting, 1973), and nitrogen and oxygen nucleophiles (Kasal, 1976; Speziale and Tung, 1963). As other *vic*-dihalides, naled may be debrominated by treating it with a reducing

agent (Morifusa, 1974; Scheybal et al., 1978; Larson and Weber, 1994). Vicinal debromination is typically the dominant pathway for the reductive debromination of vicinal dibromides. The presence of two chlorine atoms bound to one carbon makes the bromine on the same carbon of naled more susceptible to the attack of nucleophiles. The predominance of vicinal dehalogenation is attributed to the formation of an intermediate in which stabilization occurs through bridging of the bromine adjacent to the carbon from which the initial bromide was removed (Carey and Sundberg, 2004). The expulsion of a bromide ion through a bridged intermediate requires an anti orientation of the two bromine atoms. The attack of a nucleophile at one bromine enhances its nucleophilicity and permits formation of the bridged ion, which gives rise to the resulting dichlorvos fast in the following step (Scheme 5.1) (Mathai et al., 1970).

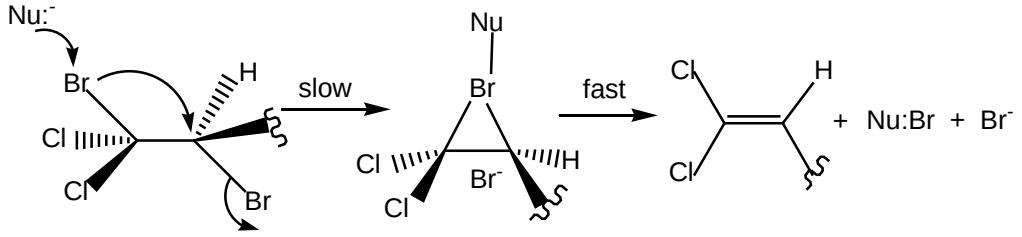

Scheme 5.1 Proposed mechanism of debromination of naled

The formation of the intermediate bridged ion is the rate-determining step, and the kinetics would be anticipated to be first-order both in nucleophilic reductant and naled.

$$rate = -d[naled]/dt = k[Nu]\cdot[naled] = k_{obs}[naled] \quad (1)$$

When the concentration of the nucleophile is much higher than that of naled, the kinetics can be treated as pseudo-first-order reaction.

The primary purpose of this part was to examine the kinetics and products of the reaction of naled with selected reduced sulfur species. The reduced sulfur species discussed here include hydrogen sulfur (H_2S), bisulfide (HS^-), thiophenol (PhSH), thiophenolate (PhS^-) and thiosulfate ($S_2O_3^{2-}$). The impact of the reduced sulfur species on the abiotic transformation of naled was investigated in well-defined aqueous solution under anaerobic conditions. Reactions were monitored at varying temperatures and concentrations of bisulfide at environmentally relevant pHs to investigate the second-order rate constant and activation parameters. The products were characterized by GC/MS, and confirmed and quantified with commercial standards.

2. Materials and Methods

2.1. Chemicals

Naled (1,2-dibromo-2,2-dichloroethyl dimethyl phosphate, 99.2%) and dichlorvos (2,2- dichlorovinyl dimethyl phosphate, 99%) were obtained from Chem Service (West Chester, PA). All solvents and reagents that were used were analytical grade or equivalent. Ethyl acetate and methanol were HPLC grade and were obtained from Fisher Scientific. All reaction solutions were prepared in an anaerobic glovebox (5% H_2, 95% N_2) and aqueous solutions were prepared from

argon-purged deionized water (DW) (Mill-Q gradient system, Millipore, Bedford, MA). The starting concentration of naled was ~ 50 μM.

2.2. Chromatographic Analysis

Ethyl acetate extracts were analyzed on a Fisons GC 8000 equipped with an AS 800 autosampler, an ECD-80 electron capture detector (Carlo Erba Instruments) containing ^{63}Ni beta emitting radioactive source of 370 MBq (10 mCi), a split/splitless injector and a 30 m DB-5, 0.25 mm i.d. × 0.25 μm fused-silica capillary column (J&W, Folsom, CA). The carrier gas was helium (99.999%) and the make up gas was methane/argon. GC/MS system to identify and analyze the degradation products was equipped with a split/splitless injector and a 30 m AT-5ms, 0.25 mm i.d. × 0.25 μm fused-silica capillary column (Alltech, Deerfield, IL). EI mass spectra were generated using electron energy of 70 eV, monitoring for ions *m/z* 80-500 in full-scan and selected ion recording (SIR) modes. The selected ions were 109, 145 and 185. The source temperature employed for the ionization technique was 200 ºC. *Temperature program:* Injector temperature and detector temperature were set at 250 ºC. The column temperature was held at 80 ºC for one minute then increased at a rate of 20 ºC/min to 250 ºC and finally held constant at 250 ºC for 4 minutes.

3. Results and Discussion

3.1. Hydrolysis of Naled in pH Buffer

Hydrolysis is a major removal process for organophosphorus insecticides and strongly dependent on the pH and other solution constituents. In aquatic systems, water and its hydrolysis products are expected to be the dominant nucleophiles. Hydrolysis of naled was investigated over pH range of 5.7 – 7.7 at 25 ºC. Dichlorvos was detected as the sole hydrolysis product of naled in our study, which demonstrated that debromination was dominant. OH^- was expected as active species and hydrolysis of naled was expected to be pH-dependent. The hydrolysis reaction of naled is treated as a pseudo-first-order reaction. The k_h is measured as the slope of the plot of ln[naled] vs. the reaction time. The kinetics data of the experiments display good fit with pseudo-first order reaction profile and the observed hydrolysis rate constants of naled at various pH values at 25 ºC are shown in Table 5.1. Hydrolysis of naled was also carried out at pH 6.95 and 7.46 at 5 ºC and 12 ºC, respectively. Time course of hydrolysis of naled at pH 6.03 at 25 ºC was shown in Figure 5.2a. The mass balance illustrated essentially 100% conversion of naled to dichlorvos. In the pH range of 5.7 – 7.7, the empirical linear relationship between pH versus log k_h can be expected as log k_h = 0.23 ($\pm$ 0.02)* pH –2.54 ($\pm$ 0.13) at 95% confidence level (Figure 5.2b).

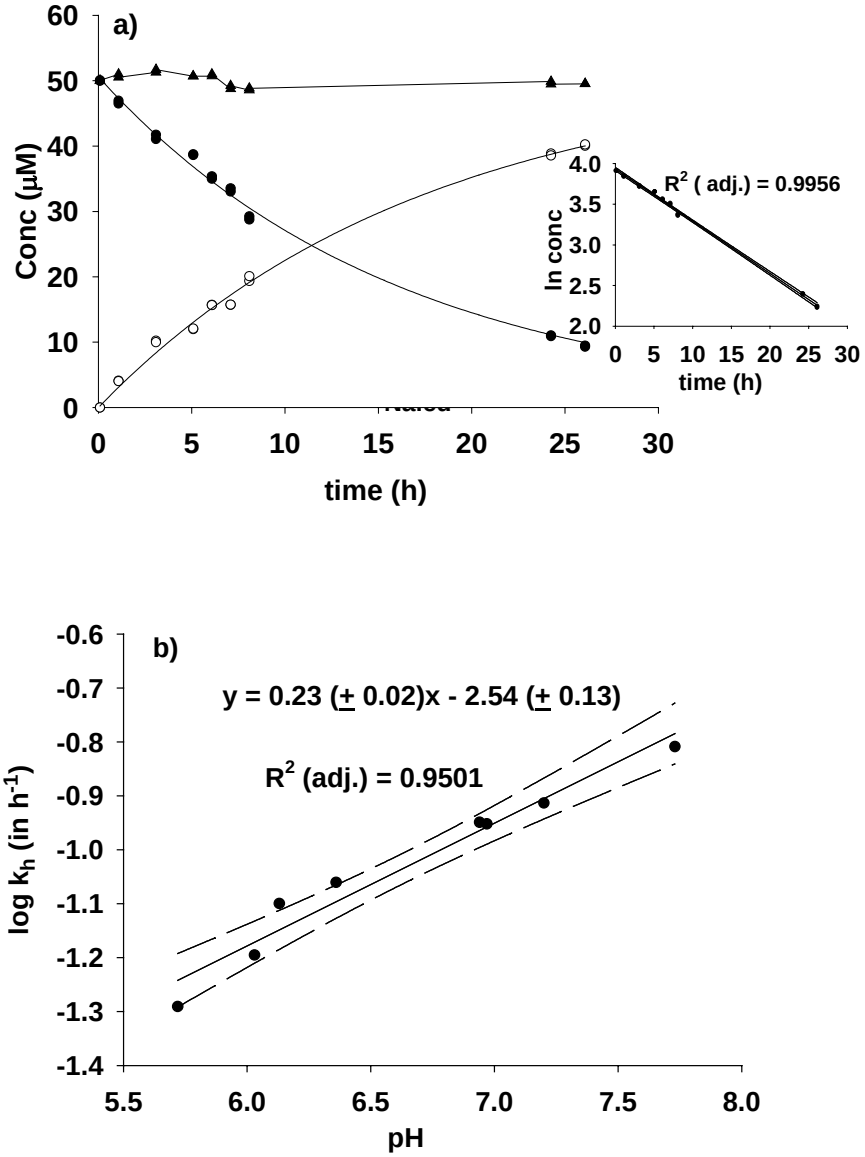

Figure 5.2 (a) Hydrolysis of naled at pH 6.03 (50 mM phosphate buffer, 100 mM NaCl, and 5% methanol) at 25 °C, indicating the degradation of naled (•), the formation of dichlorvos (o) and the mass balance (▲). Solid lines represent model fits to the data assuming exponential decay of naled to single degradation product dichlorvos simultaneously. Inset depicts the data plotted in

semilogarithmic form to obtain the observed pseudo-first-order reaction rate constants. (b) Plot of $\log k_h$ *versus pH for the hydrolysis of naled for various pH in 50 mM phosphate buffer, 100 mM NaCl, and 5% methanol at 25 °C. Solid line represents linear regression of the data; the dashed lines represent 95% confidence interval.*

Table 5.1 Hydrolysis Rate Constants of Naled in 50 mM Phosphate Buffer Containing 100 mM NaCl and 5% Methanol.

pH	Temperature (ºC)	k_h (s^{-1})*	half life (h)
5.72	25	$1.42 (\pm 0.04)\times10^{-5}$	13.5
6.03	25	$1.77 (\pm 0.06)\times10^{-5}$	10.9
6.13	25	$2.21 (\pm 0.05)\times10^{-5}$	8.72
6.36	25	$2.42 (\pm 0.07)\times10^{-5}$	7.97
6.94	25	$3.10 (\pm 0.07)\times10^{-5}$	6.21
6.97	25	$3.13 (\pm 0.09)\times10^{-5}$	6.16
7.2	25	$3.39 (\pm 0.09)\times10^{-5}$	5.68
7.73	25	$4.32 (\pm 0.10)\times10^{-5}$	4.46
6.95	12	$1.56 (\pm 0.05)\times10^{-6}$	124
7.46	12	$2.01 (\pm 0.04)\times10^{-6}$	96.3
6.95	5	$2.42 (\pm 0.05)\times10^{-6}$	79.7
7.46	5	$4.50 (\pm 0.04)\times10^{-6}$	42.8

* The rate constants of hydrolysis of naled were obtained at the 95% confidence interval.

3.2. Reduction of Naled by Reduced Sulfur Species at 5 °C

3.2.1. Reaction of naled with hydrogen sulfide at 5 °C

Our hydrolysis data demonstrated that hydrolysis of naled occurs fast and this may be one of the reasons for the paucity of published information on the fate and degradation of naled. The half-life of naled in the pH 6.03 buffer without reduced sulfur species was measured to be 10.9 h at 25 °C in our experiments. Our preliminary experiments demonstrated that the reaction of naled with bisulfide at 25 °C occurs too fast to be measured exactly with our method. Naled was not detectable 2 minutes after it was added into a pH 6.03 buffer containing 0.8 mM total hydrogen sulfide at 25 °C. To try to understand the chemical transformation of naled in the presence of reduced sulfur species, the reaction was assessed at a lower temperature. The reaction of naled with bisulfide was investigated over pH range of 5.4 – 8.0 at 5 °C. The concentrations of $[H_2S]_T$ in the reaction were 0.25 – 4.0 mM. The kinetics data of the degradation of naled in the buffer solution containing bisulfide at 5 °C display good fits with a pseudo-first-order reaction model. And hydrolysis of naled at 5 °C was also investigated to exclude the influence from buffer system. No discernible reaction of naled occurred in the control experiments conducted in the absence of bisulfide at 5 °C. Hydrolysis half-lives at pH 6.95 and 7.46 were determined at 5 °C over the expanded time courses to be 96 h and 124 h, respectively, which was more than 100 times slower

than the reaction with hydrogen sulfide. Therefore, hydrolysis can be neglected when the degradation of naled is investigated in the presence of reduced sulfur species under these conditions. Hence, the reaction rate of naled in a hydrogen sulfide solution containing H_2S and HS^- can be expressed as the following equation:

$$k_{obs} = k_h + k''_{H_2S}[H_2S] + k''_{HS^-}[HS^-] = k''_{H_2S}[H_2S] + k''_{HS^-}[HS^-] \quad (2)$$

The dominant transformation product, dichlorvos, was the only product detected during the reaction of naled with bisulfide. The time course of the reaction of naled with 0.55 mM bisulfide in pH 6.55, 50 mM phosphate buffer, 100 mM NaCl, and 5% methanol at 5 °C is shown in Figure 5.3a. The time course illustrates essentially 100% conversion of naled to dichlorvos and it can be concluded that the debromination would be the only significant reaction in the degradation of naled in the presence of bisulfide. Due to the difference in reactivity of various hydrogen sulfur species (e.g., H_2S vs. HS^-), a pH dependent pseudo-first-order rate constant is expected (Jans and Miah, 2003). This rate is divided by the total concentration of hydrogen sulfur species, which results in the apparent second-order rate constant, k''_{app}. k''_{app} is assumed to be the sum of contributions of HS^- and H_2S and can be given by the expression:

$$k''_{app} = (k_{obs} - k_h)/[H_2S]_T \approx k_{obs}/[H_2S]_T$$

$$= k''_{H_2S}\frac{[H_2S]}{[H_2S]_T} + k''_{HS^-}\frac{[HS^-]}{[H_2S]_T} \quad (3)$$

with $[H_2S]_T = [H_2S] + [HS^-]$. Substituting expression for $[H_2S]$ and $[HS^-]$ as a function of $[H_2S]_T$:

$$\alpha_{HS^-} = \frac{[HS^-]}{[H_2S]_T} = \left(1 + \frac{[H^+]}{K_a^{'}}\right)^{-1} \qquad \alpha_{H_2S} = \frac{[H_2S]}{[H_2S]_T} = \left(1 + \frac{K_a{}'}{[H^+]}\right)^{-1} \qquad (4)$$

in which, the acid dissociation constant of H_2S, K_a' is $10^{-7.28}$ at 5 °C (Millero, 1986). After rearrangement, k''_{app} can be given in term of α_{HS^-} :

$$k''_{app} = k_{obs} / [H_2S]_T = k''_{H_2S} + \alpha_{HS^-} \cdot \left(k''_{HS^-} - k''_{H_2S}\right) \qquad (5)$$

The plot of k''_{app} versus α_{HS^-} shows a linear correlation, which supports our assumption. Linear regression analysis of k''_{app} versus α_{HS^-} yielded a slope equal to 6.11 ($\pm$ 0.27)$\times 10^2$ M^{-1} min^{-1} and an intercept not significantly different from zero at 95% confidence level (Figure 5.3b). Hence, k''_{HS^-} was obtained to be 10.2 $\pm$ 0.4 M^{-1} s^{-1} and k''_{H_2S} was near zero. Therefore, of H_2S and HS^-, only HS^- is effective in transforming naled.

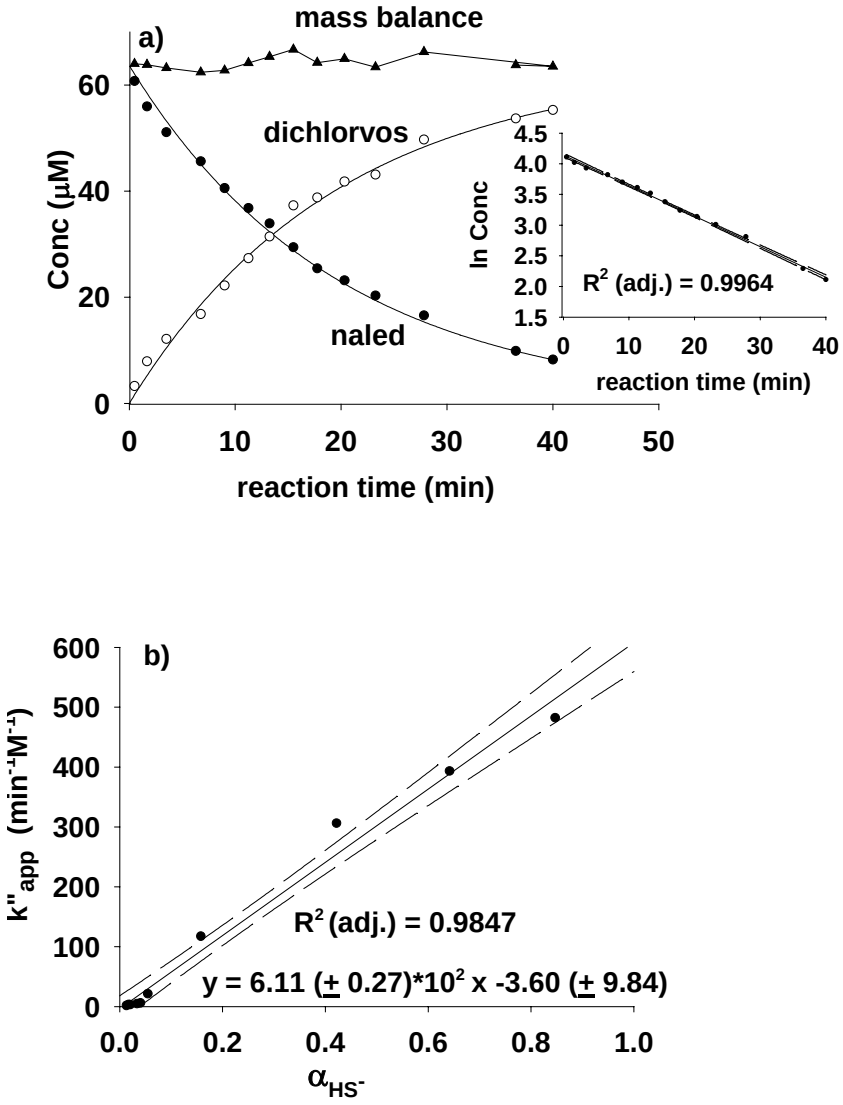

Figure 5.3 (a) Reaction of naled with 0.55 mM $[H_2S]_T$ at pH 6.55 (50 mM phosphate buffer, 100 mM NaCl, and 5% methanol) at 5 °C, indicating the degradation of naled (•), the formation of dichlorvos (o) and the mass balance (▲). Solid lines represent model fits to the data assuming exponential decay of naled to single degradation product dichlorvos simultaneously. Inset depicts the data plotted in semilogarithmic form to obtain the observed pseudo-first-order

reaction rate constants. (b) Plot of apparent second-order reaction rate constants, k''_{app} *versus* α_{HS^-} *for the reaction of naled with bisulfide for various pH in 50 mM phosphate buffer, 100 mM NaCl, and 5% methanol at 5 °C. Solid line represents linear regression of the data; the dashed lines represent 95% confidence interval.*

3.2.2. Reaction of naled with thiophenol at 5 °C

Reaction of naled with thiophenol was investigated over pH range of 5.0 – 6.5 at 5 °C. The concentrations of $[PhSH]_T$ in the reaction were 0.20 – 1.11 mM. Reduction of naled by thiophenol also followed a pseudo first-order kinetics model. Naled was again reduced to form dichlorvos, which was the only detectable product (Figure 5.4). Mass balances demonstrated almost 100% conversion of naled to dichlorvos. Due to the fact of no detectable loss of naled in buffer control experiment in absence of thiophenol over comparable time periods, it can be concluded that the disappearance of naled only results from the debromination by thiophenol. To try to understand the effect of the various thiophenol species on debromination of naled, the reactivity of thiophenol and thiophenolate was assessed as for H_2S and HS^- species.

$$k_{obs} = k_h + k''_{PhSH}[PhSH] + k''_{PhS^-}[PhS^-]$$

$$k''_{app} = (k_{obs} - k_h)/[PhSH]_T = k_{obs}/[PhSH]_T$$

$$= k''_{PhSH} + \alpha_{PhS^-} \cdot \left(k''_{PhS^-} - k''_{PhSH}\right) \quad (6)$$

in which, $\alpha_{PhS^-} = \frac{[PhS^-]}{[PhSH]_T} = \left(1 + \frac{[H^+]}{K_a^{'}}\right)^{-1}$ and the acid dissociation constant of PhSH, K_a' is $10^{-6.50}$ at 25 °C (Dean, 1985).

The plot of k''_{app} versus α_{PhS^-} shows a linear correlation, which allows the determination of the second-order reaction rate constants k''_{PhS^-} and k''_{PhSH} at 95% confidence level (Figure 5.4b). k''_{PhS^-} was obtained to be 27.3 $\pm$ 0.9 $M^{-1}s^{-1}$ and k''_{PhSH} was not significantly different from zero, which indicates that the reaction of naled with thiophenolate is much faster with respect to hydrolysis, and the two thiophenol species show significant difference in their reactivity toward naled. In addition, PhS^- is a more reactive reductant than HS^- for debromination of naled.

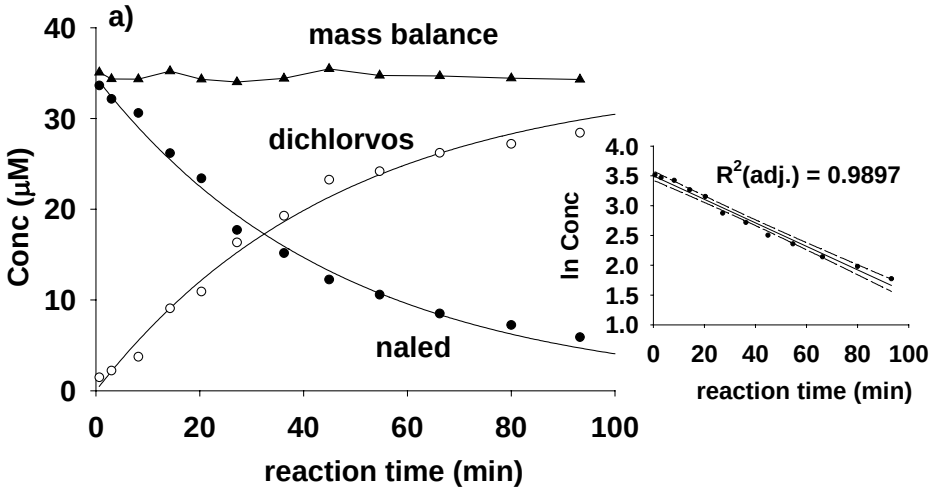

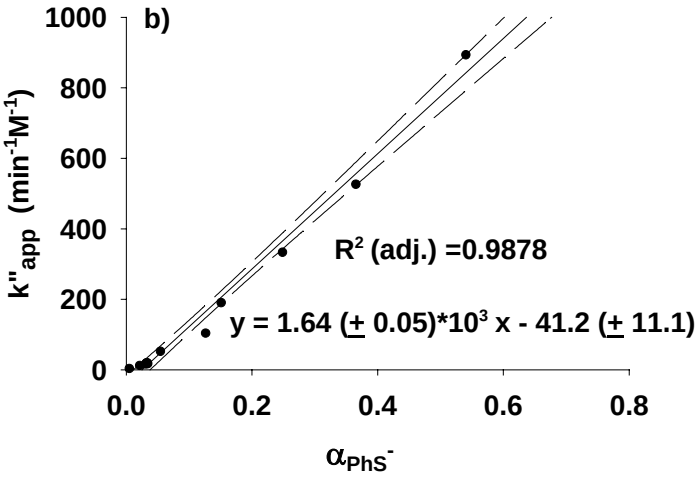

Figure 5.4 (a) Reaction of naled with 1.02 mM thiophenol at pH 5.04 (50 mM phosphate buffer, 100 mM NaCl, and 5% methanol) at 5 °C, indicating the degradation of naled (•), the formation of dichlorvos (o) and the mass balance (▲). Solid lines represent model fits to the data assuming exponential decay of naled to single degradation product dichlorvos simultaneously. Inset depicts the data plotted in semilogarithmic form to obtain the observed pesudo-first-order reaction rate constants. (b) Plot of apparent second-order reaction rate constants, k''_{app}*, versus* α_{PhS^-} *for the reaction of naled with thiophenol for various pH in 50 mM phosphate buffer, 100 mM NaCl, and 5% methanol at 5 °C. Solid line represents linear regression of the data; the dashed lines represent 95% confidence interval.*

3.3.3. Reaction of naled with thiosulfate at 5 °C

Reaction of naled with thiosulfate was investigated over pH range of 5.5 – 6.5 at 5 °C. $S_2O_3^{2-}$ is known to be the dominant species in pH buffer solutions of

sodium thiosulfate over the investigated pH range. The concentrations of [$S_2O_3^{2-}$] in the reaction were 0.15 – 0.22 mM. Naled was also reduced to form sole product, dichlorvos (Figure 5.5). Mass balances demonstrated almost 100% conversion of naled to dichlorvos. Due to the fact of no detectable loss of naled in buffer control experiment in absence of thiosulfate over comparable time periods, it can be concluded that the disappearance of naled only results from the debromination by thiosulfate. The pseudo-first-order reaction model was not applicable for the experiments with thiosulfate due to the fact that the ratio of thiosulfate to naled applied in the experiment is not high enough to meet the assumption of a pseudo-first-order reaction. Therefore, the results for the reaction of naled with thiosulfate were modeled assuming second-order kinetics (Atkins and de Paula, 2001):

$$-d[naled]/dt = k[naled][S_2O_3^{2-}]$$

$$= k[naled]\{[S_2O_3^{2-}]_0 - ([naled]_0 - [naled])\}$$

$$= k[naled](\Delta c_0 - [naled]) \quad (7)$$

where $[naled]_0$ and $[S_2O_3^{2-}]_0$ are the initial concentrations of naled and thiosulfate, respectively, and Δc_0 is the difference of the initial concentration of naled and thiosulfate. The decrease in the concentration of thiosulfate from the initial concentration at each time point was assumed to be equal to the decrease in the concentration of naled from the initial concentration. Hence, the second-order reaction rate constants of thiosulfate in the reaction with naled are obtained under

the second-order reaction kinetics model (Figure 5.5b). The second-order reaction rate constant was determined to be 5.0 $\pm$ 0.3 M^{-1} s^{-1} by averaging the second-order rate constants obtained from the experiments with different concentrations of thiosulfate (Table 5.2).

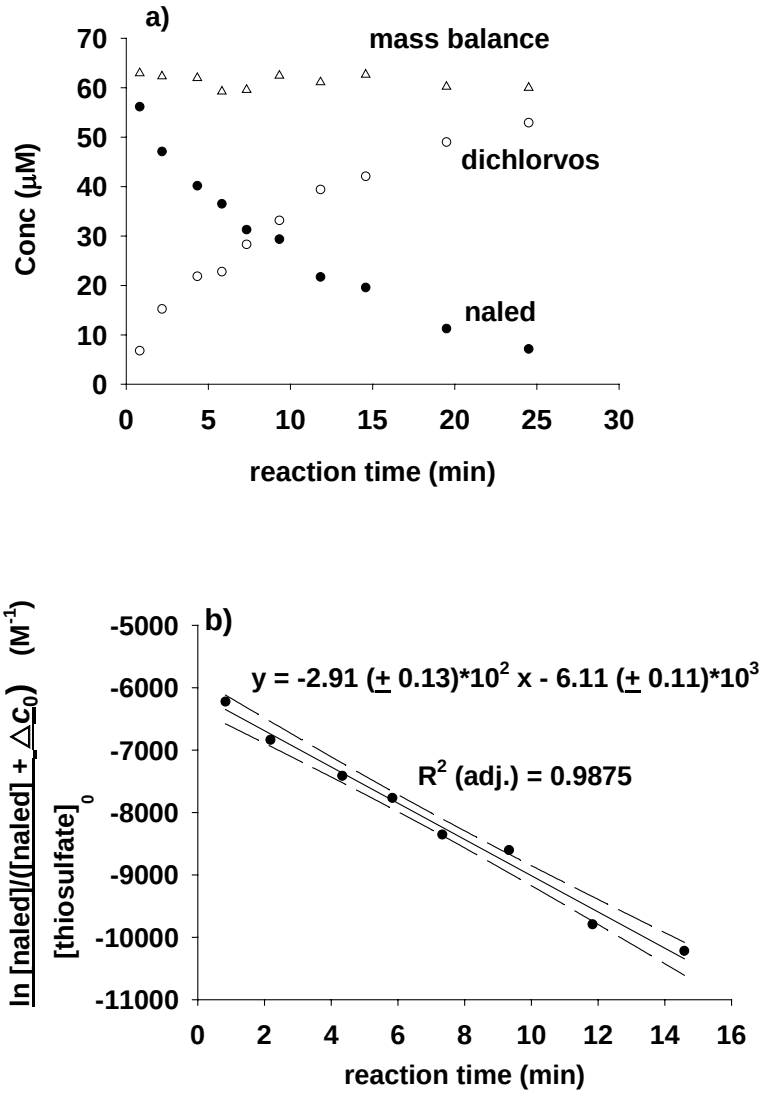

Figure 5.5 (a) Reaction of naled with 0.22 mM thiosulfate at pH 5.98 (50 mM phosphate buffer, 100 mM NaCl, and 5% methanol) at 5 °C, indicating the

degradation of naled (•), the formation of dichlorvos (o) and the mass balance (Δ). (b) The data plotted in semilogarithmic form (based on second-order reaction model) to obtain the second-order reaction rate constants for the reaction of naled with 0.22 mM thiosulfate at pH 5.98 (50 mM phosphate buffer, 100 mM NaCl, and 5% methanol) at 5 °C. Δc_0 *is the different between the initial concentrations of thiosulfate and naled,* Δc_0 *= [thiosulfate]*$_0$ *– [naled]*$_0$*. Solid line represents linear regression of the data; the dashed line represents 95% confidence interval.*

Table 5.2 The Second-order Rate Constants of the Reaction of Naled with Thiosulfate at 5 °C Obtained under the Second-order Reaction Model

pH	$[S_2O_3^{2-}]_0$ (mM)	$[naled]_0$ (μM)	$k''_{S_2O_3^{2-}}$ ($M^{-1}min^{-1}$)*
6.50	0.154	49.0	293.1 ± 13.4
5.98	0.223	56.1	290.6 ± 13.3
5.50	0.186	48.7	313.8 ± 15.5
5.76	0.176	46.3	298.6 ± 13.3
5.75	0.198	47.2	296.1 ± 15.6
5.72	0.212	52.3	319.7 ± 14.1

* The rate constants were obtained at the 95% confidence interval.

$k''_{S_2O_3^{2-}}$ = 302 (± 18) $M^{-1}min^{-1}$ = 5.03 (± 0.30) $M^{-1}s^{-1}$

3.3. Activation Parameters for Reaction with Bisulfide

To explore the extremly fast reaction of naled with bisulfide for enthalpic and entropic effects, k_{obs} was measured in bisulfide solutions (pH 5.53, $[H_2S]_T$ = 0.24 mM) over the temperature range of 5.0 °C to 20.0 °C, and the activation parameters were determined. No measurable loss of naled was observed in the absence of bisulfide at these temperatures over a comparable time period in buffer control experiments. Based on the previous discussion, $k"_{H_2S}$ can be assumed too small to make a significant contribution to the degradation of naled, the contribution of sulfur species to k_{obs} is entirely consistent with HS^- as the only reactive species in the solution. The bisulfide concentrations at the reaction temperatures were computed using the expression for the temperature dependence of pK_a of hydrogen sulfide reported by Millero (1986). Data for the temperature dependence of reaction of naled with HS^- are shown in Figure 5.6 according to a linearized version of the Eyring equation (Pross, 1995):

$$\ln(k"_{HS^-}/T) = \ln(k/h) - \Delta H^{\neq}/RT + \Delta S^{\neq}/R \qquad (8)$$

where k is the Boltzmann's constant, h is the Planck's constant, R is the gas constant, T is the temperature in Kelvin, and $\Delta H^{\neq}$ and $\Delta S^{\neq}$ are the enthalpic and entropic contributions to the overall activation barrier $\Delta G^{\neq}$, respectively. Linear regression analyses yielded a slope of $-1.96\ (\pm 0.04) \times 10^4$ and an intercept of 65.9 ($\pm$1.2) at 95% confidence level, which allow the extraction of the value of $\Delta H^{\neq}$ and $\Delta S^{\neq}$ values to be 163 ($\pm$3) kJ/mol and 351 ($\pm$10) J/mol·K respectively.

The Arrhenius activation energy, E_a, can be obtained to be 165 ($\pm$3) kJ/mol, and activation barrier $\Delta G^{\neq}$ is calculated to be 58.2 ($\pm$ 5.3) kJ/mol at 25 °C. The very fast reaction and the relative low molfraction of HS^- in the solutions under the experimental pH range may introduce a high uncertainty in the prediction of activation parameters. The positive value of $\Delta S^{\neq}$, which results in a substantial decrease in the entropic barrier, may indicate the formation of bridged transition state in the reductive elimination. As for the two-step process, the formation of the bridged intermediate is the rate-determining step. The bridged intermediate would be very short-life and transformed to dichlorvos almost instantly. The disappearance rate of naled is the same as the appearance and disappearance rate of bridged intermediate and the appearance rate of dichlorovos. The transition state involves the nucleophile and naled. Though the formation of the bridged intermediate would restrict its motions, the effect of nucleophile attached to the bridged intermediate and the leaving bromide ion still associated with intermediate would lead to lower-ordered transition state from the view of the whole system. The very positive value of $\Delta S^{\neq}$ would tend to suggest that the rather low $\Delta G^{\neq}$ is caused by a larger positive $\Delta S^{\neq}$ despite the large positive $\Delta H^{\neq}$.

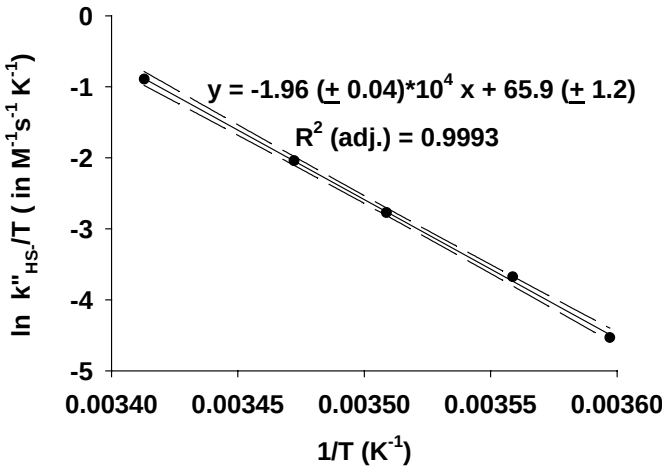

Figure 5.6 Temperature dependence of reaction of naled with bisulfide. Rate constants were determined in 50 mM phosphate buffer, 100 mM NaCl, and 5% methanol at pH 5.53. Solid line represents linear regression of the data; the dashed lines represent 95% confidence interval

Besides the reduced sulfur species we discussed here, polysulfide is a more reactive nucleophile and very important sulfur species in the natural surrounding. However, the high nucleophility results in an extremely fast reaction of naled with polysulfide, which cannot be measured by our method.

4. Conclusions

The degradation mechanisms which are of greatest environmental significance for naled in groundwaters, salt marhes and sediment porewater included reductive dehalogenation, which is much more important than hydrolysis. The results with reduced sulfur species in this work demonstrated that abiotic reactions could substantially influence the fate of naled in a sensitive coastal environmental such

as estuaries, salt marshes and sediment porewaters. From the second-order rate constants at 5 ^{o}C and the activation parameters, the second-order reaction rate constants of naled with bisulfide at 25 °C can be calculated. Based on the calculated second-order reaction rate constants of naled at 25 °C, naled is converted to dichlorvos almost instantaneously in the presence of 4.0 mM $[H_2S]_T$ at pH 7.0 at 25 °C ($t_{1/2}$ = 1s). Similarly, the half-live of naled in 0.6 mM $[S_2O_3^{2-}]$ at pH 7.0 at 25 °C could be expected to be very short. Therefore, the results of the reaction of naled with bisulfide present at environmentally relevant concentrations indicate that the degradation of naled promoted by bisulfide could play an important role in the entire chemical transformation of naled in sulfidic environments. To evaluate the potential influence of naled on the ecosystem, dichlorvos must be also taken into consideration due to its toxicity. Although reductive dehalogenation of naled results in the formation of a more toxic product, dichlorvos, the continuous degradation of dichlorvos promoted by reduced sulfur species may be a detoxification process.

Part II Dichlorvos

1. Introduction

Our results above demonstrated that dichlorvos is the sole transformation product detected in hydrolysis of naled and the reaction of naled with reduced sulfur. Numerous remediation schemes have been developed around the premise that reductive dehalogenation is a detoxification process. Reductive dehalogenation processes, however, can result in the formation of lower halogenated products that may present a greater health hazard than the parent compound. Therefore, the fate of the lower halogenated products has to be the focus of toxicological concern. Based on the kinetics we discussed above, k''_{HS^-} = 10.2 ($\pm$ 0.4) M^{-1} s^{-1} at 5 °C and E_a = 165 kJ/mol, the half-life of naled in the presence of 0.5 mM $[H_2S]_T$ at pH 6.0 at 25 °C is calculated to be about 9 seconds. The debromination of naled leads to the formation of dichlorvos, which is more toxic than naled. Dichlorvos is also a registered pesticide. The risk assessment for naled cannot be considered complete until the assessment for dichlorvos has also been included. Hence, the study of the continuous degradation of dichlorvos promoted by the reduced sulfur species is of most importance to the comprehensive understanding of the chemical fate of naled in a sulfidic environment.

Initially synthesized in the late 1940s, dichlorvos (2,2-dichlorovinyl dimethyl phosphate) was not registered for insecticidal use in the United States under the

Federal Insecticide, Fungicide, and Rodenticide Act (FIFRA) until 1948 (U.S.EPA. 1988a. Dichlorvos). Dichlorvos has been used widely as an insecticide and miticide to control internal and external parasites in livestock and domestic animals, to control insects in houses, and for crop protection. Dichlorvos is poisonous if swallowed, inhaled, or absorbed through the skin; therefore, it is a contact and stomach poison. Dichlorvos is a mutagen and has been classified as a possible human carcinogen by EPA (U.S.EPA. 1993b. Dichlorvos). Until the early 1970s, dichlorvos or mixtures containing dichlorvos were routinely used by fisheries biologists for the control of nuisance species such as carp. Dichlorvos also has been added directly to water to control parasites in intensive fish farming. Concern over problems associated with toxic and environmentally persistent organochlorine and organophosphate pesticide agents has led to restrictions on the use of such agents in natural lakes or other waterbodies, but dichlorvos has continued to be used in aquaculture to control various types of fish parasites.

Until large scale production of dichlorvos began in the late 1950s, the compound was chiefly encountered as an impurity in the pesticide trichlorfon. One method of production is the dehydrochlorination of trichlorfon in aqueous alkali at 40 – 50 ^{o}C (WHO, 1989, Dichlorvos). Dichlorvos is also produced commercially by a reaction of trimethyl phosphite and chloral (WHO, 1989, Dichlorvos; Cremlyn, 1978; Sittig, 1980). Dichlorvos is a breakdown product of trichlorfon (Scheme 5.2) and can be generated in many plants through the metabolism of naled (U.S.EPA, 1988a, Dichlorvos; Menzie, 1972; PIP-Naled,

1994; PIP-Trichlorfon, 1993). The impact of a pesticide is determined not only by its persistence in the environment but also by the identity and lifetime of its transformation products. Thus, the study of the chemical transformation of dichlorvos in the presence of reduced sulfur species is very important not only for dichlorvos itself, but also for naled and trichlorfon when the chemical fates of naled and trichlorfon in sulfidic environment are investigated.

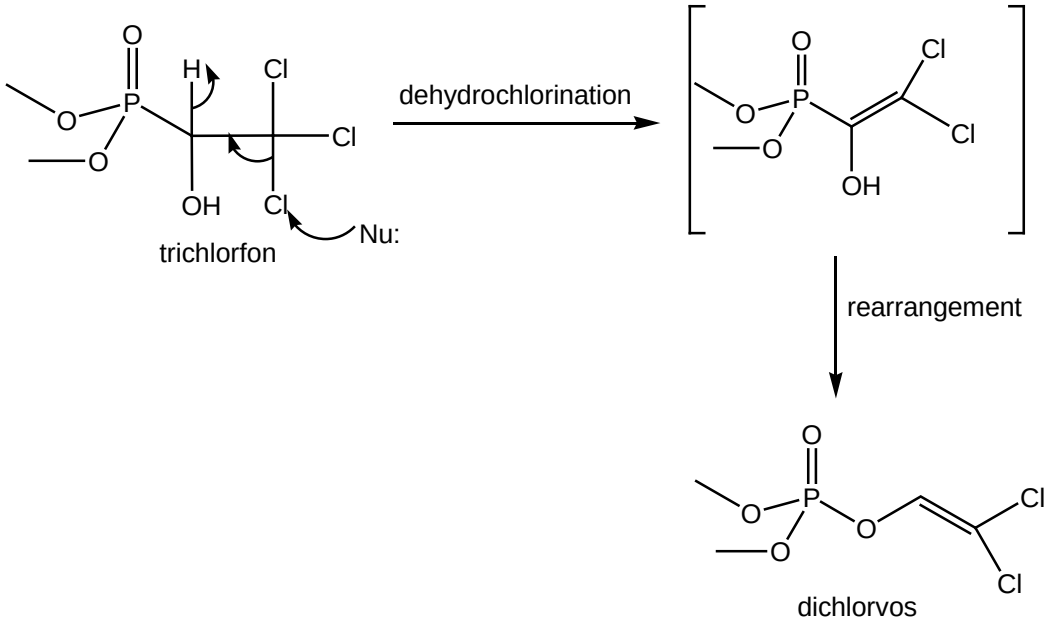

Scheme 5.2 Transformation of trichlorfon to dichlorvos.

Adsorption to soil and volatilization of dichlorvos is not significant (Howard, 1991). Dichlorvos can be expected to leach into the groundwater due to its fair water solubility and relative low K_{oc} (Kenaga, 1980). Dichlorvos does not strongly absorb ultraviolet light above 240 nm (Gore et al., 1971) and is, therefore, unlikely to be subject to direct photolysis. Treatment methods such as biodegradation (Lieberman and Alexander, 1983), oxidation with Fenton's

reagent (Lu et al., 1987), photolysis (Harada et al., 1990) and sonolysis (Schramm and Hua, 2001) have been applied to decompose dichlorvos. According to the report by Lamoreaux and Newland, when released to soils, hydrolysis and other non-biological processes account for 70% or more of the total degradation of dichlorvos, while bacterial degradation accounts for only 30% (Lamoreaux and Newland, 1978).

Over the years, the hydrolysis of dichlorvos has been widely studied (Drevenkar et al., 1976; Benoit-Marquie et al., 2004). It is known that dichlorovos is unstable towards hydrolysis and the vinyl phosphate bond is the most susceptible due to the electron deficient phosphorus atom, which leads to the formation of dimethyl phosphate and dichlorovinyl alcohol (Pearson and Songstadt, 1967). Dichlorovinyl alcohol is unstable and will quickly tautomerize to dichloroacetaldehyde (Khandelwal and Wedzicha, 1998) (Scheme 5.3, Pathway I). It has also been reported that some phosphate triesters display a cleavage of an O-C bond in water that indicates that H_2O undergoes a nucleophilic substitution at the carbon atom (Cox and Ramsay, 1963; Schmidt and Fest, 1982). Therefore, neutral-catalyzed hydrolysis of dichlorvos may happen through the nucleophilic attack of H_2O on a methoxy carbon atom (Scheme 5.2, Pathway II) or/and the phosphorous atom. Neutral hydrolysis and base-catalyzed hydrolysis have to be considered in the pH range of 6 – 8.4 investigated in this study.

Methylation of the thiol compounds was reported to take place along with the base-catalyzed cleavage of the phosphate-dichlorovinyl bond when dichlorvos

was treated with thiol compounds (Scheme 5.3, Pathway III) (Khandelwal and Wedzicha, 1998). Hence, it is suggested that dichlorvos is likely to undergo S_N2 reaction at the carbon of a methoxy group by a sulfur nucleophile in the presence of reduced sulfur species along with hydrolysis.

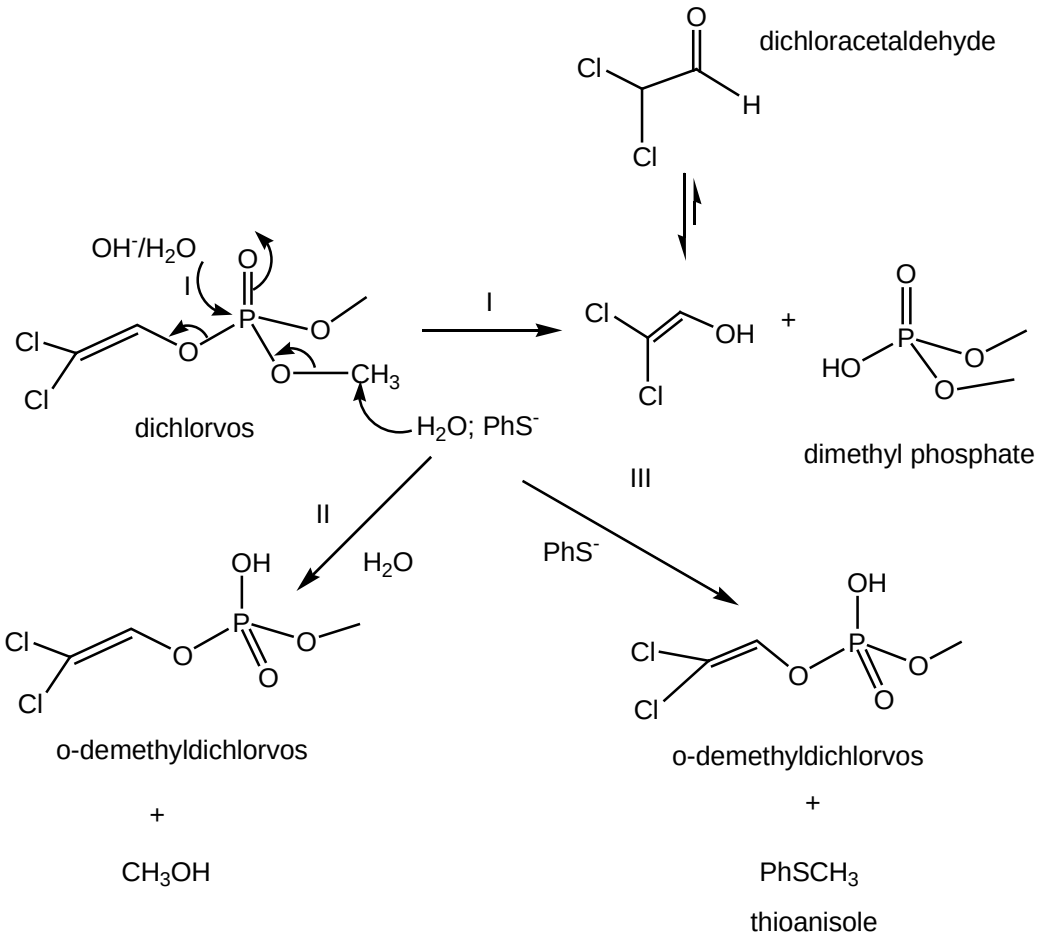

Scheme 5.3 Proposed mechanism of reactions of dichlorvos: I. Nucleophilic attack by H_2O and OH^- at central P atom; II. Nucleophilic attack by H_2O at methoxy group and III. Nucleophilic attack by sulfur species at methoxy group.

The primary purpose of this part was to examine the kinetics and products of the reaction of dichlorvos with selected reduced sulfur species in more detail. The reduced sulfur species discussed in this work include hydrogen sulfide (H_2S), bisulfide (HS^-), thiophenol (PhSH), thiophenolate (PhS^-) and thiosulfate ($S_2O_3^{2-}$). The temperature dependence of these reactions was investigated as well. The impact of the reduced sulfur species on the abiotic transformation of dichlorvos was investigated in well-defined aqueous solutions under anaerobic conditions. PhSH and PhS^- were chosen in this study as a model for aromatic sulfur nucleophiles in degradation of dichlorvos. Reactions were monitored at varying temperatures and concentrations of reduced sulfur species at environmentally relevant pH to investigate the second-order reaction rate constants and activation parameters. The reactivity of individual reduced sulfur species towards dichlorvos was explored from kinetics and enthalpic effects. The products were characterized by GC/MS. The results of this study can be incorporated in fate and exposure assessment in order to predict environmental risk associated with discharge of naled, trichlorfon and dichlorvos to coastal marine environment.

2. Material and Methods

2.1. Chemicals

Dichlorvos (2,2-dichlorovinyl dimethyl phosphate, 99%) was obtained from Chem Service (West Chester, PA). Thioanisole and dichloroacetaldehyde were obtained from TCI (Portland, OR). *o*-(2,3,4,5,6-pentafluorobenzyl)-

hydroxylamine hydrochloride (PFBHA·HCl) was obtained from TCI-SU (Tokyo, Japan). The starting concentration of dichlorvos was ~ 40 μM. All solvents and reagents that were used were analytical grade or equivalent. Ethyl acetate and methanol were HPLC grade and were obtained from Fisher Scientific (Pittsburgh, PA). Hexane (95% n-hexane) was for pesticide residue analysis and obtained from Mallinckrodt Baker, Inc. (Phillipsburg, NJ). All the reaction solutions were prepared in an anaerobic glovebox (5% H_2, 95% N_2) and aqueous solutions were prepared from argon-purged deionized water (DW) (Milli-Q gradient system, Millipore, Bedford, MA). The concentrations of $[H_2S]_T$, $[PhSH]_T$ and $[S_2O_3^{2-}]$ were 4.1 – 9.6 mM, 2.0 – 3.0 mM, and 2.2 – 5.7 mM, respectively. The reactions with hydrogen sulfide, thiophenol and thiosulfate were investigated over pH range of 6.0 – 8.4, 5.7 – 7.7, and 6.9 –7.1, respectively. The ethyl acetate extracts were subjected to GC/FID, GC/ECD or GC/MS analysis.

2.2. Product Derivatization

The possible hydrolysis products in the buffer solutions were qualitatively analyzed by GC/MS. Dichloroaldehyde can be determined via the analysis method for aldehyde and carbonyl compounds with PFBHA·HCl as a derivatizing agent. The method was first described by Yamada and Somiya (1989) and later improved by Glaze and coworkers (1989). The technique utilizes a direct aqueous derivatization with the reagent PFBHA, which reacts with the carbonyl groups to form the corresponding oximes. Two geometric isomers are formed

(pentafluorobenzyloxime *(syn)* and pentafluorobenzyloxime *(anti)*) with most aldehydes except symmetrical carbonyls where only one isomer is formed.

The detailed procedure for derivatization is given. The procedure is modified from the derivatization method for formaledehyde. Approximately 2mL aliquot of reaction solution was added into a test tube. To this 2 mL of PFBHA·HCl (prepared gravimetrically as 2 mg/ mL aqueous solution) and 5 mL of 50 mM pH 5 phosphate buffer were added. The test tube was kept in the 50 ± 0.5 ^{o}C water bath for 100 min. After the mixture had been allowed to cool to room temperature, 2~3 drops of concentrated sulfuric acid was added to quench the derivatization reaction. The derivatives were extracted into 2 mL of hexane. And the hexane extract was cleaned with 3 mL 0.1 M sulfuric acid and dried over magnesium sulfate. The hexane extract was analyzed by GC/MS. The recovery of the method for dichloroaldehyde was investigated with dichloroaldehyde standard solution. The recovery was not stable and ranged from 40 – 75%. This method cannot be used for quantification of dichloroaldehyde due to the relative bad recovery, unfortunately.

2.2. Chromatographic Analysis

Ethyl acetate extracts were analyzed on a Fisons GC 8000 equipped with an AS 800 autosampler, a FID-80 flame ionization detector (Carlo Erba Instruments) or an ECD-80 electron capture detector (Carlo Erba Instruments) containing ^{63}Ni beta emitting radioactive source of 370 MBq (10 mCi), a split/splitless injector

and a 30 m DB-5, 0.25 mm i.d. × 0.25 μm fused-silica capillary column (J&W, Folsom, CA). The carrier gas was helium (99.999%) and the make up gas was methane/argon. GC/MS system (Trio 1000 Fisons Instruments) to identify and analyze the degradation products was equipped with a split/splitless injector and a 30 m AT-5ms, 0.25 mm i.d. × 0.25 μm fused-silica capillary column (Alltech, Deerfield, IL). EI mass spectra were generated using electron energy of 70 eV, monitoring for ions *m/z* 35-500 in full-scan and selected ion recording (SIR) modes. The source temperature employed for the ionization technique was 200 ºC. *Temperature program:* Injector temperature and detector temperature were set at 250 ºC. The column temperature was held at 80 ºC for one minute, then increased at a rate of 6 ºC/min to 150 ºC, followed by heating to 250 ºC at a rate of 20 ºC/min and finally held constant at 250 ºC for 2 minutes.

3. Results and Discussion

3.1. Hydrolysis of Dichlorvos at 25 ºC

The hydrolysis reaction of dichlorvos is treated as a pseudo-first-order reaction. The hydrolysis rate constants, k_h , is measured as the slope of the plot of ln[dichlorvos] vs. the reaction time. The kinetics data of the experiments display good fit with pseudo-first order reaction profile and the observed hydrolysis rate constants of dichlorovs at various pH values are shown in Table 5.3. The time course of hydrolysis of dichlorvos at pH 6.03 was shown in Figure 5.7(a). Hydrolysis of dichlorvos is pH-dependent. Acid-catalyzed hydrolysis can be

neglected for most organophosphates. Therefore, k_h is assumed to be the sum of neutral-catalyzed hydrolysis and base-catalyzed hydrolysis:

$$k_h = k_N + k_b[OH^-] \quad (9)$$

in which k_N and k_b are rate constants for neutral-catalyzed hydrolysis and base-catalyzed hydrolysis, respectively. The good linear relationship between k_h and [OH^-] would support the assumption that there is no acid-catalyzed hydrolysis (Figure 5.7(b)). The linear regression would give the equation k_h (in s^{-1}) = 6.00 ($\pm$ 0.32) [OH^-] + 2.22 ($\pm$ 0.28) × 10^{-6}. k_N and k_b are determined to be 2.22 ($\pm$ 0.28) × 10^{-6} s^{-1} and 6.00 ($\pm$ 0.32) M^{-1} s^{-1}, respectively.

Table 5.3 Hydrolysis Rate Constants of Dichlorvos (50 mM phosphate buffer, 100 mM NaCl, and 5% methanol) at 25 °C.

pH	k_h (s^{-1})*	$t_{1/2}$ (h)
5.82	1.59 ($\pm$ 0.07)×10^{-6}	122
6.58	1.78 ($\pm$ 0.11)×10^{-6}	108
6.85	3.22 ($\pm$ 0.15)×10^{-6}	59.7
7.15	3.72 ($\pm$ 0.13)×10^{-6}	51.7
7.58	5.06 ($\pm$ 0.18)×10^{-6}	38.1
7.90	6.69 ($\pm$ 0.24)×10^{-6}	29.0
8.12	9.94 ($\pm$ 0.32)×10^{-6}	19.4
8.29	1.40 ($\pm$ 0.08)×10^{-5}	13.7

* The rate constant of hydrolysis of dichlorvos was obtained at 95% confidence interval.

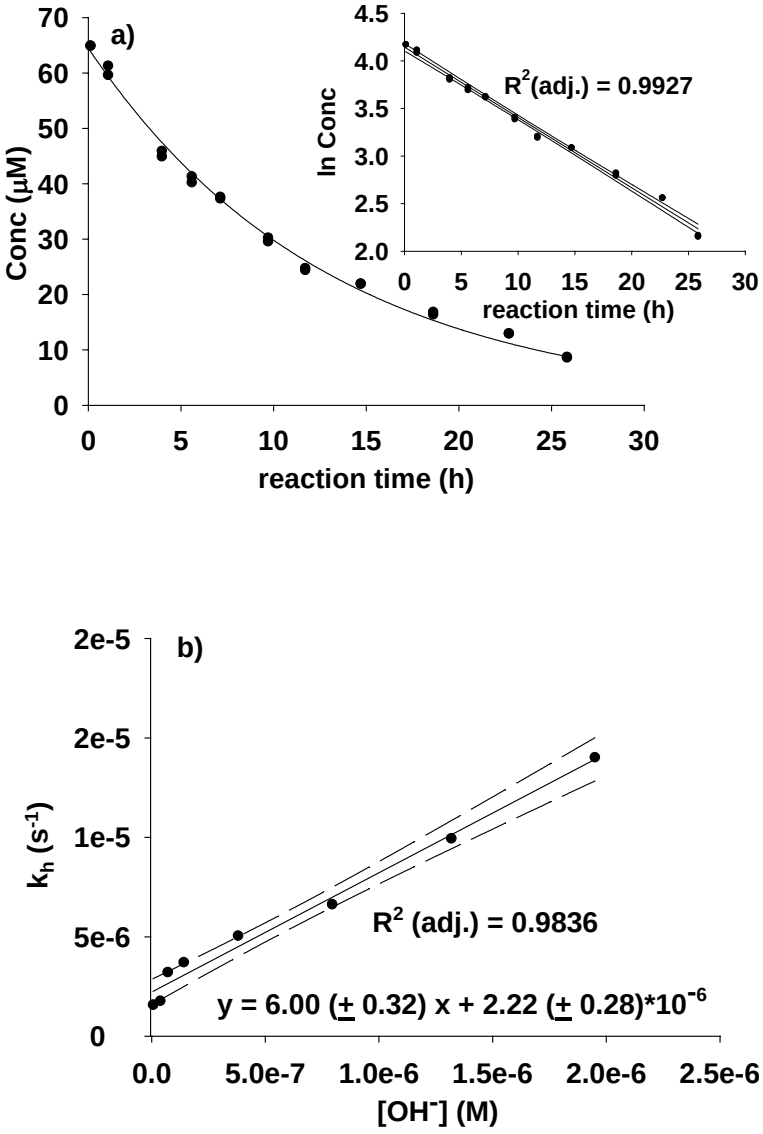

Figure 5.7 (a) Hydrolysis of dichlorvos at pH 7.90 (50 mM phosphate buffer, 100 mM NaCl, and 5% methanol) at 25 °C. Solid lines represent model fits to the data assuming exponential decay of dichlorvos. Inset depicts the data plotted in

semilogarithmic form to obtain the observed pseudo-first-order reaction rate constant. (b) Plot of hydrolysis rate constants, k_h, versus [OH⁻] for hydrolysis of dichlorvos at pH 5.80-8.30 in 50 mM phosphate buffer, 100 mM NaCl, and 5% methanol at 25 °C. Solid line represents linear regression of the data; the dashed lines represent 95% confidence interval.

To try to determine the base-catalyzed hydrolysis product, dichloroacetaldehyde, the sample was derivatized with PFBHA·HCl after the completion of the reaction in the experiment of hydrolysis of dichlorvos. The resulting sample was analyzed by GC-MS. The reaction of dichloroacetaldehyde with PFBHA·HCl is shown in Scheme 5.4.

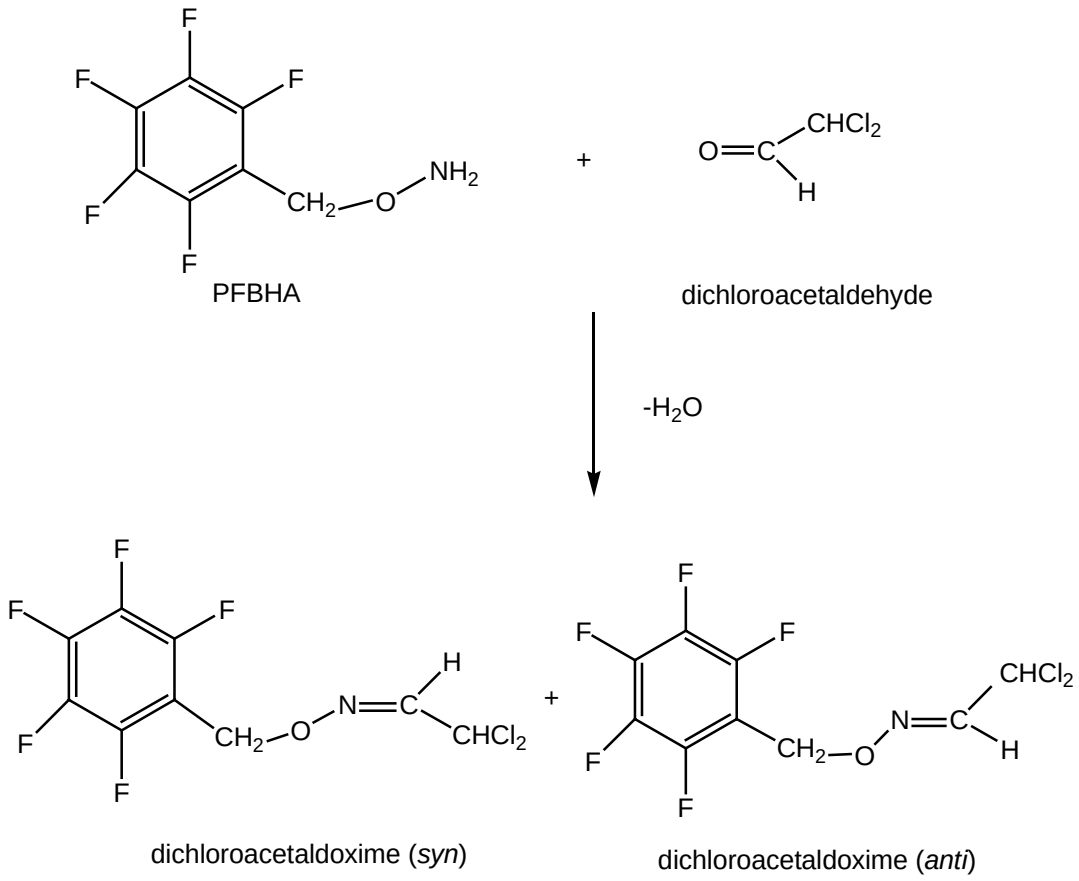

Scheme 5.4 Reaction of dichloroacetaldehyde with PFBHA.

Aldehydes are trigonal-planar in their geometry, allowing the PFBHA nucleophile to approach from either side of the molecular plane. With dichloroacetaldehyde, however, there is more crowding around the β-carbon than around the β-carbon in simple aldehydes due to the presence of two chlorine atoms. This may make the formation of dichloroacetaldoxime (*anti*) relatively favorable over dichloroacetaldoxime (*syn*). The gas chromatogram and mass spectrum of the derivatized sample in the hydrolysis of dichlorovs at pH 7.58 at 25 °C are shown Figure 5.8. Two geometric isomers of the derivatives,

dichloroacetaldoxime (*syn*) and dichloroacetaldoxime (*anti*), were detected. EI mass spectra of PFBHA dichloroacetaldoxime is shown in Figure 5.9. According to the report by Sclimenti and his coworkers (Sclimenti et al., 1990), it can be expected that the isomer pairs of PFBHA oxime of dichloroacetaldehyde are separated and the retention time of dichloroacetaldoxime (*syn*) is shorter.

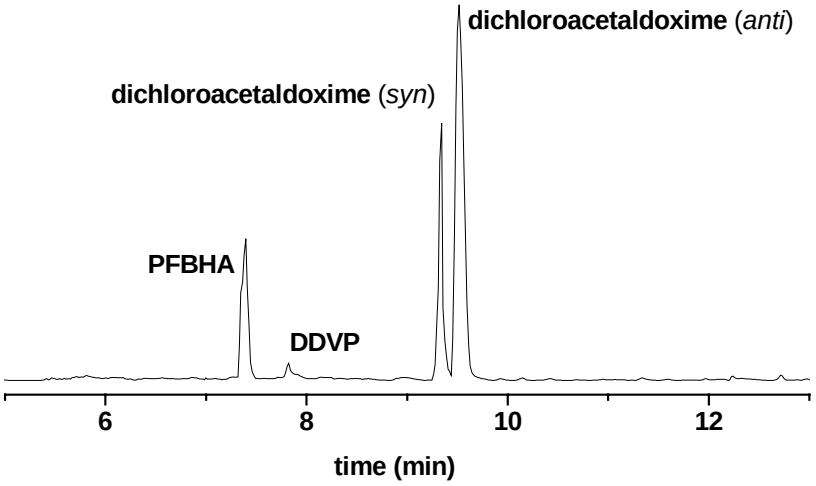

Figure 5.8 EI chromatogram of derivatized sample in the hydrolysis of dichlorvos at pH 7.58 (50 mM phosphate buffer, 100 mM NaCl, and 5% methanol) at 25 ^{o}C.

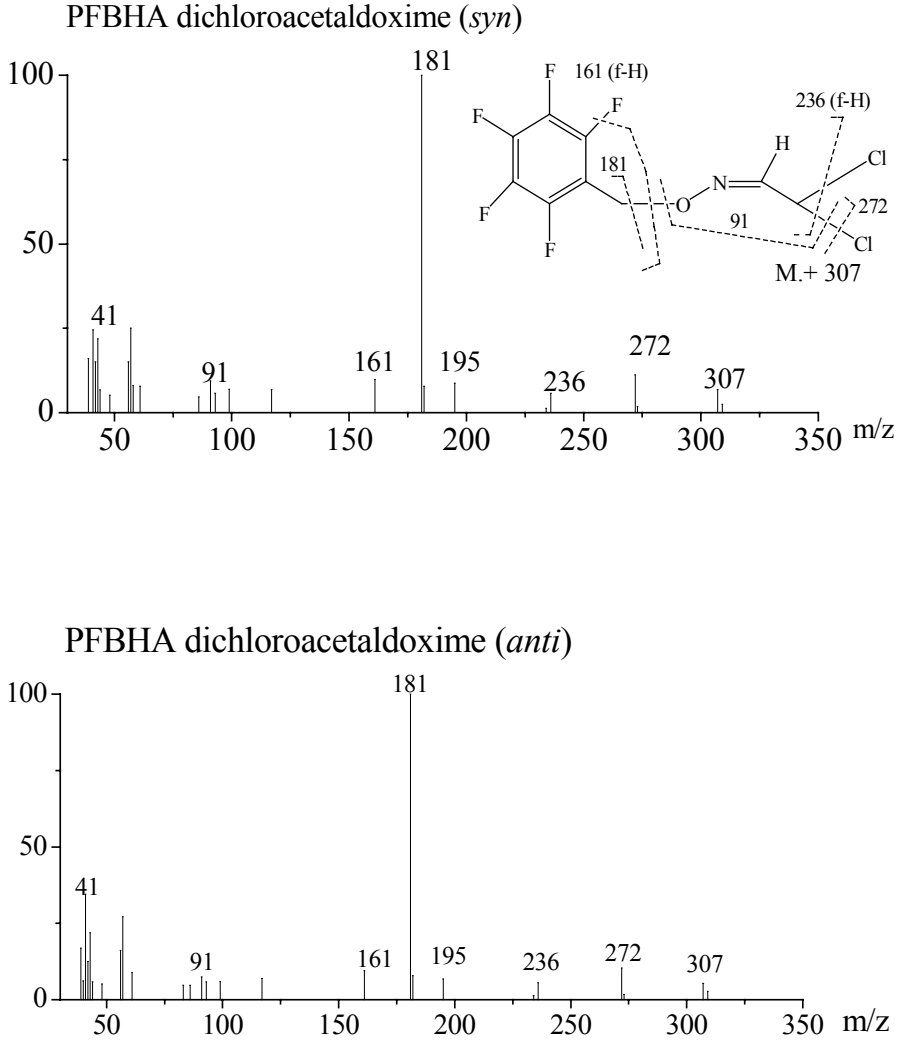

Figure 5.9 Electron ionization mass spectra of PFBHA dichloroacetaldoxime

3.2. Kinetics of the Reaction of Dichlorvos with Reduced Sulfur Species at 25 °C

3.2.1. Reaction of dichlorvos with hydrogen sulfide at 25 °C

The reaction of dichlorvos with hydrogen sulfide was assessed over a pH range (5.8 – 8.3). The observed pseudo-first-order rate constant includes the

contribution of hydrolysis and degradation promoted by hydrogen sulfide. Hydrolysis should be taken into consideration when the kinetics of the reaction of dichlorvos with hydrogen sulfide in pH constant buffer is studied.

To explore the reaction of dichlorvos with hydrogen sulfide, the difference in reactivity of various hydrogen sulfur species (e.g., H_2S vs. HS^-) was approached in the same way as the reaction of naled with hydrogen sulfide. The linear correlation between the apparent second-order reaction rate constant, k''_{app}, from the observed pseudo-first-order reaction rate constant after correction for hydrolysis, and α_{HS^-} can also be obtained, which allows the determination of the second-order reaction rate constants k''_{H_2S} and k''_{HS^-} (Figure 5.10). k''_{HS^-} was obtained to be 3.30 ($\pm$ 0.05) $\times$ 10^{-3} M^{-1} s^{-1} and k''_{H_2S} was not significantly different from zero at 95% confidence level.

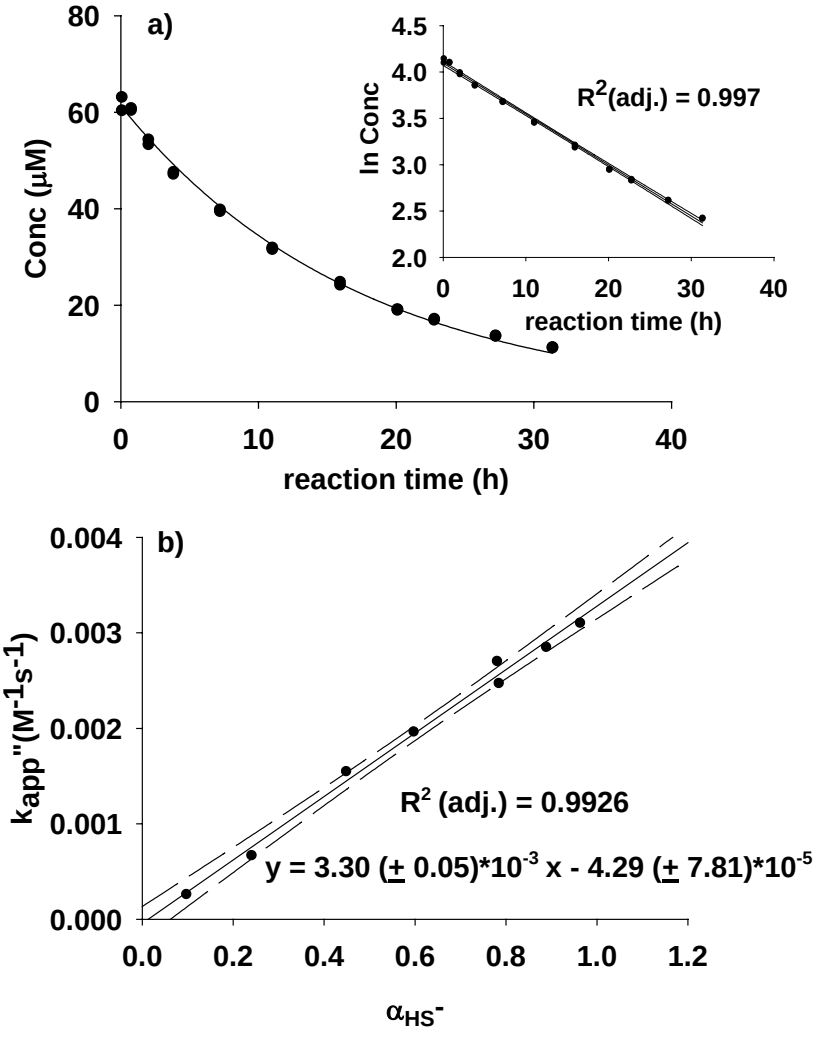

Figure 5.10(a) Reaction of dichlorvos with 5.02 mM $[H_2S]_T$ at pH 7.54 (50 mM phosphate buffer, 100 mM NaCl, and 5% methanol) at 25 °C. Solid lines represent model fits to the data assuming exponential decay of dichlorvos. Inset depicts the data plotted in semilogarithmic form to obtain the observed pseudo-first-order reaction rate constants. (b) Plot of apparent second-order reaction

rate constants, k''_{app} versus α_{HS^-} for the reaction of dichlorvos with bisulfide for various pH in 50 mM phosphate buffer, 100 mM NaCl, and 5% methanol at 5 °C. Solid line represents linear regression of the data; the dashed lines represent 95% confidence interval.

3.2.2. Reaction of dichlorvos with thiophenol at 25°C

The reaction of dichlorvos with thiophenol was assessed the same way as the reaction with hydrogen sulfide. The observed rate constant does include hydrolysis and the degradation promoted by thiophenol and thiophenolate. The different reactivity of PhS^- versus PhSH would result in a pH dependence of k_s. The corrected rate constant, k_s, obtained from k_{obs} after correction for hydrolysis, is divided by the total concentration of thiophenol species, which results in the apparent second-order rate constant, k''_{app}. Linear regression analysis of k''_{app} versus α_{PhS^-} yielded a slope equal to 2.17 ($\pm$ 0.15) $\times 10^{-2}$ M^{-1} s^{-1} and an intercept not significantly different from zero at 95% confidence level (Figure 5.11b). Hence, k''_{PhS^-} was obtained to be 2.17 ($\pm$ 0.15) $\times 10^{-2}$ M^{-1} s^{-1} and k''_{PhSH} was near zero at 95% confidence level. Therefore, like for H_2S vs. HS^-, only PhS^- was the sole reactive species in the reaction with dichlorvos. PhSH does not contribute to the degradation of dichlorvos.

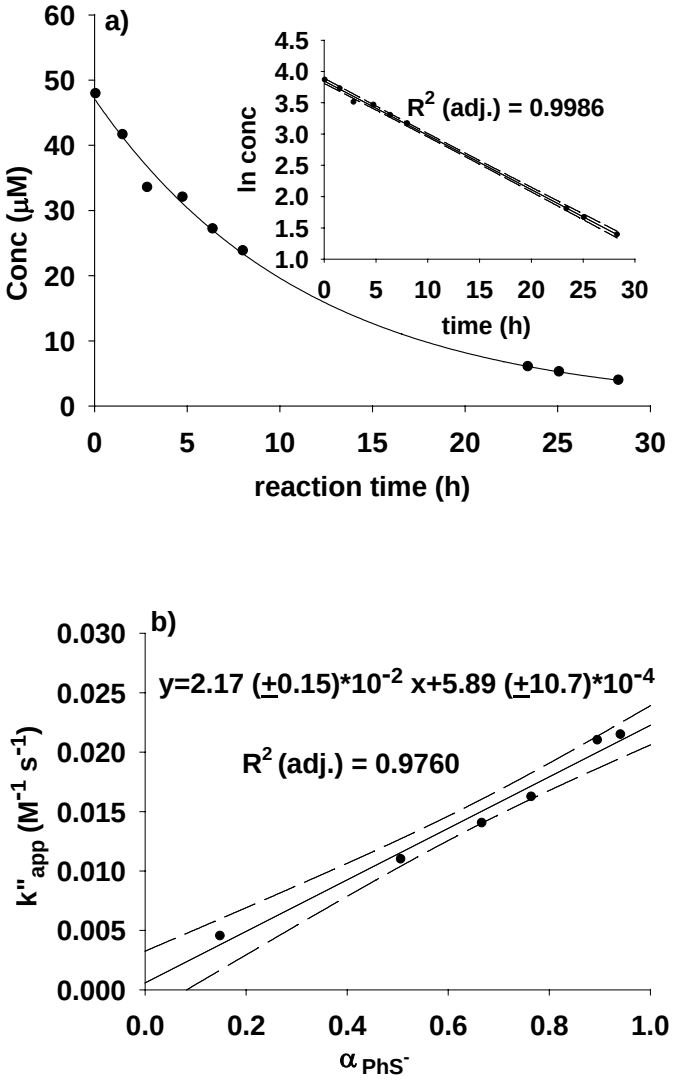

Figure 5.11 (a) Reaction of dichlorvos with 1.99 mM $[PhSH]_T$ at pH 6.51 (50 mM phosphate buffer, 100 mM NaCl, and 5% methanol) at 25 °C. Solid lines represent model fits to the data assuming exponential decay of dichlorvos. Inset depicts the data plotted in semilogarithmic form to obtain the observed pseudo-first-order reaction rate constant. (b) Plot of apparent second-order reaction rate constants, $k"_{app}$ versus α_{PhS^-} for the reaction of dichlorovos with thiophenol for various pH in 50 mM phosphate buffer, 100 mM NaCl, and 5% methanol at 25 °C.

Solid line represents linear regression of the data; the dashed lines represent 95% confidence interval.

3.2.2. Reaction of dichlorvos with thiosulfate at 25°C

$S_2O_3^{2-}$ is known to be the only dominant species in pH buffer solutions of sodium thiosulfate over the investigated pH range of 6.8-7.2, no effect of pH on k_{obs} was expected. The linear dependence of the corrected rate constant, k_s, and $[S_2O_3^{2-}]$ was observed.

$$k_s = k_{obs} - k_h = k''_{S_2O_3^{2-}}[S_2O_3^{2-}] \quad (10)$$

Figure 5.12 shows the linear plot of k_s versus $[S_2O_3^{2-}]$. A value for the second-order rate constant, $k''_{S_2O_3^{2-}}$, was therefore obtained as the slope of the plot of k_s versus $[S_2O_3^{2-}]$ to be 2.55 ($\pm$ 0.03)$\times$ 10^{-3} $M^{-1}s^{-1}$. The intercept not significantly different from zero at 95% confidence interval is consistent with Equation 10. It supports that the assumption that only $S_2O_3^{2-}$ is responsible for the loss of dichlorvos in the presence of thiosulfate besides hydrolysis. The resulting second-order constants for the reduced sulfur species in the reaction with dichlorvos are summarized in Table 5.4. Our results indicate that the reaction with PhS^- was ~7 – 8 times faster than with HS^- and with $S_2O_3^{2-}$ and there is no significant difference between the reactivity of HS^- and $S_2O_3^{2-}$ towards dichlorvos. The relative reactivity of the reduced sulfur species decreases in the following order: $PhS^- > HS^- \approx S_2O_3^{2-}$. The relative higher reactivity of PhS^- may result from the higher

electron density on the sulfur atom due to adjacent benzene ring that acts as a π-donor.

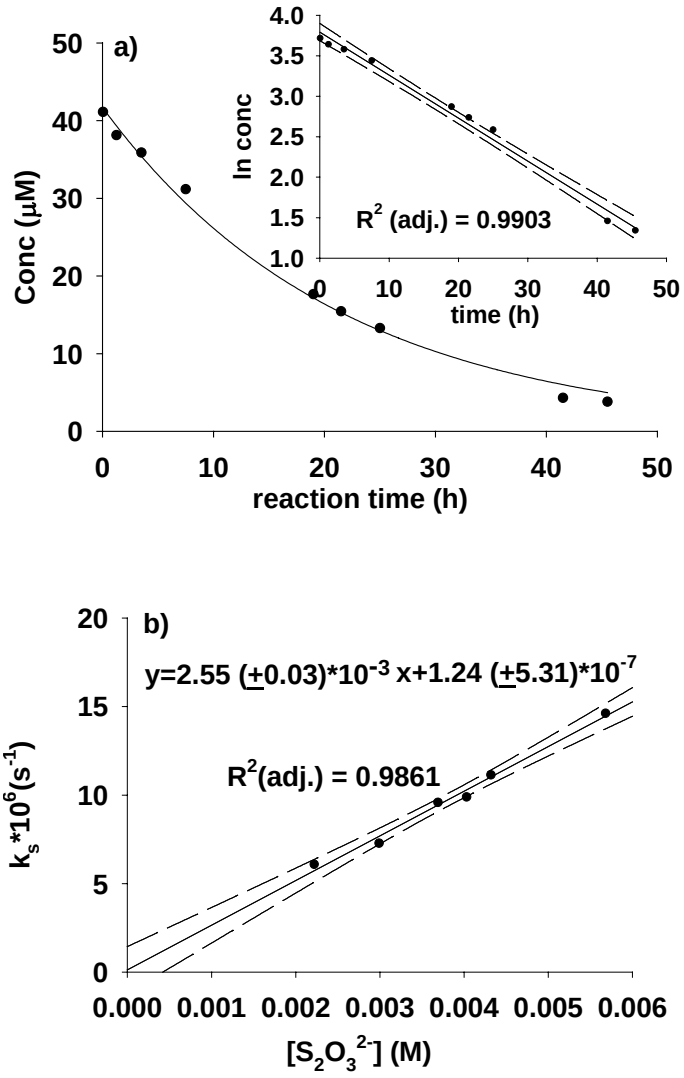

Figure 5.12 (a) Reaction of dichlorvos with 4.1 mM [$S_2O_3^{2-}$] at pH 6.95 (50 mM phosphate buffer, 100 mM NaCl, and 5% methanol) at 25 °C. Solid lines represent model fits to the data assuming exponential decay of dichlorvos. Inset depicts the data plotted in semilogarithmic form to obtain the observed pseudo-

first-order reaction rate constant. (b) Plot of the corrected rate constants, k_s, versus [$S_2O_3^{2-}$] for the reaction of dichlorovos with thiosulfate in 50 mM phosphate buffer, 100 mM NaCl, and 5% methanol at 25 °C. Solid line represents linear regression of the data; the dashed lines represent 95% confidence interval.

Table 5.4 Second-order Rate Constants for Reactions of Dichlorvos with Reduced Sulfur Species in 50 mM Phosphate Buffer, 100 mM NaCl, and 5% Methanol at 25 °C[a].

k''_{HS^-} (M^{-1} s^{-1})	k''_{H_2S} (M^{-1} s^{-1})	k''_{PhS^-} (M^{-1} s^{-1})	k''_{PhSH} (M^{-1} s^{-1})	$k''_{S_2O_3^{2-}}$ (M^{-1} s^{-1})
3.05 (± 0.05) × 10^{-3}	~ 0	2.17 (± 0.15) × 10^{-2}	~ 0	2.55 (± 0.03) × 10^{-3}

[a] Stated uncertainties represent 95% confidence limit.

3.3. Products of the Reaction of Dichlorvos with PhS^-

Product analysis is an important tool to elucidate the mechanism, especially when there multiple pathways exist. The important base-catalyzed hydrolysis product, dichloroacetaldehyde, was characterized by GC/MS after derivatization with PFBHA·HCl in the hydrolysis of dichlorvos. Since the possible transformation products of the reaction of dichlorvos with PhS^- are readily extracted into organic solvent and analyzed by GC, the reaction with PhS^- was chosen to study the degradation products of the reaction of dichlorvos with reduced sulfur species. One of the detected products was thioanisole. The formation of this supports a nucleophilic substitution at a methyl group, which

results in methylation of the thiol compound to form thioanisole. The time course of reaction of dichlorvos with 2.6 mM $[PhSH]_T$ at pH 7.70 is shown in Figure 5.13. The control experiment was conducted at pH 7.70 without thiophenol, from which the hydrolysis rate, k_h, was determined to be 0.021 h^{-1}. Over the reaction time, the concentration of thioanisole was observed to increase while dichlorvos decreased. k_{obs} and k_{PhS^-} were obtained to be 0.219 h^{-1} and 0.196 h^{-1}, respectively, by simultaneously fitting the observed parent compound degradation data and degradation product formation data using Scientist for Windows, v.2.01 (MicroMath Scientific Software). The nucleophilic attack at a methyl group by PhS^- contributed to ~90% disappearance of dichlorvos in the reaction with 2.59 mM $[PhSH]_T$ at pH 7.70 and 25 ^oC. After the completion of the reaction with thiophenol, the reaction mixture was derivatized with PFBHA·HCl, the resulting extract was analyzed by GC-MS. The EI chromatogram is shown in Figure 5.14. Thioanisole, as the major product, and the base-catalyzed hydrolysis product, dichloroacetaldehyde, were formed in the degradation of dichlorvos in the presence of PhS^-. The sum of k_{PhS^-} and k_h was equal to k_{obs} in 95% confidence interval. Hence, we can assume that dichlorvos was almost 100% transformed into thioanisole and 2,2-dichlorovinyl methyl phosphate through the reaction with thiophenol and dichloroacetaldehyde and dimethyl phosphate through base-catalyzed hydrolysis. And it can be concluded that the nucleophilic attack of PhS^- at methyl group was the dominant pathway here.

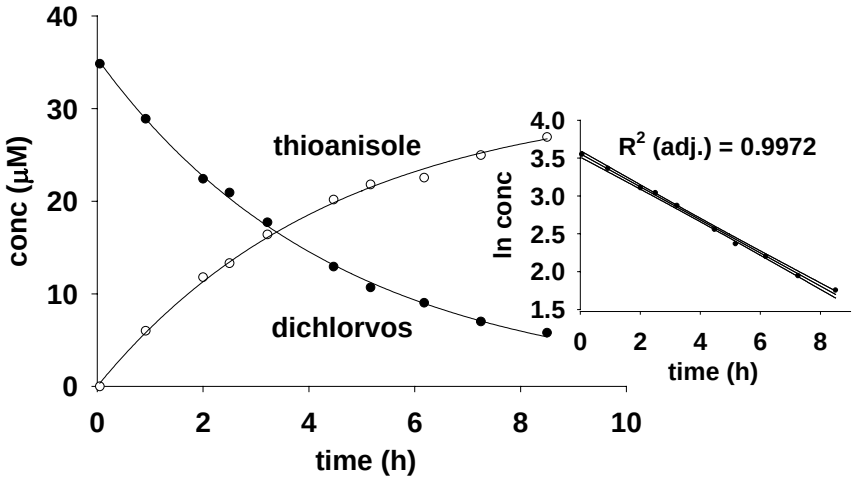

Figure 5.13 Reaction of naled with 2.6 mM $[PhSH]_T$ at pH 7.70 (50 mM phosphate buffer, 100 mM NaCl, and 5% methanol) at 25 °C, indicating the degradation of dichlorvos (•, 0.0219 h^{-1}), the formation of thioanisole (o, 0.0196 h^{-1}). Solid lines represent model fits to the data assuming exponential decay of dichlorvos to degradation product thioanisole simultaneously.

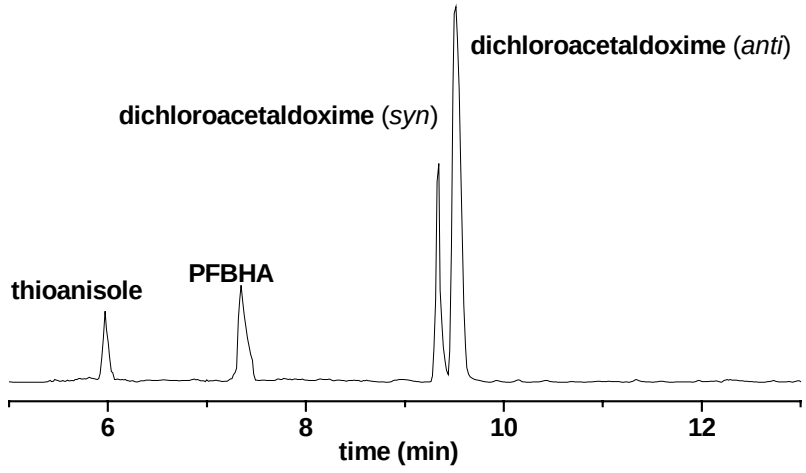

Figure 5.14 EI chromatogram of derivatized sample after completion of the reaction of dichlorvos with 2.6 mM [PhSH]$_T$ at pH 7.70 (50 mM phosphate buffer, 100 mM NaCl, and 5% methanol) and 25 ^oC.

Although HS^- and $S_2O_3^{2-}$ react at a slower rate with dichlorvos than PhS^-, we expect a similar situation for HS^- and $S_2O_3^{2-}$ acting as nucleophiles in the reaction with dichlorvos over the pH and concentration range investigated in this study. The disappearance of dichlorvos attributed to the reduced sulfur species, k_s, was predicted by multiplying the determined second-order rate constants by the concentration of [HS^-], [PhS^-] and [$S_2O_3^{2-}$]. So the percentage of the loss of dichlorvos attributed to the reduced sulfur species can be calculated from k_{obs} and k_s under the experimental conditions. The results, summarized in Table 5.5, indicate that the nucleophilic attacks of HS^-, $S_2O_3^{2-}$ and PhS^- at a methyl group would be the dominant pathways in the degradation of dichlorvos in the presence of 2.0 – 10 mM reduced sulfur species in pH range of 5.7 – 8.4 and are much more important than hydrolysis under the experimental conditions in this study.

Table 5.5 Predicted Percentage of Loss of Dichlorvos Attributed to Reduced Sulfur Species at 25 ^oC.

pH	Species	$[S(II)]_T$ (mM)	k_{obs} (h^{-1})	% of loss of dichlorvos attributed to $HS^-/PhS^-/S_2O_3^{2-}$
6.0	HS^-/H_2S	7.0	0.014	52
7.2	HS^-/H_2S	9.6	0.078	84

5.7	PhS^-/PhSH	2.1	0.042	58
7.7	PhS^-/PhSH	2.6	0.22	90
6.9	$S_2O_3^{2-}$	5.7	0.064	82
7.1	$S_2O_3^{2-}$	2.2	0.035	62

3.4. Activation Parameters for Reaction with HS^-, PhS^- and $S_2O_3^{2-}$

Difference in the second order rate constants were observed for HS^-, PhS^- and $S_2O_3^{2-}$. To explore the differences in reactivity from enthalpic and entropic effects, k_{obs} was measured in buffered solutions (pH 7.15) containing reduced sulfur species over the temperature range of 12.0 °C to 50.0 °C, and the activation parameters were determined. The control experiments were conducted in buffered solutions in the absence of reduced sulfur species at these temperatures. The hydrolysis rates at the varying temperature were listed in Table 5.6.

Table 5.6 Hydrolysis Rate Constants of Dichlorvos (50 mM phosphate buffer, 100 mM NaCl, and 5% methanol) at Temperature Range of 12 – 50 °C.

pH	Temperature (°C)	k_h $(s^{-1})^*$	$t_{1/2}$ (h)
7.15	50	$6.09 (\pm 0.08)\times10^{-5}$	3.16
7.15	40	$2.98 (\pm 0.07)\times10^{-5}$	6.45
7.15	25	$3.72 (\pm 0.12)\times10^{-6}$	51.8
7.15	20	$2.04 (\pm 0.09)\times10^{-6}$	94.4
7.15	12	$9.02 (\pm 0.17)\times10^{-7}$	213

* The rate constants of hydrolysis of dichlorvos were obtained at 95% confidence interval.

Based on the previous discussion, k''_{H_2S} can be assumed too small to make a significant contribution to the degradation of dichlorvos, the contribution of hydrogen sulfur species to k_{obs} is entirely consistent with HS^- as the sole reactive species in the solution. For the same reason, PhS^- is the sole reactive thiophenol species needed to be considered in the reaction of dichlorvos with thiophenol. $S_2O_3^{2-}$ is the only dominant species in the thiosulfate reaction solutions in the pH range investigated here. The bisulfide concentrations at the reaction temperatures were computed using the expression for the temperature dependence of pK_a of hydrogen sulfide reported by Millero (1986). pK_a of thiophenol is not as temperature-dependent as hydrogen sulfide. And pK_a of thiophenol is not available at other temperatures than 25 ^oC. The thiophenolate concentration was calaulated based on pK_a of thiophenol at 25 ^oC. Data for the temperature dependence of the reaction of dichlorvos with HS^-, PhS^- and $S_2O_3^{2-}$are shown in Figure 5.15 according to a linearized version of the Eyring equation (Pross, 1995). Linear regression analyses yielded the slopes and the intercepts, which allow the extraction of the values of $\Delta H^{\neq}$ and $\Delta S^{\neq}$. The Arrhenius activation energy (E_a) and activation barrier ($\Delta G^{\neq}$) can be calculated at 25 °C. The resulting activation parameters for the reaction of dichlorvos with reduced sulfur species are listed in Table 5.7. The $\Delta H^{\neq}$ values for HS^-, PhS^- and $S_2O_3^{2-}$are not statistically significant

different, which range from 70 – 80 kJ/mol. When trying to understand the reactivity of phosphate and thiophosphate esters, it is important to realize that such compounds may react like alkyl halides by nucleophilic displacement (S_N2) (Schwarzenbach et al., 2003). Compared to the literature values of typical S_N2 activation parameters for the reaction of alkyl halides with anionic nucleophiles ($\Delta H^{\neq}$ = 76 – 100 kJ/ mol $\Delta S^{\neq}$ = -13 – -79 J/ mol·K) (Alexander et al., 1968; Turnquist, et al., 1973; Bel'skii, et al., 2000), the $\Delta H^{\neq}$ and $\Delta S^{\neq}$ values for the reactions of dichlorvos with HS^-, PhS^- and $S_2O_3^{2-}$ fall within the range. Though precise experimental measures of $\Delta S^{\neq}$ are difficult to determine (Petersen et al., 1961), such negative values of $\Delta S^{\neq}$ determined in this study would be consistent with highly ordered transition state (Pross, 1995), which support an intermolecular S_N2 pathway in the reaction of dichlorvos with sulfur nucleophiles. Despite the small differences, the values of $\Delta S^{\neq}$ followed the order: $\Delta S^{\neq}(S_2O_3^{2-}) > \Delta S^{\neq}(PhS^-) > \Delta S^{\neq}(HS^-)$. The less negative value of $\Delta S^{\neq}$ for $S_2O_3^{2-}$ is quite likely explained by the steric hindrance, which is responsible for the lower ordered transition states involving larger thiosulfate.

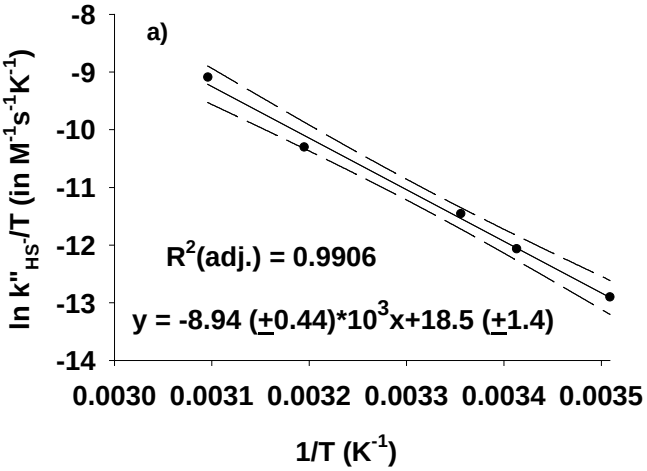
a)
-8
-9
-10
-11
-12
-13
-14
ln k"HS-/T (in M-1s-1K-1)
R2(adj.) = 0.9906
y = -8.94 (±0.44)*10^3x+18.5 (±1.4)
0.0030 0.0031 0.0032 0.0033 0.0034 0.0035
1/T (K-1)

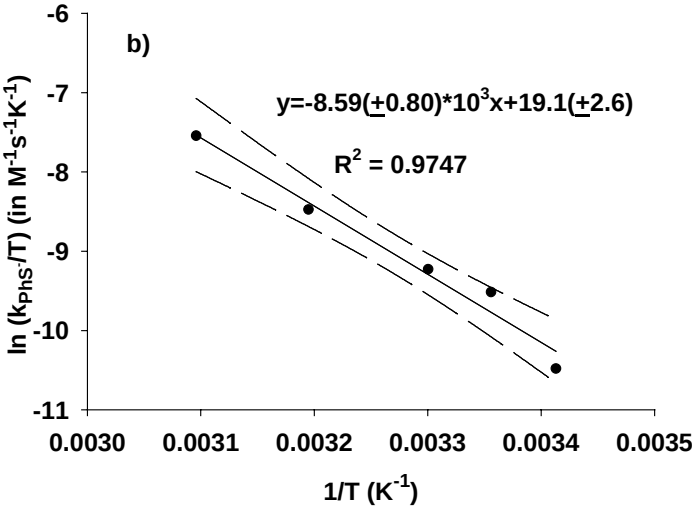
b)
-6
-7
-8
-9
-10
-11
ln (kPhS-/T) (in M-1s-1K-1)
y=-8.59(±0.80)*10^3x+19.1(±2.6)
R2 = 0.9747
0.0030 0.0031 0.0032 0.0033 0.0034 0.0035
1/T (K-1)

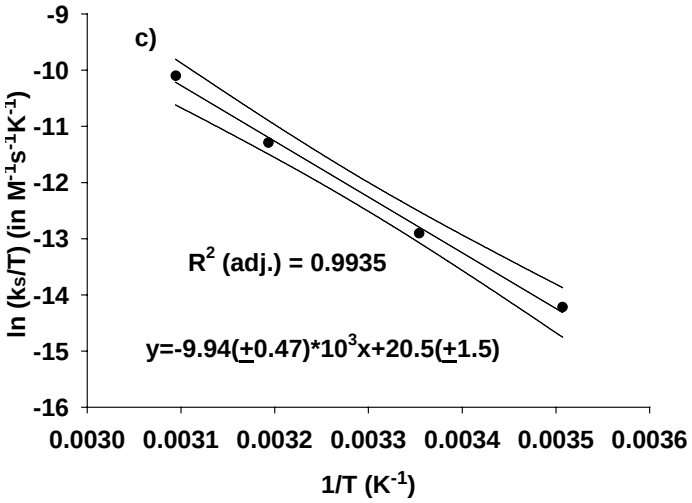

Figure 5.15 Temperature dependence of reaction of dichlorvos with a) bisulfide, b) thiophenolate and c) thiosulfate. Rate constants were determined in 50 mM phosphate buffer, 100 mM NaCl, and 5% methanol at pH 7.15 over 12 – 50 °C. Solid line represents linear regression of the data; the dashed lines represent 95% confidence interval.

Table 5.7. Calculated Activation Barriers for the Reactions of Dichlorvos with Reduced Sulfur Nucleophiles[a]

Species	$\Delta H^{\neq}$ (kJ/mol)	$\Delta S^{\neq}$ (J/mol·K)	$\Delta G^{\neq}$ (kJ/mol)[b]	E_a (kJ/mol)
HS^-	74.4 (± 3.6)	- 43.9 (± 12.0)	87.5 (± 5.1)	76.8 (± 3.6)
PhS^-	71.4 (± 6.7)	- 39.5 (± 11.8)	87.9 (± 7.5)	73.9 (± 6.7)

$S_2O_3^{2-}$	80.1 (± 3.8)	- 25.2 (± 12.6)	87.6 (± 5.4)	82.6 (± 3.8)

[a] Stated uncertainties represent 95% confidence interval.

[b] Calculated at 298.15 K.

4. Environmental Significance

Since dichlorvos is a breakdown product of trichlorfon and can be generated via the degradation of naled (U.S.EPA, 1988a, *Dichlorvos*; Menzie, 1972; PIP-Naled, 1994; PIP-Trichlorfon, 1993), it is often difficult to ascertain the original source of the chemical when dichlorvos is detected in environmental media. The chemical transformation of dichlorvos in the presence of reduced sulfur species is very important not only for understanding of the chemical fate of dichlorvos itself, but also of great importance for naled and trichlorfon in the sulfidic environments. And the chemical fate of the degradation product of dichlorvos is still of much concern. Dichloroacetaldehyde is easily transformed into dichlorethanol and dichloracetic acid. The acute toxicity of dichlorvos has been compared with the degradates. The LD_{50} values in mg/kg body-weight for intraperitoneal administration to mice are: dichlorvos, 28; o-demethyldichlorvos sodium salt, 1500; mono- and dimethylphosphate mixture, 1500; dichloroacetaldehyde, 440; 2,2-dichloroethanol, 890; dichloroacetic acid, 250 (Casida et al., 1962). The degradation of dichlorvos in the presence of the reduced sulfur species in the aqueous solutions is an important detoxification process. The half-lives of dichlorvos in anoxic environments containing reduced sulfur species can be

predicted by multiplying measured second-order rate constants given in Table 5.4 by the maximum concentrations of HS^- and $S_2O_3^{2-}$ summarized by MacCrehan and Shea (1995). The half-lives of dichlorvos in the presence of 5.6 mM HS^- and 0.6 mM $S_2O_3^{2-}$ at pH 7.0 at 25 °C were calculated to be 8.7 h, while half-lives of hydrolysis of dichlorvos at this pH was determined to be 56 h in our previous work. Our results suggest that HS^- and $S_2O_3^{2-}$ are sufficiently reactive to control the fate of dichlorvos within reduced sulfidic environments, provided these reduced sulfur species are present at sufficiently high concentrations such as 5.0 mM HS^- and 0.5 mM $S_2O_3^{2-}$ or higher (as is common in hypoxic marine environments). Unfortunately, the concentrations of aromatic sulfur moieties in the natural environments are not available to the best of our knowledge. However, many other types of organosulfurous compounds such as thiolanes, thianes, thiophenes, and so on are reported in marine sediments (Damste et al., 1989). The study on the reaction of dichlorvos with thiophenol and thiophenolate species can provide a platform from which further investigation of the role of aromatic organosulfur species in the degradation of dichlorvos would be performed.

Literature Cited

1. Adam, P.; Philippe, E.; Albrecht, P. Photochemical sulfurization of sedimentary organic matter: a widespread process occurring at early diagenesis in natural environments? *Geochim. Cosmochim. Acta.* **1998,** *62*, 265-271.

2. Alexander, R.; Ko, E.C.F.; Parker, A.J.; Broxton, T.J. Solvation of ions. XIV. Protic-dipolar aprotic solvent effects on rates of bimolecular reactions. Solvent activity coefficients of reactants and transition states at 25 ^{o}C. *J. Am. Chem. Soc.* **1968**, *90*, 5049-5069.

3. Arnold, W.A.; Winget, P.; Cramer, C.J. Reductive dechlorination of 1,1,2,2-tetrachloroethane. *Environ. Sci. Technol.* **2002**, *36,* 3536-3541.

4. Atkins, P.; De Paula, J. *Physical Chemistry*. Seventh Edition. W. H. Freeman: New York, 2001.

5. Baciocchi, E.; Schiroli, A. Dehalogenation reactions of vicinal dihalides. II. Substituent and leaving-group effects in the reactions of 1,2-dihalo-1,2-diphenylethanes with iodide, bromide, and chloride ions. *J. Chem. Soc. B, Phys. Org.* **1969**, *5,* 554-558.

6. Barbash, J. E., and M. Reinhard, The Reactivity of Sulfur Nucleophiles Toward Halogenated Organic Compounds in Natural Waters. In *Biogenic Sulfur in the Environment*, E. S. Saltzman, W. J. Cooper, Eds. ACS Symposium Series 393, American Chemical Society:Washington, DC, 1989. (1989a)

7. Barbash, J. E.; Reinhard, M. Abiotic dehalogenation of 1,2-dichloroethane and 1,2-dibromoethane in aqueous solution containing hydrogen sulfide. *Environ. Sci. Technol.* **1989**, *23*, 1349-1358. (1989b)

8. Bel'skii, V.E. Isokinetic relationships for nucleophilic substitution reactions at the saturated carbon atom. Reactions in aqueous solution. *Russ. Chem. Bull.* (*Engl. Transl.*) **2000**, *49*, 806-811.

9. Benoit-Marquie, F.; De Montety, C.; Gilard, V.; Martino, R.; Maurette, M.T.; Malet-Martino, M. Dichlorvos degradation studied by ^{31}P-NMR. *Environ. Chem. Letter* **2004**, *2*, 93-97.

10. Berner, R.A. Sedimentary pyrite formation: an update. *Geochim. Cosmochim. Acta.* **1984,** *48*, 606-616

11. Borchardt, L. G., and D. B. Easty. Gas chromatographic determination of elemental and polysulfide sulfur in kraft pulping liquors. *J. Chromatogr.* **1984**, *299*, 471-476.

12. Borowitz, I.J.; Weiss, D.; Crouch, R.K. Debromination of stilbene dibromides and other vicinal dibromides by tricovalent phosphorus. *J. Org. Chem.* **1971**, *36*, 2377-2379.

13. Boulegue, J.; Lord, C. J. III; Church, T. M. Sulfur speciation and associated trace metals (Fe, Cu) in the pore waters of Great Marsh, Delaware. *Geochim. Cosmochim. Acta.* **1982**, *46*, 453-464.

14. Bradman, M. A.; Harnly, M. E.; Draper, W.; Seidel, S.; Teran, S.; Wakeham, D.; Neutra, R. Pesticide exposures to children from California's Central Valley: results of a pilot study. *J. Expo. Anal. Environ. Epidemiol.* **1997**, 7, 217-234.

15. Brassell, S.C.; Lewis, C.A.; de Leeuw, J.W.; de Lange, F.; Damsté, J. S. Isoprenoid thiophenes: Novel products of sediment diagenesis? *Nature* **1986,** *320,* 160-162.

16. Brock, T.D.; Smith, D. W.; Madigan, M.T. *Biology of Microorganisms.* Fourth edition, Prentice-Hall: Englewood Cliff, NJ, 1984.

17. Buckley, T.; Liddle, J.; Ashley, D.; Paschal, D.; Burse, V.; Needham, L.; Akland, G. Environmental and biomarker measurements in nine homes in the lower Rio Grande Valley: multimedia results for pesticides, metals, PAHs, and VOCs. *Environmental International* **1997**, *23*, 705-732.

18. Calvert, D.E.; Karlin, R.E. Relationship between sulphur, organic carbon and iron in the modern sediment of the Black Sea. *Geochim. Cosmochim. Acta.* **1991,** *53*, 2483-2490.

19. Camann, D.; Harding, H.; Clothier, J.; Kuchibhatla, R.; Bond, A. Dermal and in-home exposure of the farm family to agricultural pesticides. In: *Measurement of Toxic and Related Air Pollutants.* Air & Waste Management Association: Pittsburgh, PA, 1995.

20. Camann, D.; Akland, G.; Buckley, J.; Bond, A.; Mage, D. Carpet dust and pesticide exposure of farm children. In: *Unpublished presentation at International Society of Exposure Analysis Annual Meeting,* 5 November 1997, Research Triangle Park, North Carolina.

21. Capel, P. D.; Giger, W.; Reichert, P.; Wanner, O. Accidental input of pesticides into Rhine River. *Environ. Sci. Technol.* **1988,** *22*, 992-997.

22. Capozzi, G.; Modena, G. Oxidation of thiols. In: *The chemistry of the thiol group*; Patai, S. Eds.,Wiley: New York, 1974.

23. Carey, F.A.; Sundberg, R.J. *Advanced Organic Chemistry: Part A: Structure and Mechanisms*. Fourth edition. Kluwer Academic Publishers: Plenum US, 2004.

24. Casida, J.E.; McBride, L.; Niedermeier, R.P. Metabolism of 2,2-dichlorovinyl dimethyl phosphate in relation to residues in milk and mammalian tissues. *J. Agric. Food. Chem.* **1962**, *10*, 370-376.

25. Chapman, R. A.; Harris, C. R. Insecticidal activity and persistence of terbufos, terbufos sulfoxide and terbufos sulfone in soil. *J. Econ. Entomol.* **1980**, *73*, 536-543.

26. Chapman, R. A.; Tu, C. M.; Harris, C. R. Biochemical and chemical transformations of phorate, phorate Sulfoxide, and phorate sulfone in natural and sterile mineral and organic soil. *J. Econ. Entomol*. **1982**, *75*, 112-117.

27. Colt, J. S.; Zahm, S. H.; Camann, D. E.; Hartge, P. Comparison of pesticides and other compounds in carpet dust samples collected from used vacuum cleaner bags and from a high-volume surface sampler. *Environ. Health. Perspect.* **1998**, *106*, 721-724.

28. Cox, J. R.; Ramsay, O.B. Mechanism of nucleophilic substitution in phosphate ester. *Chem. Rev.* **1964**, *64*, 317-352.

29. Cremlyn, R. Pesticides: Preparation and mode of Action. J. Wiley and Sons: Chichester, UK, 1978.

30. Criddle, C.S.; Macarty, P.L.; Elliott, M.C., Barker, J.F. Reduction of hexachloroethane to tetrachloroethylene in groundwater. *J. Contam. Hydrol.* **1986**, *1*, 133-142.

31. Damsté, J.S.; de Leeuw, J.W.; Kock-van Dalen, A.C.; de Leeuw, M.A.; de Lange, F.; Rijpstra, W.I.C. The occurrence and identification of series of organic sulphur compounds in oils and sediment extracts: I. A study of Rozel Point Oil (USA). *Geochim. Cosmochim. Acta.* **1987,** *51*, 2369-2391.

32. Damsté, J. S.; Rijpstra, W. I. C.; De Leeuw, Jan W.; Schenck, P. A. The occurrence and identification of series of organic sulfur compounds in oils and sediment extracts: II. Their presence in samples from hypersaline and non-hypersaline palaeoenvironments and possible application as source,

palaeoenvironmental and maturity indicators. *Geochim. Cosmochim. Acta.* **1989**, *53*, 1323-1341.

33. Dean, J.A. *Lange's Handbook of Chemistry*. McGraw-Hill: New York, 1985.

34. Devlin, C.J.; Walker, B.J. Stereochemistry of phosphine-induced debromination reactions. *J. Chem. Soc., Perkin Trans. 1,* **1972**, *9-10,* 1249-1253.

35. Drevenkar, V.; Fink, K.; Stipcevic, M.; Tkalcevic, B. The fate of pesticides in aquatic environment. II. Hydrolysis of dichlorvos in a model system and in river water. *Arh .hig. rada.* **1976,** *27,* 297

36. Eskenazi, B.; Maizlish, N. A. Effect of occupational exposure to chemicals on. neurobehavioral functioning. In *Medical Neuropsychology: The Impact of Disease on Behavior.* Tarter, R.E.; Thiel, D.H.V.; Edwards, K.L. eds. Plenum Press: New York City, 1988.

37. EXTOXNET TIBs - Cholinesterase Inhibition, 1993 Extension Toxicology Network, Pesticide Information Project, Cornell University, Ithaca, NY. http://extoxnet.orst.edu/tibs/cholines.htm (accessed on June, 5, 2005)

38. Faust, S. D.; Gomaa, H. M. Chemical hydrolysis of some organic phosphorus and carbamate pesticides in aquatic environments. *Environ. Letter.* **1972**, *3,* 171-201.

39. Feldman, R. G. *Organophosphates. Occupational and Environmental Neurotoxicology.* Lippincott-Raven: Philadelphia, 1998

40. Furukawa, N.; Ogawa, S.; Kawai, T. Sulphoxide Substitution Pyridines as Phase-transfer Catalysts for Nucleophilic Displacements and Alkylations. *J.Chem. Soc., Perkin Trans. I* **1984**, 1833.

41. Gan, Q.; Singh, R.M.; Jans, U. Degradation of naled and dichlorvos promoted by reduced sulfur species in well-defined anoxic aqueous solutions. *Environ. Sci. Technol.* **2006**, *40*, 778-783.

42. Giggenbach, W. Optical spectra and equilibrium distribution of polysulfide ions in aqueous solutions at 20 ^{o}C. *Inorg. Chem.* **1972,** *11*, 1201-1207.

43. Glaze, W. H.; Koga, M.; Cancilla, D. Ozonation byproducts. 2. Improvement of an aqueous-phase derivatization method for the detection

of formaldehyde and other carbonyl compounds formed by the ozonation of drinking water. *Environ. Sci. Technol.* **1989**, *23*, 838-847.

44. Godfrey, J. T.; Foster, G. D.; Lippa, K. A. Estimated annualloads of selected organic contaminants to Chesapeake Bay via a major tributary. *Environ. Sci. Technol.* **1995**, *29*, 2059-2064.

45. Gohre, K.; Miller, G.C. Photooxidation of thioether pesticides on soil surfaces. *J. Agric. Food Chem.* **1986**, *34*, 709-713.

46. Gore, R. C.; Hannah, R. W.; Pattacini, S. C.; Porro, T. J. Pesticide residues: Infrared and ultraviolet spectra of seventy-six pesticides. *J. Assoc. Off. Anal. Chem.* **1971**, *54*, 1040-1082.

47. Haag, W.R.; Mill, T. Some reactions of naturally occurring nucleophiles with haloalkanes in water. *Environ Toxicol Chem***, 1988,** *7,* 917-924.

48. Haag, F.; Reinhard, M.; McCarty, P.L.Degradation of Toluene and p-Xylene in Anaerobic Microcosms: Evidence for Sulfate as a Terminal Electron Acceptor," *Env. Tox. Chem.* **1991**, *10*, 1379-1389.

49. Hallberg, G. R. Pesticide pollution of groundwater in the humid United States. *Agric. Ecosyst. Environ.* **1989,** *26,* 299-367.

50. Harada, K.; Hisanaga, T.; Tanaka, K. Photocatalytic degradation of organophosphorus insecticides in aqueous semiconductor suspension. *Water Research* **1990**, *24*, 1415-1417.

51. Hedderich, R.; Klimmek, O.; Kroger, A; Dirmeier, R.; Keller, M.; Stetter, K.O. Anaerobic respiration with elemental sulfur and with disulfides. *FEMS Microbiol. Rev.* **1998**, *22*, 353-381.

52. Hennessey, M.K.; Nigg, H.N.; Habeck, D.H. Mosquito (Diptera: Culicidae) adulticide drift into wildlife refuges of the Florida Keys. *Environ. Entomol.* **1992**, *21,* 714-721.

53. Hine, J. *Physical Organic Chemistry,* Second edition, McGraw-Hill: New York, 1962.

54. Hofmann, P.; Huc, A. Y.; Carpentier, B.; Schaeffer, P.; Albrecht, P.; Keely, B.; Maxwell, J. R.; Sinninghe Damsté, J. S.; de Leeuw, J. W.; Leythaeuser, D. Organic matter of Mulhouse basin, France: A synthesis. *Org. Geochem.* **1993**, *20*, 1105-1123

55. Holden, P.W. *Pesticides and groundwater quality.* National Academy Press: Washington, DC, 1986.

56. Holden, A. J.; Chen, L.; Shaw, I. C., Thermal stability of organophosphorus pesticide triazophos and its relevance in the assessment of risk to the consumer of triazophos residues in food. *J. Agric. Food Chem.* **2001**, *49*, 103-106.

57. Hong, F.; Pehkonen S. Hydrolysis of phorate using simulated environmental condition; rates, mechanism, and product analysis. *J. Agric. Food. Chem.* **1998**, *46*, 1192-1199.

58. Hong, F.; Pehkonen S. O.; Brooks, E. Pathways for the phorate: product studies by ^{31}P NMR and GC-MS. *J. Agric. Food. Chem.* **2000**, *48*, 3013-3017.

59. Hong, F.; Win, K. Y.; Pehkonen S. O. Hydrolysis of terbufos using simulated environmental condition; rates, mechanism, and product analysis. *J. Agric. Food. Chem.* **2001,** *49*, 5866-5873.

60. Howard, P.H. *Handbook of Environmental Fate and Exposure Data for Organic Chemicals. Vol. III. Pesticides.* Lewis: Chelsea, MI, 1991.

61. Howard, P.H.; Meylan, W.M. *Handbook of Physical Properties of Organic Chemicals*. CRC/Lewis Publishers: Boca Raton, FL,1997.

62. Ibne-Rasa, K.M.; Muhammad, N.; Hasibullah. Reaction of vic-dibromides with thiourea. *Chem. Ind.* **1966**, *33*, 1418.

63. Jafvert, C.T.; Wolfe, N.L. Degradation of selected halogenated ethanes in anoxic sediment-water systems. *Environ. Toxicol. Chem.* **1987**, *6*, 827-837.

64. Janout, V.; Prochazka, M.; Palecek, M. Reaction of 1,2-dihalides with thiolates. *Coll. Czech. Chem. Commun.* **1976**, *41*, 617-622.

65. Jans, U.; Miah, M.H. Reaction of chlorpyrifos-methyl in aqueous hydrogen sulfide/bisulfide solutions. *J. Agric. Food Chem.,* **2003**, *51,* 1956-1960.

66. Kamiya, M.; Kameyama, K., Effects of selected metal ions on photodegradation of organophosphorus pesticides sensitized by humic acids. *Chemosphere* **2001**, *45*, 231-235.

67. Kasal, A. Steroids. CLXXXIII. Reductive debromination of dibromo steroids. *Coll. Czech. Chem. Commun.* **1976**, *41*, 2040-2046.

68. Kenaga, E. E. Predicted bioconcentration factors and soil sorption coefficients of pesticides and other chemicals. *Ecotox. Environ. Safety* **1980**, *9*, 26-38.

69. Khandelwal G. D.; Wedzicha, B.L. Reaction of dichlorvos, dichloroacetaldehyde and related compounds with nucleophiles and phenols. *Food Chemistry* **1998**, *61*, 191-200.

70. Kirby, A. J.; Warren, S. G. *The Organic Chemistry of Phosphorus.* Elsevier: New York, 1967.

71. Klecka, G.M.; Gonsior, S.J. Reductive dechlorination of chlorinated methanes and ethanes by reduced iron(II)porphyins. *Chemosphere* **1984**, *13*, 391-402.

72. Kohnen, M.E.; Damsté, J.S.; Bass, M.; Kock-van Dalen, A.C.; de Leeuw, J.W. Sulphur-bound steroid and phytane carbon skeletons in geomacromolecules: Implications for the mechanism of incorporation of sulphur into organic matter. *Geochim. Cosmochim. Acta.* **1993**, *57*, 2515-2528.

73. Kohn, G. K; Baker, D. R. Eds. The Agrochemical Industry. In *Riegel's Handbook of Industrial Chemistry.* Kent, J.A. Ed. Van Nostrand Reinhold: New York, 1992.

74. Krein, E. B.; Aizenshata, Z. The formation of sulfur compounds during diagenesis: Simulated sulfur incorporation and thermal transformation. *Org. Geochem.* **1994**, *21*, 1015-1025.

75. Kwok, W.K.; Mathai, I.M.; Miller, S.I. Debromination of meso- and DL-stilbene dibromides by lithium bromide in dimethylformamide. *J. Org. Chem.* **1970**, *35*, 3420-3423.

76. Lamoreaux, R.J.; Newland, L.W. The fate of dichlorvos in soil. *Chemosphere* **1978**, *7*, 807-814.

77. Larson, R.A.; Weber, E.J. *Reaction Mechanisms in Environmental Organic Chemistry*. Lewis: Boca Raton, FL, 1994.

78. Leonard, R. A. Herbicides in surface water. In: *Environmental Chemistry of Herbicide,* Grover, R., Ed.; CRC Press: Boca Raton, FL,1988.

79. Lewis, R.G.; Fortmann, R. C.; Camann, D. E. Evaluation of methods for monitoring the potential exposure of small children to pesticides in the residential environment. *Arch. Environ. Contam. Toxicol.* **1994**, *26*, 37-46.

80. Licht, S.; Davis, J. Disproportionation of aqueous sulfur and sulfide: Kinetics of polysulfide decomposition. *J. Phys. Chem.* B **1997**, *101*, 2540-2545.

81. Lieberman, M. T.; Alexander, M. Microbial and nonenzymic steps in the decomposition of dichlorvos (2,2-dichlorovinyl O,O-dimethyl phosphate). *J. Agric. Food Chem.* **1983,** *31*, 265-267.

82. Lippa, K.A.; Roberts, A.L. Nucleophilic aromatic substitution reaction of chloroazines with bisulfide (HS^-) and polysulfide (S_n^{2-}). *Environ. Sci. Technol.* **2002**, *36*, 2008-2018.

83. Lippa, K.A.; Demel, S.; Lau, I.H.; Roberts, A.L. Kinetics and mechanism of the nucleophilic displacement reaction of chloroacetanilide herbicides: Investigation of α-substituent effects. *J. Agric. Food Chem.* **2004**, *52,* 3010-3021.

84. Liu, B.; McConnell, L. L.; Torrents, A., Hydrolysis of chlorpyrifos in natural waters of the Chesapeake Bay. *Chemosphere* **2001**, *44*, 1315-1323

85. Loch, A.R.; Lippa, K.A.; Carlson, D.L.; Chin, Y.P.; Traina, S.J.; Roberts, A.L. Nucleophilic aliphatic substitution reactions of propachlor, alachlor, and metolachlor with bisulfide (HS^-) and polysulfide (S_n^{2-}). *Environ. Sci. Technol.* **2002**, *36*, 4065-4073.

86. Lu, M. C., Chen, J.-N.; Chang, C.-P. Effect of inorganic ions on the oxidation of dichlorvos insecticide with Fenton's reagent. *Chemosphere* **1997**, *35*, 2285-2293.

87. Luther, G. W. III. The frontier-molecular orbital theory approach in geochemical processes. In: *Aquatic Chemical Kinetics: Reaction Rates of Processes in Natural Waters*; Stumm, W., Ed.; John Wiley, New York, 1990; 173-198.

88. Luther, G.W.III; Giblin, A.E; Varsolona, R. Polarographic analysis of sulfur species in marine porewaters *Limnol. Oceanogr,* **1985**, *20*, 727-736.

89. MacCrehan, W.; Shea, D. Temporal relationship of inorganic sulfur compounds in anoxic Chesapeake Bay sediment porewater. In *Geochemical Transformations of Sedimentary Sulfur*, Vairavamurthy, M.A.; Schoonen, M.A.A. Eds. American Chemical Society: Washington, DC, 1995.

90. Mathai, I.M.; Schug, K.; Miller, S.I. Stereoselectivity in debromination of the stilbene dibromide by several metal and inorganic reductants in several solvents. *J. Org. Chem.* **1970**, *35*, 1733-1736.

91. Meikle, R. W.; Youngson, C. R., The hydrolysis rate of chlorpyrifos, *O,O*-diethyl *O*-(3,5,6-trichloro-2-pyridyl) phosphorothioate, and its dimethyl analog, chlorpyrifos-methyl, in dilute aqueous solution. *Arch. Environ. Contam. Toxicol.* **1978**, *7*, 13-22.

92. Menzie, C. M. Fate of pesticides in the environment. *Ann. Rev. Entomol.* **1972,** *17*, 199-222.

93. Meyer, B.; Peter, L.; Spitzer, K., Trends in the charge distribution in sulfanes, sulfanesulfonic acids, sulfanedisulfonic acids, and sulfurous acid. *Inorg. Chem.* **1977**, *16*, 27-33.

94. Miller, P.L.; Vasudevan, D.; Gschwend, P. M.; Roberts, A.L. Transformation of hexachloroethane in a sulfidic natural water. *Environ. Sci. Technol.* **1998**, *32,* 1269-1275.

95. Millero, F.J. The thermodynamics and kinetics of hydrogen sulfide systems in natural waters. *Mar. Chem.*, **1986**, *18*, 121-147.

96. Mileson, B.E.; Chambers, J.E.; Chen, W.L.Common mechanism of toxicity: a case study of organophosphorous pesticides. *Toxicol. Sci.* **1998**, *41*, 8-20.

97. Mopper, K.; Taylor B.F. Biogeochemical cycling of sulfur: thiols in coastal marine sediments. In: *Organic Marine Geochemistry* Sohn, M.L.Ed. ACS Symposium Series 305, American Chemical Society: Washington, DC, 1986.

98. Morifusa, E. *Organophosphate Pesticides: Organic and Biological Chemistry*. CRC Press: Cleveland, OH, 1974.

99. Mortland, M. M.; Raman, K. V. Catalytic hydrolysis of some organic phosphate pesticides by copper(II). *J. Agric. Food. Chem.* **1967**, *15*, 163-167.

100. Mossman, D.J.; Schnoor, J.L.; Stumm, W. Predicting the effects of a pesticide release of the Rhine River. *J. Water Pollut. Control Fed.* **1988**, *60*, 1806-1812.

101. Mostaghimi, S.; McClellan, P.W.; Cooke, R. A. Pesticide contamination of groundwater in Virginia: BMP impact assessment. *Water Sci. Technol.* **1993**, *28*, 379-387.

102. Mühlmann, R.; Schrader, A. Hydrolyse der insektiziden phosphoruräester. *Z. Naturforsch.* **1957**, *12b*, 196-208.

103. Nash, R. G. Plant uptake of insecticides, fungicides and fumigants from soils. In *Pesticides in Soil and Water*. Weed, S.B.; Weber, J.B.; Guenzi, W.D. Eds. Soil Science of America Inc.: Madison, WI, 1974.

104. New York State Department of Health. *West Nile Virus Response Plan.* Feb, 2000. http://www.health.state.ny.us/nysdoh/westnile/final.htm (accessed January 3, 2005).

105. Noblet, J. A.; Smith, L. A.; Suffet, I. H. M., Influence of natural dissolved organic matter, temperature, and mixing on the abiotic hydrolysis of triazine and organophosphate pesticides. *J. Agric. Food Chem.* **1996**, *44*, 3685-3693.

106. Pearson, R.G.; Songstadt, S. Application of the principle of hard and soft acid and bases to organic chemistry. *J. Am. Chem. Soc.* **1967**, *89*, 1827-1837.

107. Peijnenburg, W.J.G.M.; 'T Hart, M. J.; Den Hollander, H.A.; Van de Meent, D.; Verboom, H.H.; Wolfe, N.L. QSARs for predicting biotic and abiotic reductive transformation rate constants of halogenated hydrocarbons in anoxic sediment systems. *Sci. Total Environ.* **1991**, *109/110,* 283-300.

108. Petersen, R. C.; Markgraf, J. H.; Ross, S. D. Solvent Effects in the Decomposition of 1,1'-Diphenylazoethane and 2,2'-Azobis-(2-methylpropionitrile) *J. Am. Chem. Soc.* **1961**, *83*, 3819-3823.

109. Pickerling, T. L.; Tobolsky, A. V. Inorganic and Organic Polysulfides. In: *Sulfur in Organic and Inorganic Chemistry*; Senning, A., Ed.; Marcel Dekker, New York, 1972.

110. PIP-Naled. 1994. EXOTOXNET Profile for Naled. Extension Toxicology Network, Pesticide Information Project, Cornell University, Ithaca, NY. http://extoxnet.orst.edu/pips/naled.htm (accessed on Oct, 5, 2005)

111. PIP-Phorate. 1993. EXOTOXNET Profile for Phorate. Extension Toxicology Network, Pesticide Information Project, Cornell University,

Ithaca, NY. http://extoxnet.orst.edu/pips/phorate.htm (accessed on Dec, 15, 2005)

112. PIP-Terbufos. 1994. EXOTOXNET Profile for Terbufos. Extension Toxicology Network, Pesticide Information Project, Cornell University, Ithaca, NY. http://extoxnet.orst.edu/pips/terbufos.htm (accessed on Dec, 15, 2005)

113. PIP-Trichlorfon. 1993. EXOTOXNET Profile for Trichlorfon. Extension Toxicology Network, Pesticide Information Project, Cornell University, Ithaca, NY. http://extoxnet.orst.edu/pips/trichlor.htm (accessed on Oct, 5, 2005)

114. Plumb, R. H. Jr. The occurrence of Appendix IX organic constituents in disposal site ground water. *Ground Water Monit. Revue.* **1991**, *11*, 157-164.

115. Posner, G.H.; Ting, J. S. Reductive elimination of bromine from 1,2-dibromoalkanes using organometallic reagents. *Syn. Commun.* **1973**, 3, 281-285.

116. Pross, A. *Theoretical and Physical Principles of Organic Reactivity.* John Wiley and Sons: New York, 1995.

117. Pyzik, A.J.; Sommer, S.E. Sedimentary iron monosulphides: Kinetics and mechanism of formation. *Geochim. Cosmochim. Acta,* **1981**, *45*, 687-98

118. Racker, K.D. Degradation of organophosphorus insecticides in environmental matrices. In *Organophosphates, Chemistry, Fates and Effects.* Chamber, J.E.; Levi, P.E. Academic Press: San Diego, CA, 1992.

119. Racke, K. D.; Steele, K. P.; Yoder, R. N.; Dick, W. A.; Avidov, E., Factors affecting the hydrolytic degradation of chlorpyrifos in soil. *J. Agric. Food Chem.* **1996**, *44*, 1582-1592.

120. Ramasamy, K.; Kalyanasundaram, S.K.; Shanmugam, P. Debromination of vic-dibromides using sodium hydrogen telluride reagent. *Synthesis* **1978**, *4*, 311-312.

121. Roberts, A. L.; Sanborn, P.L.; Gschwend, P.M. Nucleophilic substitution reactions of dihalomethanes with hydrogen sulfide species. *Environ. Sci. Technol.* **1992**, *26*, 2263-2274.

122. Roberts, A.L.; Gschwend, P.M. Interaction of abiotic and microbial processes in hexachloroethane transformation in groundwater. *J. Contam. Hydrol.,* **1994**, *16*, 157-174.

123. Roberts, A.L.; Totten, L.A.; Arnold, W.A.; Burris, D.R.; Campbell, T.J. Reductive elimination of chlorinated ethylenes by zero-valent metals. *Environ. Sci. Technol.* **1996**, *30,* 2654-2659.

124. Roinestad, K. S.; Louis, J. B.; Rosen, J. D. Determination of pesticides in indoor air and dust. *J AOAC Int.* **1993**, *76*, 1121-1126.

125. Rowland, S.; Rockey, C.; Al-Lihaibi, S. S.; Wolff, G. A. Incorporation of sulphur into phytol derivatives during simulated early diagnensis. *Org. Geochem.* **1993**, *20*, 1-5.

126. Schenau, S.J.; Passier, H.F.; Reichart, G..J.; de Lange, G.J. Sedimentary pyrite formation in the Arabian Sea. *Marine Geology* **2002**, *185*, 393-402.

127. Scheybal, A.; Gabrio, T.; Konrad, H. Zum Abbauverhalten von Naled-Untersuchungen mit Hilfe von ^{82}Br-Naled. *Z. Chem.* **1978**, *18*, 404-405.

128. Schmidt, K. J.; Fest, C. *The Chemistry of Organophosphorus Pesticides.* Springer-Verlag: New York, 1982.

129. Schouten, S.; van Driel, G. B.; Sinninghe Damsté, J. S.; de Leeuw, J. W. Natural sulphurization of ketones and aldehydes: A key reaction in the formation of organic sulphur compounds. *Geochim. Cosmochim. Acta.* **1993**, *57,* 5111-5116.

130. Schramm, J. D.; Hua, I. Ultrasonic irradiation of dichlorvos: Decomposition mechanism. *Water Research* **2001**, *35*, 665-674.

131. Schroeder, J.P.; Tew, L.B. Peters, V.M. Dehalogenation of vicinal dibromoalkanes with triethyl phosphite. *J. Org. Chem.*, **1970**, *35*, 3181-3184.

132. Schwarzenbach, G. and Fischer, A. Die Acidität der Sulfane und die Zusammensetzung wässeriger Polysulfidelösungen. *Helv. Chim. Acta.* **1960**, *43*, 1365-1388.

133. Schwarzenbach, R. P.; Giger, W.; Schaffner, C.; Wanner, O. Groundwater contamination by volatile halogenated alkanes: abiotic formation of volatile sulfur compounds under anaerobic conditions *Environ. Sci. Technol.* **1985**, *19*, 322-327.

134. Schwarzenbach, R. P.; Gschwend, P. M.; Imboden, D. M., *Environmental Organic Chemistry*. Wiley-Interscience: New York, 2003.

135. Sclimenti, M. J.; Krasner, S. W.; Glaze, W. H.; Weinberg, H. S. Ozone disinfection by-products: optimization of PFBHA derivatization method for analysis of aldehydes. In *Proceedings of the American Water Works Association Water Quality Technology Conference.* American Water Works Association: Denver, CO, 1990.

136. Senesi, N.; Steelink, C. Application of ESR spectroscopy to the study of humic substances. In: *Humic Substance II: In Search of Structure.* Hayes, M. H. B.; MacCarthy, ed. P. Wiley-Interscience: New York, 1989.

137. Simcox, N. J.; Fenske, R. A.; Wolz, S. A.; Lee, I. C.; Kalman, D. A. Pesticides in household dust and soil: exposure pathways for children of agricultural families. *Environ. Health Perspect.* **1995**, *103*, 1126-1134.

138. Sittig, M. *Pesticide Manufacturing and Toxic Materials Control Encyclopedia.* Noyes Data Corporation: Park Ridge, NJ. 1980.

139. Smolen, J. M.; Stone, A. T., Divalent metal ion-catalyzed hydrolysis of phosphorothionate ester pesticides and their corresponding oxonates. *Environ. Sci. Technol.* **1997**, *31*, 1664-1673.

140. Solomons, T.W.G. *Organic Chemistry,* Sixth Edition, John Wiley & Sons: New York, 1996.

141. Speziale, A.J., Tung, C.C. Debromination of N,N-diethylcinnamamide dibromide. *J. Org. Chem.*, **1963**, *28*, 1353-1357.

142. Starr, H. G. Jr; Aldrich, F. D.; MacDougall, W. D.; Mounce, L. M. Contribution of household dust to the human exposure to pesticides. *Pestic. Monit. J* **1974**, *8,* 209-212.

143. Steen. W.; Bond, A.; Mage, D. *Agricultural Health Study-Exposure Pilot Study Report.* U.S. Environmental Protection Agency: Research Triangle Park, NC, 1997.

144. Stumm, W.; Morgan, J.J. *Aquatic Chemistry*, Second edition, Wiley-Interscience: New York, 1981

145. Swain, C.G.; Scott, G. B. Quantitative correlation of relative rates. comparison of hydroxide ion with other nucleophilic reagents toward alkyl halides, esters, epoxides and acyl halides. *J. Am. Chem. Soc.,* **1953**; *75*; 141-147.

146. Szeto, S. Y.; Brown, M. J.; Mackenzie, J. R.; Vernon, R.S. Degradation of terbufos in the soil and its translocation into cole crops. *J. Agric. Food Chem.* **1986**, *34*, 876- 879.

147. Szeto, S. Y.; Price, P. M.; Mackenzie, J. R.; Vernon, R. S. Persistence and uptake of phorate in mineral and organic Soils. *J. Agric. Food Chem*. **1990**, *38*, 501-504.

148. Thompson, W.T. *Agricultural Chemicals. Book I. Insecticides.* Thompson Publications: Fresno, CA, 1985.

149. Thurman, E. M.; Goolsby, D. A.; Meyer, M. T.; Kolpin, D.W. Herbicides in Surface Waters of the Midwestern United States: The Effect of Spring Flush. *Environ. Sci. Technol.* **1991,** *25***,** 1794-1796.

150. Thurman, E. M.; Meyer, M. T.; Mills, M. S.; Zimmerman, L. R.; Perry, C. A.; Goolsby, D. A. Formation and Transport of Deethylatrazine and Deisopropylatrazine in Surface Water. *Environ. Sci. Technol.,* **1994**, *28*, 2267-2277.

151. Totten, L.A.; Jans, U.; Roberts, A.L. Alkyl bromides as mechanistic probes of reductive dehalogenation: reaction of vicinal dibromide stereoisomers with zerovalent metals. *Environ. Sci. Technol.* **2001**, *35,* 2268-2274.

152. Tsai Lee, C.S.; Mathai, I.M.; Miller, S.I. Stereoselectivity and dehalogenation mechanism. The elimination reactions of meso- and dl-stilbene dibromides with iodide in methanol. *J. Am. Chem. Soc.* **1970**, *92,* 4602-4609.

153. Turnquist, C.R.; Taylor, J.W.; Grimsrud, E. P.; Williams, R. C. Temperature dependence of chlorine kinetic isotope effects for aliphatic chlorides. *J. Am. Chem. Soc.* **1973**, *95*, 4133-4138.

154. U.S. Environmental Protection Agency. 1988a. *Dichlorvos: Initiation of special review.* Notice. *Fed. Regist.* **1988**, *53,* 5542-5549. [EPA Notice OPP-30000/56; FRL-3332-71.]

155. U.S. Environmental Protection Agency. 1993b. *Dichlorvos (DDVP, Vapona) Revocation of food additive tolerance: Final rule.* Notice. *Fed. Regist.* **1993**, *58*, 59663. [EPA Notice OPP-300237A; FRL-4188-7.]

156. U.S. Environment Protection Agency. 1996. OPP annual report for 1996 Part 1. http://www.epa.gov/oppfod01/annual/1996/part1.htm (Accessed on Dec. 12, 2005).

157. U.S. Environment Protection Agency. 1996. Food Quality Protection Act (FQPA) of 1996. http://www.epa.gov/oppfead1/fqpa/ (accessed on Oct. 12, 2005).

158. U.S. Environment Protection Agency. 1999. 735-F-99-014. Organophosphate Pesticides in Food - A Primer on Reassessment of Residue Limits. http://www.epa.gov/pesticides/op/primer.htm (accessed on Oct. 12, 2005).

159. U. S. Environment Protection Agency. 2000. *Organophosphate Pesticides Information. Disulfoton summary.* http://www.epa.gov/pesticides/op/disulfoton/disulf_summ.htm (accessed Dec. 12, 2005)

160. U.S. Environmental Protection Agency. 2001. 738-F-00-014. *R. E. D. Facts. Phorate.* http://www.epa.gov/oppsrrd1/REDs/factsheets/phorate_fs.htm (accessed Nov. 11, 2005).

161. U.S. Environmental Protection Agency. 2001. 738-F-01-015 *R. E. D. Facts. Terbufos.* http://www.epa.gov/REDs/factsheets/terbufos_ired_fs.htm accessed Nov. 11, 2005).

162. Valent USA Corporation. March 1993. Dibrom concentrate—for use in mosquito control programs. (Cited in EXTOXNET. 1996b. *Naled.* http://extoxnet.orst.edu/pips/naled.htm Accessed January 3, 2005.)

163. Wang, T. C.; Hoffman, M. E. Degradation of organophosphorus pesticides in coastal water. *J. Assoc. Off. Analyt. Chem.* **1991**, *74*, 883-886

164. Wauchope, R. D. J. The pesticide content of surface water draining from agricultural fields – A review. *Environ. Qual.* **1978**, *7*, 459-7472.

165. Wanner, O.; Egli, T.; Fleischmann, T.; Lanz, K.; Reichert, P.; Schwarzenbach, R. P. Behavior of the insecticides disulfoton and thiometon in the Rhine River: a chemodynamic study. *Environ. Sci. Technol.,* **1989**, *23*, 1232-1242.

166. Ware, G.W.; Whitacre, D.M. *The Pesticide Book.* Sixth edition. MeisterPro Information Resource: Willoughby, Ohio, 2004.

167. Wauchope, R. D. J. The pesticide content of surface water draining from agricultural fields – A review. *Environ. Qual.* **1978**, *7*, 459-7472.

168. Weber, E.J.; Wolfe, N.L. Kinetic studies of thr reduction of aromatic azo compounds in anaerobic sediment-water system. *Environ. Toxicol. Chem.* **1987**, *6*, 911-919.

169. Whitmore, R. W.; Immerman, F. W.; Camann, D. E.; Bond, A. E.; Lewis, R. G.; Schaum, J. L. Non-occupational exposures to pesticides for residents of two U.S. cities. *Arch. Environ. Contam. Toxicol.* **1994**, *26*, 47-59.

170. WHO. 1989. Dichlorvos. Environmental Health Criteria #79. World Health Organization, Geneva, Switzerland.

171. Wolfe, N. L.; Zepp, R. G.; Gordon, J. A.; Baughman, G. L.; Cline, D. M. Kinetics of chemical degradation of malathion in water. *Environ. Sci. Technol.,* **1977**, *11*, 88-93.

172. Wu, T.; Jans, U. Nucleophilic substitution reaction of chlorpyrifos-methyl with sulfur species. *Environ. Sci. Technol.* **2006**, *42*, 784-790.

173. Yamada, H.; Somiya, I. The determination of carbonyl compounds in ozonated water by PFBOA method. *Ozone: Sci. Eng.* **1989**, *11,* 127-141.

174. Zoro, J.A.; Hunter, J.M.; Eglinton, G.; Ware, G. Degradation of p,p'-DDT in reducing environments. *Nature* **1974**, *247*, 235-236.